Manufacture of Red Blood Cells from Stem Cells

Thesis submitted to Heriot Watt University for the degree of Doctor of Philosophy in Chemical Engineering

by

Nicola Goddard

Institute of Biochemistry, Biophysics and Bioengineering
Department of Engineering and Physical Sciences

August 2016

Abstract

Although the current system of blood transfusion is relatively safe and established within the UK, periodic shortages of certain blood groups and residual risks of emerging transfusion transmitted infections (TTIs) make an industrial manufacture process for the generation of red blood cells more desirable. The generation of red blood cells from human embryonic stem cells has been completed in vitro but the major challenge lies in making the process highly scalable and economically viable.

Initially human embryonic and induced pluripotent stem cells were trialled for use on the project however these were found to be inconsistent, a major issue in cellular therapies. They were replaced with CD34+ cord blood stem cells which are morphologically and physiologically divergent. In order to assess their suitability for a GMP-complaint manufacturing process an ultra-scale down (microfluidic) approach was taken to assess the cells' reactions to the changeable physical environment associated with scale-up procedures. Cellular responses to hypoxia and shear stress were evaluated at successive time-points in the step-wise haematopoietic differentiation process and recommendations made for optimum scale-up conditions. Conversely further challenges in the manufacture of red blood cells from stem cells were uncovered regarding the differences between stem cell derived red blood cells and their adult equivalents.

For my late Grandfather who started me on this path

Acknowledgements

First I would like to thank my supervisor Professor Nik Willoughby for giving me this opportunity and for his ongoing support and encouragement. I would like to thank Dr Fiona Dempsey for sharing her expertise in cell culture and GMP with me and for her constant support and guidance that went beyond her duties as a post-doc. I would also like to thank Dr Maïwenn Kersaudy-Kerhoas for being my mentor and giving me guidance in microfluidics when I needed it most.

I would like to thank the exceptional mechanical engineers and technicians at Heriot Watt, in particular John Mason, Richard Kinsella and Eileen McEvoy. Not only was their expertise indispensable to my project, they are great people who always made me smile even when I didn't feel like it.

A special gratitude goes to my parents Peter and Catherine Goddard who always told me 'life is what you make it' and supported my decision to change career when others laughed at me. They have shown unwavering faith in my abilities and been my biggest supporters.
Finally the biggest thank you has to go to my husband Aaron Stewart who has been a rock for me throughout. He kept me company on late nights and weekends in the lab, put up with my tears and tantrums and on the hard days told me to never give up.

ACADEMIC REGISTRY

Research Thesis Submission

Name*:*			
School:			
Version: *(i.e. First, Resubmission, Final)*		Degree Sought:	

Declaration

In accordance with the appropriate regulations I hereby submit my thesis and I declare that:

1) the thesis embodies the results of my own work and has been composed by myself
2) where appropriate, I have made acknowledgement of the work of others and have made reference to work carried out in collaboration with other persons
3) the thesis is the correct version of the thesis for submission and is the same version as any electronic versions submitted*.
4) my thesis for the award referred to, deposited in the Heriot-Watt University Library, should be made available for loan or photocopying and be available via the Institutional Repository, subject to such conditions as the Librarian may require
5) I understand that as a student of the University I am required to abide by the Regulations of the University and to conform to its discipline.
6) I confirm that the thesis has been verified against plagiarism via an approved plagiarism detection application e.g. Turnitin.

* *Please note that it is the responsibility of the candidate to ensure that the correct version of the thesis is submitted.*

Signature of Candidate*:*		Date:	

Submission

Submitted By *(name in capitals):*	

Signature of Individual Submitting:	
Date Submitted:	

For Completion in the Student Service Centre (SSC)

Received in the SSC by *(name in capitals):*			
Method of Submission *(Handed in to SSC; posted through internal/external mail):*			
E-thesis Submitted (**mandatory for final theses)**			
Signature:		Date:	

Table of Contents

List of Tables

Chapter 1

Chapter 2

Chapter 5

Chapter 6

List of Figures

Chapter 1

Chapter 2

Chapter 3

Chapter 4

Chapter 5

Chapter 6

Chapter 1 - Introduction

Blood transfusion involves the intravenous transfer of whole blood or its components from one person to another. In the case of red blood cell transfusion, cells may be administered as part of whole blood but are more often separated from other blood components (white blood cells, platelets and plasma) as red cell concentrates [1].
Red cell transfusion is an essential medical procedure used to treat blood loss following surgical procedures or trauma and treat anaemia or haemorrhage associated disorders. These diverse applications place high demand on stocks with around 2.2 million units of blood component used in the UK each year [2]. Stocks are currently maintained through altruistic donation of anonymous individuals who have corresponding blood type to the recipient or who have the universal blood donor type, O negative.
The current system is normally efficient and sustainable yet there are several uncertainties over whether service can be maintained indefinitely since numerous external factors have a direct negative impact on its operation. Stringent eligibility criteria, short shelf life, proportional inconsistencies of blood groups in the population and interruptions of normal service by holiday periods and state events result in shortened and/or erratic supply [2]. Pressure will only increase with the population's life expectancy on an already laboured system.
Furthermore, despite rigorous donor health checks and sensitive serological and nucleic acid screening for transfusion transmitted infections (TTIs) there are residual risks with blood transfusion. Transmission of highly infectious, occasionally fatal viruses HIV and Hepatitis B and C still occur, particularly in developing countries where infection rates are higher and screening is not as widely accessible [3]. Novel TTIs continue to emerge and are readily spread by international travel and trade placing potential risk on the system for years to come [4].
There is then ample motivation for a replacement or supplement product for red blood cell donation which will ensure its safety and supply. The generation of manufactured red blood cells from stem cells is emerging as an attractive solution to these problems.

1.1 Stem cells for use in cellular therapies

Regenerative Medicine describes the process by which human cells, tissues or organs are replaced or regenerated in order to restore normal function. Cellular therapy, a sub category of regenerative medicine, is a form of medical or surgical treatment in which new cells are introduced to a tissue in order to treat or prevent a disease.
The discipline has undergone recent and rapid expansion due to unprecedented applications in tissue regeneration and repair through the use of stem cells. These cells have the ability to self-renew as well as differentiate into a number of different cell types [5].

1.2 Good manufacturing process

Good manufacturing process (GMP) is a regulatory system for ensuring that commercial therapeutic products are produced in accordance with quality standards and meet the guidelines set down by the relevant licensing and regulatory authorities. Products must be of consistently high quality, have a specific action and be appropriate for the intended use. This is crucial for cellular therapies whereby cells or their products are administered directly to a patient putting them at risk of immune rejection [6], teratoma [7], disease [8] and other undesirable responses. It is therefore imperative that the manufacture of cell therapy products is robust and reproducible so that the physiological response is predictable. It is also desirable that the manufacturing process be xeno-free to protect from cross-contamination [9] and that superfluous proteins and nucleic acids [10] be removed to prevent immune rejection and development of teratomas.

1.3 Benefits of red blood cell manufacture from stem cells

The manufacture of red blood cells from stem cells could potentially overcome the two main issues with the current donation system; safety and supply.

1.3.1 Safety

Red blood cells (erythrocytes) are among the simplest cells in the body since they lack a nucleus and other membrane-bound organelles [11]. Once matured they are devoid of genetic material and can therefore be sterilised using radiation to destroy remnant nucleic acids. Irradiation of donated red blood cells is possible (and is usually administered to high risk patients) but not practical since it significantly shortens the shelf life of an already limited product [12]. Red blood cells manufactured from stem cells could be routinely irradiated eradicating the development of TTIs and tumours, addressing the current safety issues with red blood cell transfusion.

1.3.2 Supply

Individuals with the O RhD negative (O-) blood group are called ‘universal donors’ since their erythrocytes lack detectable antigens and their blood can be given to any patient, regardless of blood type. Presently 4% of the eligible UK population donates amongst which there is a mixed distribution of blood groups [13]. As can be seen from Table 1.1 all donated blood is distributed leading to consistently low stock levels. Consequently, this leaves the system vulnerable to shortages, particularly for rare blood types.

The advantage of using erythrocytes manufactured from stem cells is that cells can be produced to meet demand, entirely of the O- universal blood type. The cells produced would also be a population of entirely ‘new’ cells, so that the shelf life (currently 31 days) would be increased significantly.

Table 3.1 Distributions of blood groups amongst UK donors as of March 2016 (https://www.blood.co.uk/why-give-blood/the-need-for-blood/blood-groups/ accessed June 2016). It is imperative sufficient quantities are collected to meet hospital and patient demand

ABO Blood Group	Donor population with this group	Blood issued to hospitals
A +	30%	30%
A -	8%	8%
B +	8%	8%
B -	2%	2%
O +	36%	36%
O -	12%	13%
AB +	3%	2%
AB -	1%	1%

1.4 Competitor products

There have been several outlier replacement products such as perfluorocarbons, synthetic haemoglobins and erythropoietic stimulating hormones which have not met safety standards owing mainly to problems with biocompatibility [2]. The advantage of manufactured red blood cells is that they lack Major Histocompatibility Complexes (MHC) and (assuming the correct blood type) there is no risk of immune rejection [6]. Since the manufactured red blood cells would be recognised as 'self' they would be naturally broken down at the end of their 120 day life cycle.

1.5 Types of stem cell

It is possible to derive red blood cells from any of the three main subcategories of human stem cells; embryonic (ES), induced pluripotent (iPS) and adult (AS) stem cells. Due to differences in source/microenvironment and consequent changes to *in vitro* culture each type of stem cell has its own set of advantages and challenges as shall be assessed in the following sections. Some are from a research point of view only as shall be specified where appropriate.

1.5.1 Embryonic stem cells

Embryonic stem cells (ES cells) begin with the zygote. Symmetric cell division ensues yielding identical daughter cells until the 8 cell stage of the morula (Figure 1.1). At this point all cells are totipotent with the ability to give rise to any cell necessary for foetal development.

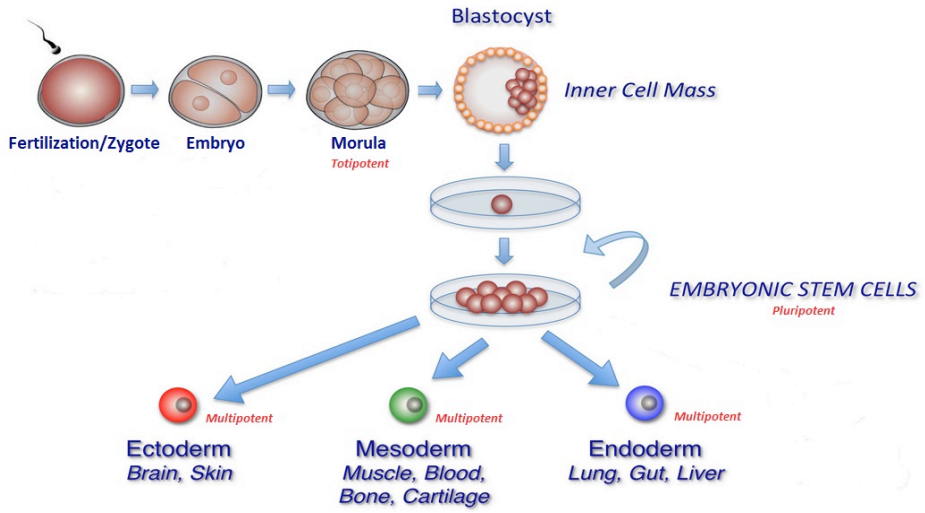

Figure 1.1; Stepwise differentiation and potency of human embryonic stem cells

The first phase of differentiation begins with the formation of the blastocyst. The outer cells of the morula form the outer trophoblast layer which will eventually become the placenta and other extraembryonic tissues. The inner cells give rise to the inner cell mass (ICM) from which pluripotent ES cells are derived; cells which are able to differentiate into any of the three germ layers (mesoderm, endoderm, and ectoderm) which comprise the embryo proper [14]. These cells can be manipulated *in vitro* to transit down a desired lineage yielding cells of a particular type, tissue or organ.

1.5.1.1 Advantages:

(a) They are immortal; the first successful culture of a pluripotent and permanent human ES line was completed by Thomson et al in 1998 and still exists to this day [15]. Hence a desired distinct cell type can be cryopreserved and banked indefinitely until needed, eliminating the inconvenience and cost to re-source.

(b) They are pluripotent; ES cells are highly susceptible to manipulation *in vitro* since they respond to a wide variety of biochemical cues (Research only)[15].
(c) They express low levels of MHC complexes; ES cells have a reduced risk of graft rejection which comprises a major issue for allogenic therapies [14].

1.5.1.2 Disadvantages:

(a) Haematopoietic differentiation of ES cells is a 31 day process requiring germ-line specification, lineage commitment and maturation though the erythroid series. This requires many expensive growth factors such as cytokines and increases the risk of error/variation between cultures.
(b) Blood type specification is not apparent in early stage ES cells and so an additional processing step would be required prior to differentiation to identify suitable donors (research only)[16].
(c) The use of ES cells is controversial.

1.5.2 Induced pluripotent stem cells

Induced pluripotent stem cells (iPS) are adult somatic cells which have been reprogrammed to behave like pluripotent ES cells. In 2006, Yamanaka generated the first induced pluripotent cell lines by re-programming mouse fibroblasts using four transcription factors (Oct3/4, Sox2, Klf4, c-Myc, now known as 'Yamanaka factors' [17]. Transcription factors control which genes are expressed and thus addition of these four particular factors induces artificial transcription of embryonic genes, yielding pluripotent stem cells.
Using this technology cells that are terminally differentiated can be extracted from a donor of desired blood type (O-) and induced to artificial embryonic pluripotency before directed differentiation to a desired cell type i.e. haematopoietic. Hence although iPS maintenance and differentiation is identical to ES cells there are some added benefits to their use:

1.5.2.1 Advantages:

(a) Immortality
(b) Pluripotency
(c) Low expression of MHC complexes
(d) Can be extracted from a donor of desired blood type
(e) Their use is not controversial

1.5.2.2 Disadvantages:

(a) Haematopoietic differentiation of iPS cells is a 31 day process

1.5.3 Adult Stem Cells

Adult stem cells (AS) are lineage committed multipotent stem cells which are able to develop into more than one cell type within a restricted lineage. They reside in stem cell niches in several locales in the adult or juvenile body and continually repair/ replenish organs and tissues, particularly those with a high turn-over (such as blood, skin and intestine) or which have been subject to injury [19].

1.5.3.1 Advantages:

a) They are multipotent; although multipotency could be seen as a drawback from a research point of view, a stem cell which has already undergone germ layer specification and haematopoietic lineage commitment would be beneficial to a bioprocess; by eliminating these early development steps the differentiation period is shortened by 10 days reducing reagent and labour costs.
b) They are adult; mature cells express detectable identification markers (for example AB+ blood group) so that a potential donor can be carefully selected to reduce immune rejection.
c) The use of AS cells is not controversial

1.5.3.2 Disadvantages:

a) They are finite; although AS cells harbour the possibility of becoming immortal through genetic manipulation, in their natural state they are finite. Therefore their use requires continual resourcing which can be costly and invasive. Immortalisation of AS cells requires additional, often time consuming and costly, research and development.
b) They are multipotent; AS cells respond to a smaller pool of biochemical cues so that they are not so susceptible to manipulation *in vitro*.

1.5.4 Cord blood stem cells

CD34+ (haematopoietic stem cell) cord blood stem cells are isolated from umbilical cord or placental tissues using immunomagnetic separation. Essentially CBS cells are adult stem cells despite their neonatal origin; they have the same aforementioned attributes of AS cells although they exhibit some slight morphological and phenotypical differences to adult haematopoietic stem cells [19]. Little research has been completed on these differences and one of the aims of this research was to ensure that the erythroid cells generated were equal to their adult counterparts and hence safe for use in blood transfusion.

1.6 Haematopoietic differentiation

Traditionally propagation of ES cells required culture on ‘feeder cells’; mouse or human embryonic fibroblasts (MEFs) which secrete diffusible cellular metabolites to developing stem cells [9]. The feeder cells were thought to be critical to the growth process since some metabolites have short half-lives and need to be secreted continuously throughout the culture process [20]. However feeder cells do not have a predictable or reproducible secretome which undermines any scientific experimental model, particularly in industry where even small differences in culture conditions can have a huge impact on the end product. Furthermore, the use of xenogeneic or allogeneic sources of feeder cells supports cross-contamination of pathogens and cell by-products which could be detrimental to cells and render the end product unusable.

Similarly foetal bovine serum (FBS) is often used to supplement cell culture growth medium and raises concerns regarding cross-contamination and incorporation of non-human constituents into the cell environment. Consequently a serum-free feeder-free culture system is desirable for the haematopoietic differentiation of ES (and other stem) cells. Each of the haematopoietic differentiation protocols used in this research (described step-wise in Chapter 2) for ES/iPS and CBS cells were developed by Mountford lab, University of Glasgow [unpublished data, personal communication].

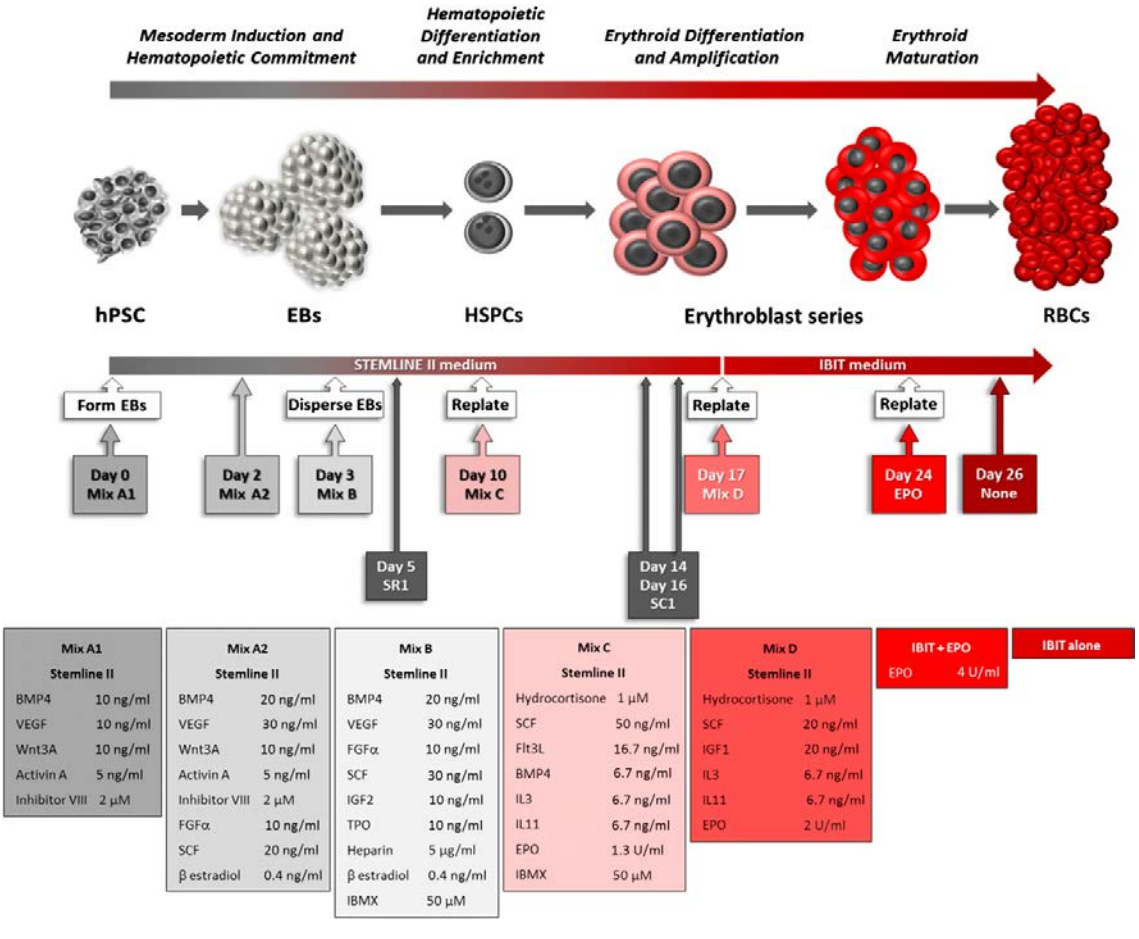

Figure 1.2; Diagram representing the serum-free feeder-free erythroid differentiation of ES/iPS cells as orchestrated by the addition of cytokines and hormones [21]. For CBS cells the process begins at day 10 since cells are already lineage committed.

1.6.1 ES and iPS cells

The 31 day haematopoietic differentiation process is initiated with ES/iPS cells grown to near confluence in 6 well plates. The cells are cultured in several different media/growth factor mixes which direct germ layer specification to mesodermal cells and then lineage commitment to haematopoietic progenitor cells. The growth factors listed in table 1.2 have been found to reside in haematopoietic stem cell niches and where possible their functions are described although some of their mechanisms remain elusive. Growth factors is the all-encompassing term for substances necessary for the growth and development of cells. Cytokines are small signalling proteins released by cells that have specific autocrine or paracrine effects on cellular behaviours. Hormones control and regulate the development of cells; their action *en vivo* is primarily endocrine [21].

Table 1.2; Function of growth factors used for haematopoietic differentiation

Name	**Function**
Bone Morphogenetic Protein 4 (BMP4)	Transforming cytokine which induces the expression of primitive streak genes which direct development to mesodermal and endodermal lineages [22]
Vascular Endothelial Growth Factor (VEGF)	Cytokine which generates robust Colony Forming Units (CFU). Although BMP4 is sufficient to initiate haematopoietic gene expression addition of VEGF generates 3-4 times more CFU [23]
Wnt 3A	Cytokine which triggers canonical Wnt signalling; as intracellular beta-catenin levels rise, beta-catenin binds to TCF/LEF transcription factors leading to expression of Wnt target genes. Wnt genes have many functions in embryogenesis but here they promote self-renewal of haematopoietic stem cells [24]
Activin A	Cytokine which inhibits posterior hox genes to suppress haematopoiesis momentarily during mesoderm

	specification. This is to prevent primitive haematopoiesis and enable the definitive [25] Activin A also promotes mesoderm specification and contributes to the expansion of cells already committed to being haematopoietic [26]
GS3K Inhibitor VIII	Cytokine which inhibits Glycogen Synthase Kinase 3 Beta (GSK3b) to enhance Wnt3a activity and improve quality of cells post day 24 of the protocol [21]
Fibroblast Growth Factor (FGFα)	Cytokine which induces differentiation toward mesoderm and primes for the haemato-endothelial compartment. Increases proliferation more than two-fold in combination with SCF [21]
Stem Cell Factor (SCF)	Cytokine which binds to and activates the receptor tyrosine kinase c-kit which leads to its autophosphorylation and signal transduction. It is necessary for normal haematopoiesis and proliferation, increasing cell yield more than two-fold [27]
β-Estradiol	Hormone which induces differentiation toward mesoderm and primes for the haemato-endothelial compartment [28]
Insulin-like Growth Factor 1&2	Mitogenic hormones which stimulate proliferation and cell survival [29]
Thrombopoietin (TPO)	Glycoprotein hormone which regulates the expansion and maturation of megakaryocytes. It also promotes self-renewal of haematopoietic stem cells to establish long-term culture initiating cells [30]
Heparin	Anticoagulant which is used to maintain proliferation and prevent terminal differentiation [31]
3-Isobutyl-1-methylxanthine (IBMX)	Cytokine which inhibits cGMP phosphodiesterases elevating intracellular cAMP levels to activate PKA. This results in reduced proliferation but increased differentiation [32]
FMS-like tyrosine kinase 3	Cytokine which binds to tyrosine kinase receptor c-kit

ligand (Flt3L)	recruiting colony stimulating factors and interleukins to induce growth and differentiation [33]
Interleukins 3 and 11 (IL3 and IL11)	Interleukins are cytokines which function in immune system signalling. They also support proliferation and differentiation of haematopoietic cells IL3 promotes proliferation of haematopoietic progenitor cells and stimulates differentiation of multipotent haematopoietic stem cells into myeloid progenitor cells [34] IL11 is key regulator of several stages in haematopoiesis especially initiating maturation of megakaryocytes [35,36]
Erythropoietin (EPO)	Hormone which regulates proliferation and differentiation of erythroid cells. Upon binding with its receptor tyrosine phosphorylation of JAK2 is induced which activates an autophosphorylation leading to transcription and mitogenesis [37]
Hydrocortisone	Hormone released during the stress response. Increases glucose production by gluconeogenesis. Immunosuppressant and antidiuretic hormone. Used to stimulate erythroid colony growth and may play a role in regulation of erythropoiesis [38]
Insulin	Hormone which regulates the cellular uptake, utilization, and storage of glucose, amino acids, and fatty acids and inhibits the breakdown of glycogen, protein, and fat [39]

1.6.2 CBS cells

CD34 positive CBS cells are grown in suspension culture. The CBS cell haematopoietic differentiation requires fewer signalling molecules (as described in Chapter 2) than that required for ES/iPS differentiation since the cells are already committed to a haematopoietic lineage.

1.7 Scale-up to bioreactor culture

At commencement of this research red blood cells were being successfully differentiated from ES cells in 6-well plates at Glasgow University (Figure 1.3) A typical red blood cell concentrate or unit of blood contains around 2.5 $x10^{12}$ erythrocytes [2].

Day	Fold Expansion
0-3	2-4
3-10	20-50
10-17	60-100
17-24	2-8
24-31	0.5-2
TOTAL	**320000**

Figure 1.3; Red blood cells fabricated from ES cells at Mountford Lab, Glasgow 03/12/12 day 21 of protocol [personal communication]

ES cells were routinely seeded at 1 $x10^{6}$ cells/well so that the total maximum fold-expansion would result in 1.92 $x10^{12}$ erythrocytes, not far off one unit. However since the proliferating cells must be transferred to new plates this culture method is unrealistic in terms of space, labour and quality control. In order to transform the haematopoietic differentiation protocol into a commercially and clinically viable process it was necessary to transfer it to a vessel more amenable to scale-up.

A 5L (recommended working volume 1.25-3.75L) Celligen BLU Disposable Unit Bioreactor (New Brunswick) was purchased for the project with a view to producing one unit of blood (Figure 1.4).

Figure 1.4; Celligen BLU bioreactor, Eppendorf, http://newbrunswick.eppendorf.com/en/products/bioreactors/ 25/04/13

Historically stirred tank bioreactors were designed for use with bacterial cells which are smaller and inherently more robust. The Celligen BLU bioreactor was designed for use with mammalian cells and a trial with HL60 cells at the beginning of the project successfully supported 3.4 $x10^6$ cells/mL or 1.275 $x10^{10}$ cells per 3.75 L culture (unpublished).

Stem cells are unique in their *en vivo* microenvironments and are prone to spontaneous differentiation in extraneous conditions. Bioreactors have instrumentation which allows the user to harmonise conditions inside the vessel with specific requirements of the cells to optimise cell growth, proliferation and ultimately differentiation. Although mammalian cell cultures are habitually grown at 37°C, pH 7, 21% oxygen and 5% carbon dioxide [40], these parameters are unknown and untested for haematopoietic stem cells, warranting further investigation.

1.8 Considerations for bioreactor culture

1.8.1 Oxygen and stem cells

In order to sustain lifelong cell regeneration, *en vivo* stem cells must be conserved in an environment free from endogenous and exogenous stresses which cause DNA damage. Hypoxia is one of the mechanisms by which stem cell niches realise this through reduced exposure to reactive oxygen species which induce an oxidative stress response leading to dysfunction [41].

Embryonic [42] and induced pluripotent [43] stem cells which are cultured under hypoxic conditions have been shown to upregulate growth factors which maintain the pluripotent state to promote self-renewal. Conversely hypoxic culture conditions have been shown to induce differentiation and proliferation in several types of multipotent (adult) stem cells including neural[44], haematopoietic[45] and mesenchymal[46].

These changes are bought about by upregulation of Hypoxia Inducible Factor (HIF-1-α), a transcriptional regulator for which expression is upregulated at low oxygen tensions [43] and induces different responses in stem cells dependent on their level of potency/development.

Since mesenchymal and haematopoietic stem cell niches have 2-8% and 1-6% oxygen concentrations respectively [47] and given that haematopoietic stem cells pass through both these phases during their step-wise development, oxygen intensity needs to be investigated and carefully controlled at each stage in order to drive proliferation and differentiation of desired cell types.

1.8.2 Oxygen and red blood cells

Table 1.3; Rate of Oxygen Consumption of Various Types of Cells in Culture [48]

Cell Type	Rate of Oxygen Consumption (amol cell-1 s-1)
Red blood cell (Human)	4×10^{-5}
Red blood cell (Rabbit)	2×10^{-2}
HL60 with knock out mitochondria	4.7
HL60	11.5
Murine macrophages (J774A.1)	31
Mouse embryonic fibroblasts (MEF)	60
Baby Hamster Kidney (BHK)	83
Chinese hamster ovary cells(CHO)	86

The oxygen requirement of erythrocytes is markedly low in comparison with other cell types (See table 1.3) wherein the vast majority of energy is generated from the Citric Acid Cycle, which takes place aerobically in mitochondria (Figure 1.5).

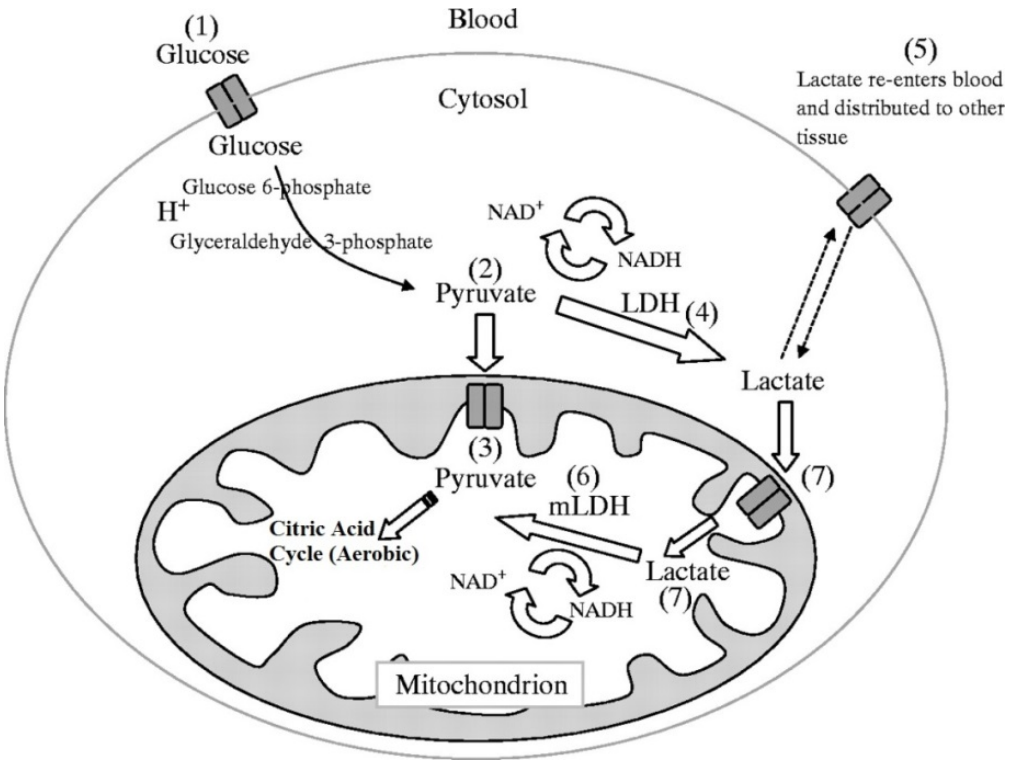

Figure 1.5; Fate of glucose entering a cell; cells containing mitochondria harness pyruvate produced by glycolysis to generate energy through the aerobic citric acid cycle. Cells which lack mitochondria anaerobically convert pyruvate to lactate via LDH [49]

Mature red blood cells lack mitochondria (and other membrane bound organelles) relying almost entirely on anaerobic glycolysis for ATP production. The pyruvate produced by glycolysis is harnessed by lactate dehydrogenase which catalyses its conversion into lactate. Effectively around 87.5% of the glucose entering an erythrocyte is converted to lactate [50].

ES cells do have mitochondria but their immaturity and paucity [51] mean that they similarly rely mainly on glycolysis for energy production. Theoretically speaking there should be a metabolic shift from glycolysis toward aerobic respiration during haematopoietic differentiation consistent with mitochondrial maturation. Since mature red blood cells lack mitochondria their eventual omission should mark another metabolic conversion from aerobic respiration to glycolysis. Owing to this there should be a distinctive optimum oxygen concentration for each stage of development/differentiation.

Static cell cultures are generally carried out at ambient (21%) oxygen however this can cause problems when moving into a stirred tank mammalian cell culture. Sparging is required in order to adequately oxygenate the column of media inside the vessel but this is highly detrimental to cells (Figure 1.6 [52]).

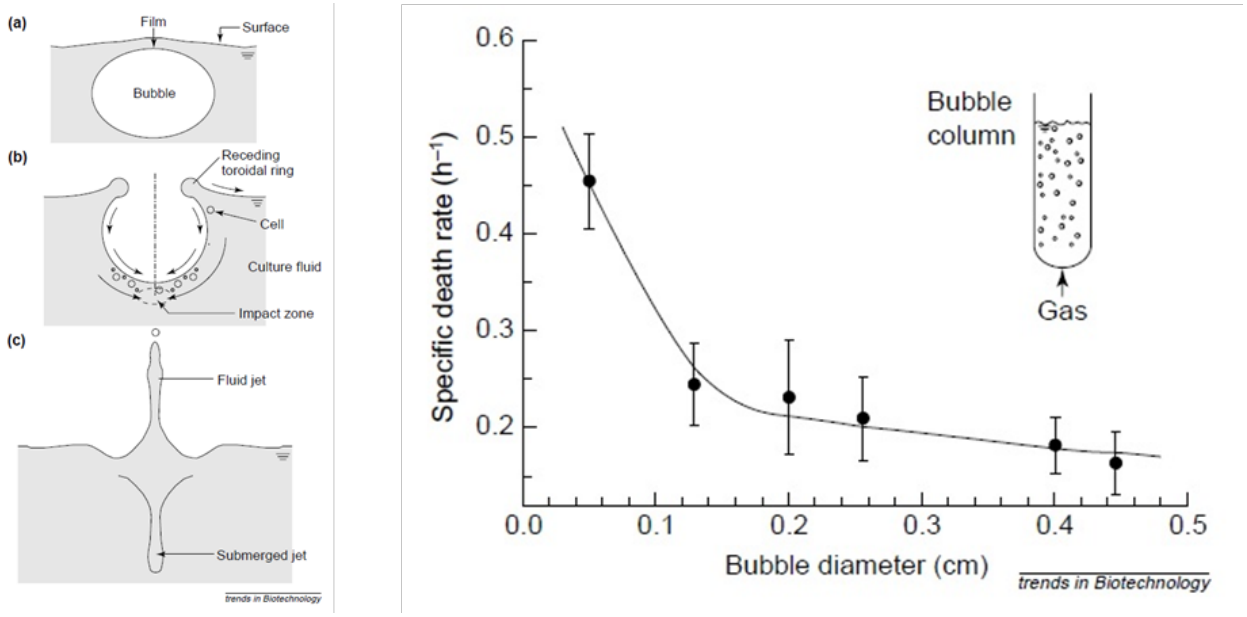

Figure 1.6; Images extracted from Chisti, 2000 [52]. Cells which attach to bubbles are destroyed when the bubble disengages with the culture surface creating a fluid and submerged jet with a higher energy dissipation than mammalian cells can withstand. Smaller bubbles have higher energy dissipation resulting in increased death rate

Taking all of these factors into consideration it was hypothesized that lowering the oxygen concentration of the differentiation culture would act as a double-edged sword by (a) increasing proliferation by hypoxia induced erythropoiesis and/or reduced reactive oxygen species and (b) preventing cell death by bubble damage.

1.8.3 Oxygen and agitation

Bubbles with smaller diameters reach greater velocities and therefore have higher energy dissipation, consequently leading to elevated cell death. These smaller bubbles are created by fragmentation during mechanical agitation [52].
Agitation or mixing in stirred tank bioreactors is used to ensure homogenous distribution of nutrients and other soluble components such as waste products, suspended cells and dissolved gases. In this respect a high agitation rate would be preferential since it would ensure proper mixing. However there is an upper limit on agitation rate since higher speeds cause bubble fragmentation which leads to cell death. In order to calculate the most suitable stirrer speed the Reynolds number equation is used;

$$Re_i = \frac{N_i D_i^2 p}{\mu}$$

in which N_i is stirrer speed, D_i is impellor diameter, p is fluid density, μ is fluid viscosity. The turbulent regime in stirred tank bioreactors is fully developed when $Re^i > 10^4$. Solving this equation should yield a stirrer speed at the boundary of laminar and turbulent flow which achieves proper mixing with the least amount of bubble fragmentation [40].
Gassed liquids have a lower density and therefore require lower stirrer speeds than nonaerated fluids. The stirrer speed calculated by the Reynolds equation can therefore be reduced by up to 20% for upward-pumping pitched-blade turbines (as used in the Celligen BLU Bioreactor)[40]. This calculation of stirrer speed is a crude method and requires some further experimentation to find the optimum speed. It was the intention of this research to find a more suitable approach to this estimate which would not require extensive reagent usage.

1.8.4 Agitation rate and shear stress

Shear stress is a tangential force applied to a surface; in bioreactors it is the tangential flow of culture media against the surface of cells. Agitation in stirred tank bioreactors causes a residual shear stress inside the vessel which does not ordinarily cause cell death (without sparging) since it generally remains lower than the cell's shear threshold. For example an agitation rate of up to 100rpm in a Rushton turbine bioreactor results in a shear stress of approximately 0.4 N m^{-2} which lies within the optimum shear range of most cell types (0.2-3 N m^{-2}) [53].

Conversely shear stresses within this range can also cause stem cells to differentiate. For example mechanical shear stresses of 1.5 N m^{-2} have been shown to induce mesenchymal stem cells to differentiate into osteoblasts [54] and promote angiogenesis in vascular endothelium [55]. Since the optimum shear and its effect on differentiation is unknown for haematopoietic stem cells, it was the aim of this research to find the optimum shear which would support differentiation of haematopoietic stem cells to erythrocytes whilst promoting cell proliferation.

1.8.5 pH and Stem Cells

Traditionally animal cells are cultured in incubators which maintain CO_2 at 5%, which in turn maintains the pH of the growth medium at 7.4 [40]. However cell yield and development may be optimised by adjusting the pH.

For example one study found that the optimum pH for murine embryoid bodies was 7.3, not only in cell yield but in producing the correct cell types. A pH which deviated from this optimum by only 0.15 resulted in suboptimal cultures which did not comprise cells of all 3 germ layers [56][57]. Hence finding the correct pH prior to differentiation is paramount to ensure the correct cell types are present.

Furthermore, the optimum pH range for differentiating human erythroid cells was found to be between 7.5 and 7.6 which not only induced higher production of haemoglobin in erythroid cells but also may have acted as a trigger for differentiation [58]

Since little research has been completed in this field effects of carbon dioxide and pH on stem cell culture and differentiation need to be examined and optimised for each stage of development.

During this research the intention was to investigate the effects of oxygen, carbon dioxide/pH and shear stress on differentiating haematopoietic stem cells. Due to time constraints alteration of CO2/pH levels and any corresponding effects were not assessed and these parameters will need to be investigated in the future.

1.8.6 Red Blood Cells and Platelet Aggregation

En vivo platelet aggregation occurs only when subendothelial collagen is exposed by blood vessel damage [59]. This coupled with Von Willebrand factor, which is released at the site of injury, recruits platelets to the exposed site. Upon this interaction integrin receptors on platelet walls are activated and bind to the collagen. Once bound the platelet/s release adenosine triphosphate (ADP) causing a procoagulant conformational change which aids further binding and recruitment of platelets to form aggregates [59]. Hence red blood cells are not ordinarily involved in platelet aggregation but they do contain ADP which is released following membrane damage to induce the procoagulant shape change [59].
To date there are no known mechanisms by which red blood cells are able to repair membrane damage since they lack a nucleus. However this seems counter-intuitive since the heme and haemoglobin released by such damage could cause acute kidney injury [60].

1.9 Ultra-scale down – Microfluidics

Although the aim of this research was to scale-up the haematopoietic differentiation protocol to a 5L bioreactor the cost of reagents and the unknown effects of the physical bioreactor environment render it an expensive and high risk operation. An ultra-scale down method was proposed by which the optimum parameter conditions could be tested prior to use of the Celligen BLU Bioreactor.

Human cells and capillaries are generally in the range 5-30 μm which renders microfluidics an appealing mode of cell biology study from a practical point of view; more physiologic cell volume to extracellular fluid ratios (usually >1) are attainable which are more representative of en vivo conditions and hence yield more realistic results [61].
Micro-scaling of physical forces is also advantageous. Although the laws of physics remain the same as in a macroscopic system, frictional forces become predominant over inertial forces leading to formation of laminar flows. Particles in laminar regimes flow parallel to one another forming streamlines as opposed to turbulent flow in macroscale systems (Figure 1.7) [40].

This is highly advantageous since flows in microfluidic devices can be modelled and tightly controlled [62] particularly in reference to stem cells and their differentiating counterparts which are sensitive to even the slightest fluctuations in their physical environment [41-45]. Furthermore the laminar perfusion system can be used to implement biosensors before and after the culture chamber so that utilization of molecules of interest can be accurately monitored throughout the culture period.
The small scale microfluidic system can be subjected to a spectrum of conditions and easily integrated into a monitoring system such as microscopic imaging [62]. It was the intention of this research to use microfluidic devices in conjunction with fluorescent biosensors for in-situ imaging and quantification of cellular metabolites.

Crucially low reagent usage and reusable devices can decrease experimentation costs. Although miniature (for example Ambr, TAP Biosytems) bioreactors are available these are expensive, the reagent usage is much higher, the environment is not so

carefully modelled/defined and they cannot easily be used in conjunction with biosensors [63].

The estimated cost to run a haematopoietic differentiation culture in the Celligen BLU Bioreactor purchased for the use on the project is >£5000. Hence an ultra-scale down to microfluidic proportions was favourable for the initial stages of this research until the suitable physical environment of the differentiating culture is known.

1.10 Microfabrication techniques

1.10.1 Polydimethylsiloxane devices using soft-lithography

Polydimethylsiloxane (PDMS) is the most common material used for the fabrication of microfluidic devices since it is inexpensive, non-cytotoxic, autoclavable and gas permeable to allow for cell respiration. Devices are usually fabricated using soft-lithography whereby a mould is prior-made using photolithography (Figure 1.7a-c) and then the PDMS is applied and cured to obtain the device (d-f)[64].

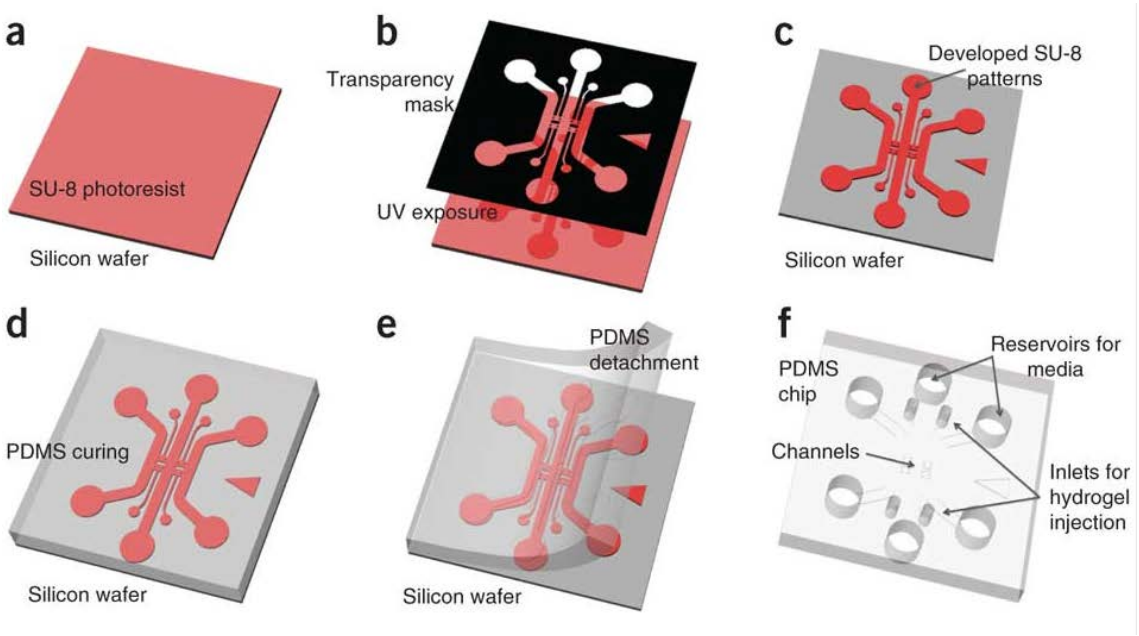

Figure 1.8 [64]; Steps a-c show the process for photolithography, steps d-f show soft-lithography. (a) SU-8 photoresist is spin-coated onto a silicon wafer (b) a transparency or 'photoresist' mask is aligned and UV light applied (c) the exposed regions are polymerised by UV light (negative photoresist) and following submersion in developing solution the unexposed areas are dissolved (d) PDMS is poured onto the SU-8/silicon mould (e) The PDMS is cured and peeled away from the mould (f) the PDMS device is punched with inlets, outlets and applied to a substrate

The disadvantage of this method is that the photolithography steps require specialist training, equipment and access to a clean room. Often fabrication of photolithography moulds is outsourced to a dedicated company which can be time-consuming, expensive and the geometries are finite. Since it was perceived that the microfluidic device would take some development this was not considered a viable option for the purposes of this research.

1.10.2 Silicone devices using photolithography

This fabrication method uses Ultraviolet (UV) light to transfer a geometric pattern from a photomask onto a light-sensitive chemical photoresist. The ‘photomask’ is the microchannel geometry patterned onto a chromium-lined glass or quartz plate. The photo-resist material (often SU-8) is a viscous fluid which is spin-coated onto a silicon wafer and then hardened by baking. The two are aligned and exposed to UV light. Depending on whether a negative or positive photoresist is used the exposed area is removed or preserved during submersion in development fluid. The device can then be bonded to a substrate of choice [65].
As mentioned previously, photolithography was not considered suitable for this project mainly due to restrictions on channel geometry.

1.10.3 Silicone devices using femtosecond laser writing

Microchannel geometries are etched into the interiors of silicon wafers (and other transparent materials) using a femtosecond laser. The etched material is then dissolved in a weak acid to expose the channel. The advantages of this method are that it creates a closed channel system less prone to leaks and contamination, has the potential for complex circuits and is cost effective [66]. Silicone was considered an ideal substrate for the device since it is clear, gas impermeable, non-cytotoxic and can be sterilised by autoclave [67]. Initially devices were fabricated using this method however it was considered too restrictive in terms of time, size and adaptability.

1.10.4 Poly (methyl methacrylate) devices using laser cutting

Laser cutting can be used to cut or etch into a number of different materials. Poly (methyl methacrylate) PMMA is particularly useful for microdevices since it is transparent, non-cytotoxic and inexpensive [68]. Usually the device is constructed of 3 or more layers (base, channels, and lid) which are then aligned and bonded permanently using heat/sealant or temporarily using gaskets [69]. This method was used primarily for the development of the device since it is inexpensive and fast allowing for several geometries to be trialled before deciding on a final design. The disadvantage of this method is that PMMA cannot be sterilized by autoclaving which leaves the system vulnerable to contaminations.

1.10.5 Other Polymers

Due to the high volume of laboratory and manufacturing work required for the project other methods of fabrication were not suitably researched at the time. Other autoclavable polymers (such as cyclic olefin copolymer (COC) and polycarbonate (PC)) were considered briefly, however hot embossing is required for fabrication [69]. Since no autoclavable polymers could be found which were amenable to the fabrication methods used/available it was felt that too much time would be required for development and they were dismissed in favour of other autoclavable materials such as glass and steel which could be machined on-site.

1.10.6 Glass and stainless steel devices by machining

Microfluidic devices can be fabricated using traditional machining methods such as milling, turning and drilling. As will be explained in Chapter 3 a second larger device was fabricated using this method. Machining was also used to add supplementary features to PMMA devices.

1.11 Microfluidic biosensors

1.11.1 Oxygen sensors

The classical oxygen sensor is the Clark electrode sensor which works by detecting current flow caused by reduction of oxygen [64]. The miniaturisation of these sensors to feature in microfluidic devices requires the use of microscale electrodes which consume oxygen intended for quantification. They also require electrical connection difficult to integrate on a microfluidic device and can render it susceptible to contamination. Optical oxygen sensors are a far less intrusive form of sensor, easily integrated into a microfluidic platform and do not consume oxygen. Most operate on the principle of reversible luminescence quenching by oxygen [65].

The most widely used sensors for luminescent quantification and detection of oxygen are Ruthenium based probes. Their high luminescence, photo stability, biocompatibility and ease of integration into microfluidic devices through polymer encapsulation make them ideal candidates for oxygen detection in microfluidic devices [65] ruthenium-tris(4,7-disphenyl-1, 10-phenanthroline) dichloride Ru(dpp) complex is dissolved in ethanol and mixed with PDMS polymer base and curing agent [70] the mixture can then be applied to a microfluidic sensing chip.

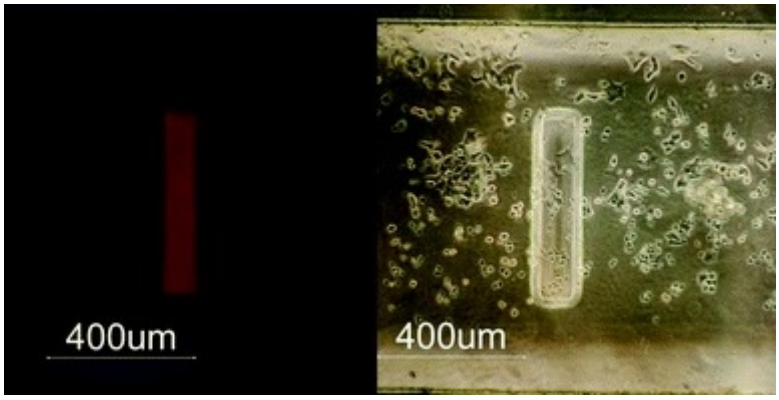

Figure 1.9; Fluorescence (left) and brightfield (right) images of oxygen ruthenium biosensor microtrenches [70]

The fluorescence of the ruthenium complex is efficiently and reversibly reduced by molecular oxygen due to dynamic quenching [64] The decrease in fluorescence intensity is then measurable using standard fluorescence microscopy setups and the Stern-Volmer Equation;

$$\frac{I}{I_0} = 1 + kp_{O_2}$$

Where *I* is the fluorescence in the presence of the quencher (oxygen), *Io* is the fluorescence in the absence of the quencher and k is the Stern-Volmer constant. Plots of

I/Io can then be used to determine changes in oxygen concentration [71]. Although these biosensors were developed commercially over the duration of this research, the novel application was in their implementation in a novel microfluidic device which could be used to measure in-situ oxygen consumption rates of differentiating stem cells.

1.11.2 Glucose sensors

It was hoped that the microfluidic sensing chip would also implement a glucose sensor since it is the chief source of energy for cells, particularly red blood cells. Optical glucose sensors work based on the activity of the carbohydrate-binding protein (lectin) Concanavalin A (ConA) which has high affinity for glycoconjugates [70]. Change in glucose concentration is detected through fluorescence resonance energy transfer (FRET) between fluorescein isothiocyanate (FITC)-bound dextran and ConA tetramethylrhodamine (TR) conjugate. In the absence of glucose FITC-bound dextran is bound to ConA-TR conjugate and FITC fluorescence is quenched through FRET. When glucose concentration increases it competes with the FITC-bound dextran displacing it and FITC fluorescence is detectable in proportion to glucose concentration [70]. These fluorescent probes can be similarly integrated into microfluidic chips by immobilisation with PDMS and quantified using fluorescence microscopy. Although a glucose

biosensor was successfully fabricated it was not compatible with sterilisation methods necessary for the microdevice and requires further development.

1.11.3 Carbon dioxide/pH and lactate sensors

It was the intention at the beginning of this research to develop optical CO_2 and lactate sensors however these were unsuccessful. Presently there are no such sensors which are amenable to integration into a microfluidic system.

1.12 Offline analysis

1.12.1 Flow cytometry

Flow cytometry is the simultaneous measurement of a range of characteristics of cells that pass in single file (in suspension) past one or more lasers. Each ‘event’ created as one cell passes the laser gives information about its size and complexity. Additionally the cells can be labelled with fluorescence to identify desirable traits. The advantage of using flow cytometry as an analysis method is that samples are quick and easy to prepare and data for an entire cellular population is collected quickly [72]. There are also a wide range of fluorescence probes available for rapid identification of a myriad of cellular features and processes as shall be discussed in the following sections.

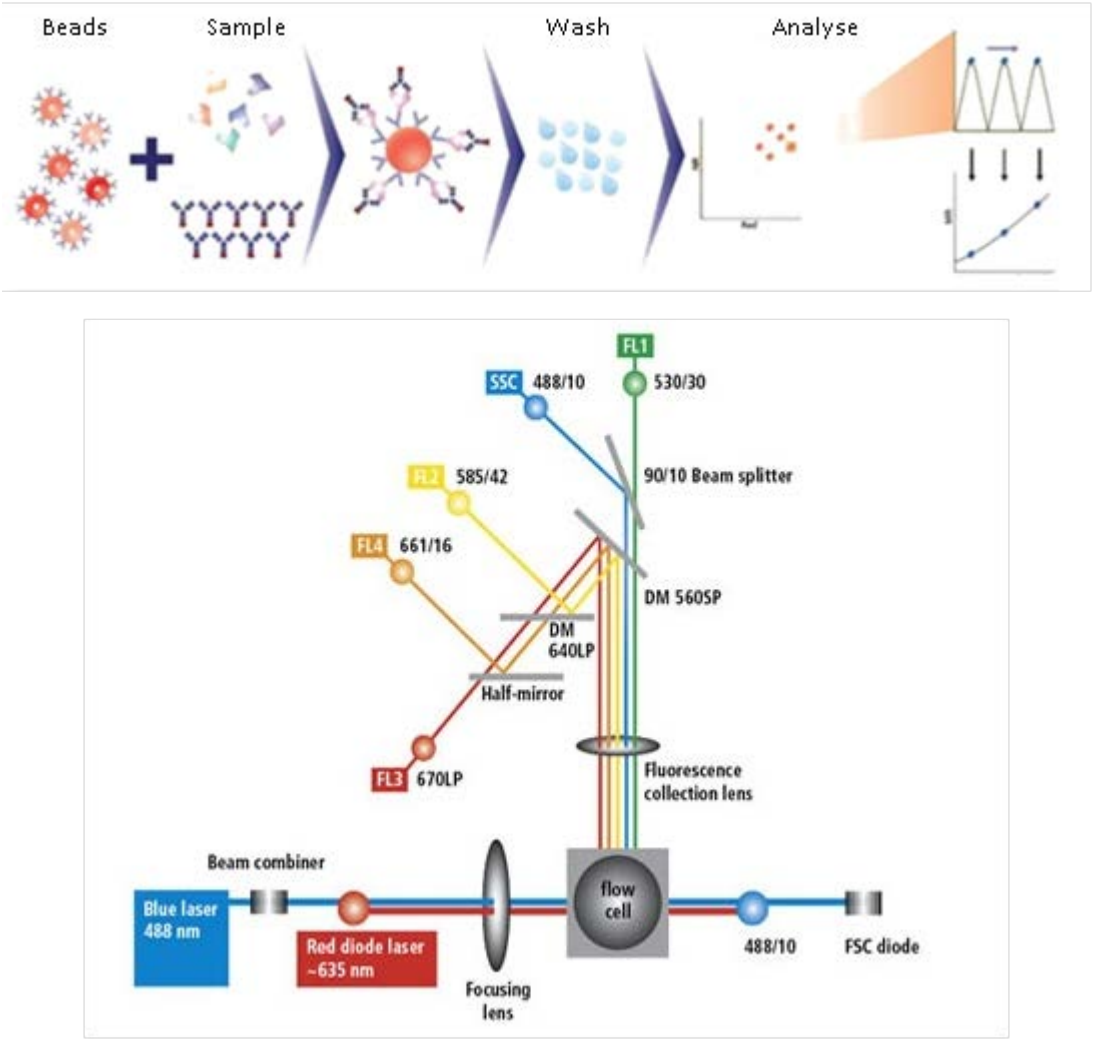

Figure 1.10; Process of flow cytometry. First cells are labelled with fluorescent probes then the cell suspension enters the flow cell and as each cell passes the lasers an 'event' is created which gives information about the fluorescent properties of the cell. Information on cell size and complexity are collected using transmitted light. Images taken from BD Biosciences 29/06/16

1.12.2 Cell surface markers

Cells have a unique combination of surface markers which are often transient in nature and can be used to identify key points in haematopoietic differentiation. A marker profile was developed at Mountford Laboratories, University of Glasgow [personal communication, unpublished data] and adopted at Heriot Watt University as part of the differentiation process transfer. Table 1.4 shows the markers and the cell types they are used to identify throughout the protocol. SSEA3, SSEA4 and TRA-160 markers are usually only found on ES cells and can therefore be used to gauge pluripotency of a population. Following differentiation they are downregulated.

Table 1.4; Cell Surface Markers and their identifying cell type

Name	**Cell Type**
SSEA3	Pluripotent
SSEA4	Pluripotent
TRA-160	Pluripotent
CD34	Haematopoietic stem cell
CD45	Leukocyte common antigen
CD31	Haemangioblast
CD43	Haemangioblast
CD235a	Haemangioblast and erythrocyte
CD71	Transferrin receptor on erythroid cells
CD36	Early erythroid
CD41a	Haemangioblast and platelets
CD42b	Platelets

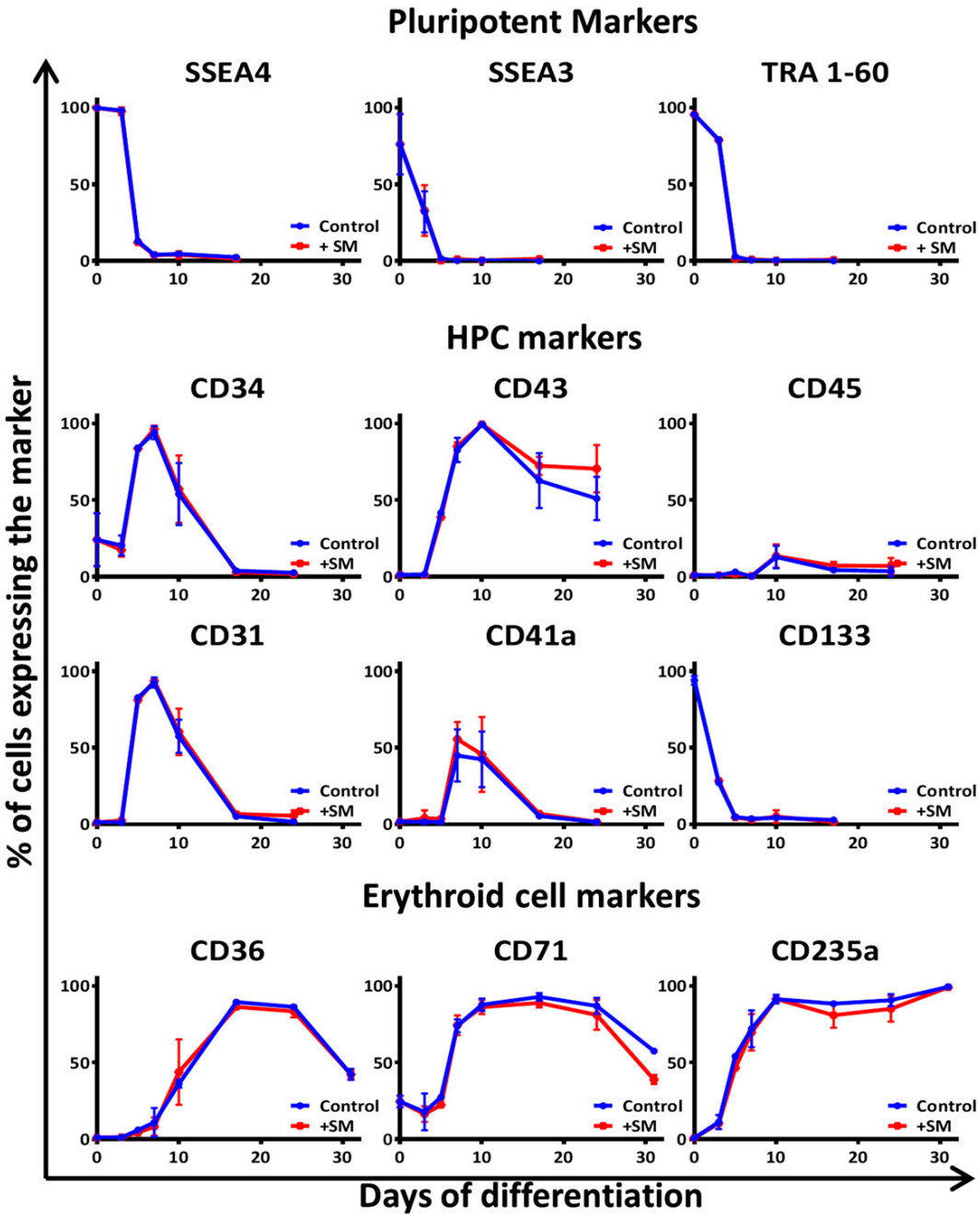

Figure 1.11; Analysis of CD markers on differentiating ES cells as obtained using flow cytometry at Mountford Laboratories University of Glasgow[21] Since CBS cells are already lineage committed their marker profile should start at day 10. The same panel was used for analysis at Heriot Watt although without CD133

Haemangioblastic markers CD34, CD31, CD43 and CD41a mark a transient stage of multipotency whereby cells have the potential to become haematopoietic or endothelial. Following this they undergo further lineage commitment to early erythroid as indicated by CD36 (although there is a short transient peak in leukocyte marker CD45). The late

erythroid markers CD235a and CD71 should then remain elevated if the differentiation is successful [21]. Although CD41a is known to be a haemangioblast marker it is more commonly known as a marker for platelets and megakaryocytes. In order to confirm platelet presence in parts of this research CD42b was added to the panel.

1.12.3 Apoptosis/Necrosis

There are two kinds of cell death. Apoptosis is a programmed, autonomous dismantling of the cell and its components whilst necrosis describes accidental cell death caused by unexpected trauma. During apoptosis phosphatidylserine (PS) is transferred from the inside of the plasma membrane to the outer leaflet due to phospholipid flipping [73]. Necrotic cells exhibit inflammation and loss of plasma integrity since this type of cell death is unplanned [74].

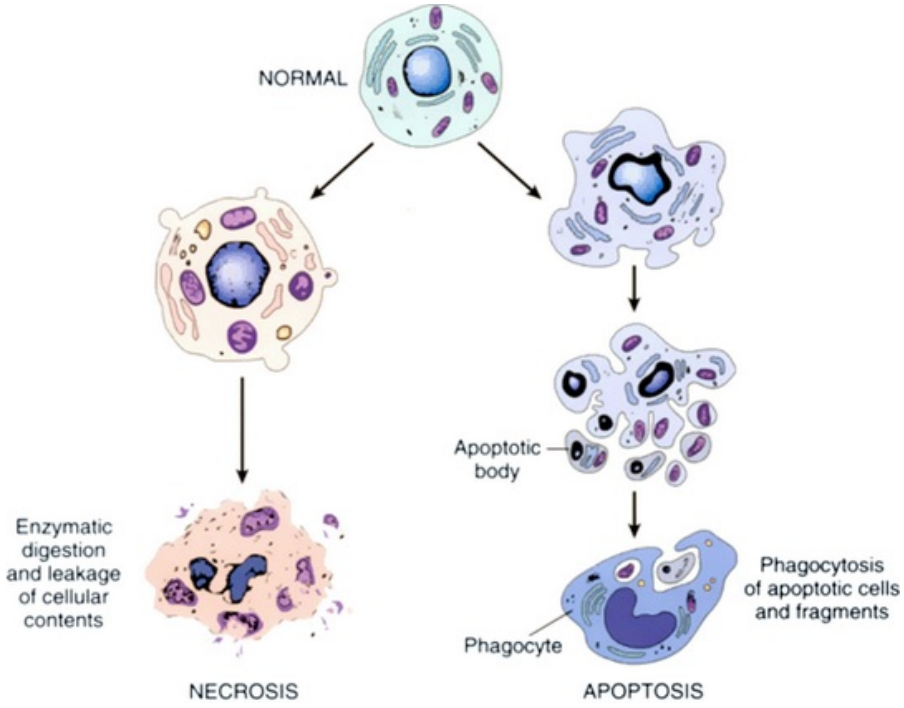

Figure 1.12; Morphologic differences observed for the two types of cell death, necrosis (left) and apoptosis (right) [http://medicinembbs.blogspot.co.uk/2011/03/programmed-cell-death-apoptosis.html June 2016]

Although morphologic differences should be visible under a microscope (Figure 1.10) an entire population can be more easily and accurately analysed by flow cytometry. Apoptosis is detected using a fluorescent probe specific to exposed PS on the cell surface whilst a membrane impermeable dye is used to detect necrosis as it diffuses through the degraded cell walls of necrotic cells (Abcam). These stained cell populations are then sampled for flow cytometry analysis.

1.12.4 Mitochondria

Mitochondria are double membraned organelles. The outer membrane has larger pores which allows for passage of ions and small molecules. The inner membrane surrounding the mitochondrial matrix is much more selective and is studded with proteins involved in electron transport and ATP synthesis as shown in Figure 1.11 [75].

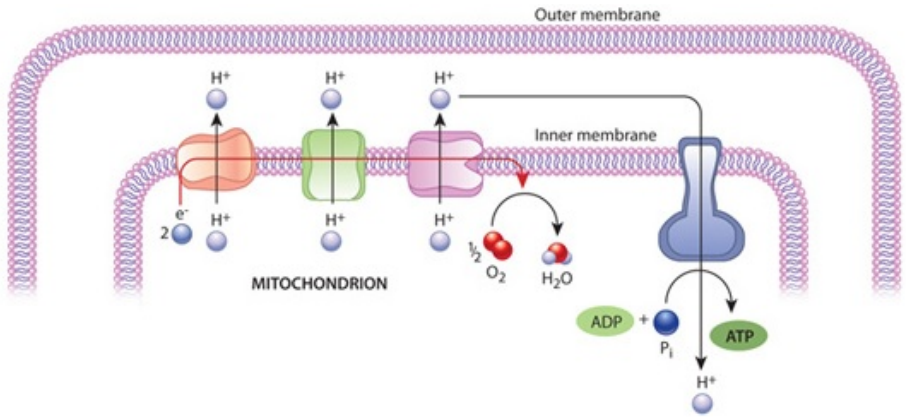

Figure 1.13; Mitochondrial double membrane which surrounds the mitochondrial matrix where the aerobic citric acid cycle takes place. http://www.nature.com/scitable/topicpage/mitochondria-14053590, 15/06/16

The intermembrane space has a high concentration of hydrogen ions which creates a proton gradient. Mitochondria can be stained with fluorescent probes which accumulate in live mitochondria via this potential gradient. Once stained the mitochondria can be analysed using flow cytometry or fluorescence microscopy.

1.12.5 Hypoxia inducible factor subunit 1-alpha

Hypoxia Inducible Factor 1 alpha (HIF-1-α) is a subunit of a master regulator of cellular responses to hypoxia, HIF-1 [76]. It induces the transcriptional activation of many genes involved in energy metabolism, erythropoiesis, apoptosis and several other responsive adaptations. Hif-1drives expression of glycolytic genes since glycolysis is necessary to produce energy when oxygen is low. It is also represses mitochondrial function by inducing pyruvate dehydrogenase kinase 1 (PDK1) which phosphorylates and inhibits pyruvate dehydrogenase from using pyruvate to fuel the mitochondrial TCA cycle [77]. Hence upregulation of HIF-1-a is considered to be a marker of cellular response to hypoxia. HIF-1-α can be labelled with fluorescent probes and assessed using techniques such as Western blot and immunochemistry.

1.12.6 Reactive oxygen species

Reactive Oxygen Species (ROS) are a natural by-product of cellular metabolism. It is believed that stem cell niches are hypoxic in order to protect from oxidative stress inflicted by ROS [77]. Cytoplasmic ROS can be labelled with fluorescent probes for visualisation by microscopy and/or flow cytometry.

Chapter 2 – Materials and Methods

2.1 Cell lines

2.1.1 RC9b human embryonic stem cells

The RC9 cell line was purchased from Roslin Cells and renamed RC9b to distinguish new banks which were created at Glasgow/Heriot Watt Universities. They are clinical grade pluripotent human embryonic stem cells (hESC) derived from B+ blastocysts. Since embryonic stem cells are in a state of self-renewal they are immortal and can be passaged continuously. However their pluripotency depreciates with each passage due to spontaneous differentiation and cultures were therefore routinely discarded at Passage 38 based on pluripotency markers and karyotype analysis.

2.1.2 SFC i55 human induced pluripotent stem cells

Human induced pluripotent stem cells (iPS) were produced from dermal fibroblast cell lines generated from donors with an O negative blood group. The fibroblasts were reprogrammed using Oct 4, Sox 2, c-Myc and Klf 4 transcription factors to produce pluripotent stem cells. The resultant cells were then screened for pluripotency markers (TRA1-60, OCT4, SSEA-4 and lack of expression of early differentiation marker SSEA-1), ability to differentiate into blood cells and single-nucleotide polymorphism (SNP) analysis/karyotyping to ensure cell line stability. The most reliable cell line produced was SFC i55 which was then expanded for further laboratory use. Since iPS cells mimic hESCs they were maintained and discarded in the same manner.

2.1.3 Human CD34+ Cord Blood Stem Cells

Primary human CD34+ cells are haematopoietic progenitors and were purchased from Stemcell Technologies Incorporated. The cells were isolated from umbilical cord blood using positive immunomagnetic separation from mothers who tested negative for HIV-

1, HIV-2 and Hepatitis B. Hepatitis C tests were completed at time of collection. Cord blood cells are finite and had to be continuously resourced.

2.2 Model cell lines

Haematopoietic differentiation of the aforementioned stem cells involves both adherent and suspension stages and their development is directed by the use of expensive cytokines/growth factors. Since it was anticipated this research would entail augmented reagent usage, two haemocytic model lines were selected for preliminary experimentation based upon robustness, cost efficiency and simplicity of culture/maintenance. They also share similar characteristics such as size, shape and elasticity.

2.2.1 Haemocytic suspension cells; HL60

HL60 leukocytes were first derived from the peripheral blood of a 36 year old female patient with acute promyelocytic leukaemia in 1977. They are haemocytic suspension cells which are supplemented with serum so that they do not require expensive growth factors and they are immortal which makes them an ideal model cell line for preliminary scale-up experiments.

2.2.2 Haemocytic adherent cells; J774

The J774 monocyte macrophage cell line was first isolated in 1968 from sarcoma cells of the murine reticulum. J774s are haemocytic adherent cells which serum supplemented so that they do not require expensive growth factors and are immortal, making them an ideal cell line for mimicking the adherent stages of haematopoietic stem cells. Both J774 and HL60 cell lines were purchased from Sigma Aldrich for use on this project.

2.3 Aseptic technique

Stem cells (and their model equivalents) must be cultured without the use of antibiotics and therefore a high standard of aseptic technique was applied to all applications. Cell cultures were carried out in a class II laminar hood which was designated exclusively for stem cell use and wiped down prior and post culture with Distel followed by 70% ethanol. All plastics and tools were pre-sterilised and sprayed with 70% ethanol prior to introduction to the hood. Many of the experiments carried out during this research took place in non-sterile environments. In these instances all equipment was routinely cleaned by sonication and sterilised by autoclave and/or UV radiation. Inoculation took place in a sterile hood and sterile connections made before the removal and integration into the experimental apparatus.

2.4 Cell culture protocols

2.4.1 Stem cell maintenance

Since cord blood cells are finite and continuously resourced maintenance was required for RC9b and SFC i55 cells only. First subculture post-defrost cells were split 1:3 with subsequent subcultures split 1:6. Cells were always subcultured again within 10 days of defrost to prevent spontaneous differentiation.

1) Coating 6 well plates:

Costar 3516 6 well plates were coated with 1mL of Stem Cell Technologies Vitronectin XF at a final concentration of 10µg/mL. Stock vitronectin (250 µg/mL) was removed from -80 °C freezer and defrosted to room temperature. In a polypropylene tube 40 µL of stock vitronectin was added to 960 µL Dulbecco's PBS (Ca^{2+}/Mg^{2+} free) for each well and mixed by pipetting. The diluted vitronectin was added 1mL per well and the plate sealed with Parafilm® to prevent evaporation. The plate was then shaken on a rocking platform at room temperature for >1 hour to ensure an even coating. Following this the excess vitronectin was aspirated to waste and each coated well washed with 2mL Dulbecco's PBS (Ca^{2+}/Mg^{2+} free).

2) Preparation of culture media:

The required volume of StemPro® Complete medium (ThermoFisher) was prepared according to Table 2.1 and pre-warmed to 37 °C

Table 4.1; StemPro® hESC SFM Complete Medium

	Final Conc	**For 15 mL**	**For 10 mL**	**For 5 mL**
DMEM/F12 + GlutaMAX (1X)	1X	13.56 mL	9.04 mL	4.52 mL
StemPro® hESC SFM growth supplement (50X)	1X	0.3 mL	0.2 mL	0.1 mL
BSA 25%	1.8%	1.08 mL	720 µL	360 µL
FGF-basic (20 µg/mL)	20 ng/mL	15 µL	10 µL	5 µL
2-mercaptoethanol (50 mM)	0.1 mM	30 µL	20 µL	10µL

3) Subculturing cells:

Cells to be subcultured had their media changed 1-2 h prior to passage using 3 mL of pre-warmed StemPro® Complete growth medium per well. A StemPro® EZPassage™ tool (ThermoFisher) was used to cut the stem cell monolayer three times top to bottom and three times left to right across the well. The 'squares' of cells were then collected using a 5 mL pipette, pipetting up and down over the centre of the well to ensure all cell squares were aspirated. The cell suspension was used to seed directly into prepared vitronectin coated plates e.g. for a 1:6 subculture 0.5 mL of the cell suspension was placed into each of the 6 wells. StemPro® Complete medium was added to each well to ensure a total volume of 2 mL/well. Plates were gently rotated by hand left to right and up /down to ensure the cells were evenly spread across the seeded wells. Plates were placed in an incubator at 37 °C 5% CO_2 and media changed daily until next passage/subculture.

2.4.2 Haematopoietic differentiation of RC9b/SFC i55

2.4.2.1 Day 0 cell counting

Wells of RC9b/SFC i55 which had grown to 80-85% confluent were used as starting material.

Prior to initiation of the protocol one well was sacrificed for cell counting. Cell culture media was aspirated to waste and the cell monolayer washed with Dulbecco's PBS (Ca^{2+}/Mg^{2+} free). 1mL TrypLE™ Select, a recombinant cell-dissociation enzyme, (ThermoFisher), was added to the well and the cells were incubated for 10 minutes at 37 °C. Following this, cells were removed from incubator and fully dissociated by pipetting up/down with a 5mL pipette. Once dissociated the cells were added to a 15mL centrifuge tube and washed with 14mL Dulbecco's PBS (Ca^{2+}/Mg^{2+} free). The cells were centrifuged at 1200rpm for 3 minutes and supernatant removed before resuspending in 1mL Dulbecco's PBS (Ca^{2+}/Mg^{2+} free). A cell sample was then counted on a haemocytometer using the trypan blue exclusion method.

2.4.2.2 Trypan blue exclusion method

The trypan blue exclusion method is based on the principle that viable cells have intact membranes which exclude specialized dyes including trypan blue. Only cells which are dead (with impaired membranes) are able to absorb the dye and are therefore easily distinguished from viable cells.

A small sample of cell suspension (usually 20µL) was diluted 1:1 with trypan blue in a microcentrifuge tube or bijou and mixed by pipetting up and down. Cells were then loaded into haemocytomer chambers and counted at x10 magnification using a Nikon microscope. In order to calculate cell density the number of cells counted was multiplied by the dilution factor and 10^4 to determine number of cells in 1mL. For example if 73 cells were counted in total then;

$$73 \times 2 \times 10^4 = 1.46 \times 10^6 \text{ cells/mL.}$$

Cells which were deep blue in colour were considered dead and excluded in the following equation to calculate cell viability;

$$\left(\frac{Total\ no.of\ cells - \ no.of\ blue\ cells}{Total\ no.of\ cells}\right) \times 100 = Cell\ viability$$

For example if 2 of the 73 cells were deep blue/dead then;

$$\left(\frac{73-2}{73}\right) x100 = Cells\ are\ 97.3\%\ viable$$

2.4.2.3 Differentiation

Following cell counting media was removed from remaining wells and aspirated to waste with care not to disturb the stem cell monolayers. The cells were washed in Dulbecco's PBS (Ca^{2+}/Mg^{2+} free) by adding 3mL to each well and leaving for 1 minute before aspirating to waste. 3mL/well Stemline® II medium (Sigma Aldrich) supplemented with cytokines and small molecules as shown in Table 2.2 (below) was added to each well. Using a StemPro® EZPassage tool cells were cut into rough squares by cutting three times top to bottom and three times left to right across the well. The cell 'squares' were then dissociated from wells by pipetting up/down with a 5mL pipette. Cells were pooled in a 15mL centrifuge tube before addition to a Costar Ultra-low Attachment 6 well plate at 1.5 x10^6 cells per well. Additional media/cytokine mix was added to a final volume of 3mL per well.

Table 2.2; Day 0 Cytokine mix

Factor	[Final]	[Stock]	1ml (1x)	3ml (1x)	6ml (1x)	12ml(1x)
BMP4	**10ng/mL**	50ng/µL	0.2µL	0.6µL	1.2µL	2.4µL
VEGF	**10ng/mL**	50ng/µL	0.2µL	0.6µL	1.2µL	2.4µL
Wnt3A	**10ng/mL**	10ng/µL	1.0µL	3.0µL	6.0µL	12µL
Activin A	**5ng/mL**	10ng/µL	0.5µL	1.5µL	3.0µL	6.0µL
Inhibitor VIII	**2µM**	2mM	1.0µL	3.0µL	6.0µL	12µL

2.4.2.4 Day 2

By day 2 the cells had formed embryoid bodies (three-dimensional aggregates of pluripotent stem cells) and were now tubular/rounded in shape rather than square. At this stage 0.5mL Stemline® II media was added per well with a x6 concentration of cytokines as shown in Table 2.3. This assumes a loss of 0.5mL media through evaporation to bring the final volume back to 3mL.

Table 2.3; Day 2 Cytokine Mix

Factor	[Final]	[Stock]	1ml(1x)	1ml(6x)	2ml(6x)
BMP4	**20ng/mL**	50ng/µL	0.4µL	2.4µL	4.8µL
VEGF	**30ng/mL**	50ng/µL	0.6µL	3.6µL	7.2µL
Inhibitor VIII	**2µM**	2mM	1.0µL	6.0µL	12.0µL
Wnt3A	**10ng/mL**	10ng/µL	1.0µL	6.0µL	12.0µL
Activin A	**5ng/mL**	10ng/µL	0.5µL	3.0µL	6.0µL
FGFα	**10ng/mL**	50ng/µL	0.2µL	1.2µL	2.4µL
SCF	**20ng/mL**	50ng/µL	0.4µL	2.4µL	4.8µL
β-Estradiol	**0.4ng/mL**	0.4ng/µL	1.0µL	6.0µL	12.0µL

2.4.2.5 Day 3

At day 3 the embryoid bodies were harvested from the wells and pooled into a 15mL centrifuge tube. The cells were centrifuged at 100g for 1 minute and the supernatant aspirated to waste. 1mL TrypLE® Select was added and cells mechanically dissociated by pipetting up and down gently. The cells were then transferred to an empty well of a 6 well plate and incubated at 37°C for 10min occasionally pipetting up and down to aid dissociation. After 10min the dissociated cells were placed in a 15mL centrifuge tube with 14mL of Dulbecco's PBS (Ca^{2+}/Mg^{2+} free) and centrifuged for 3min at 310g. The supernatant was aspirated to waste and the cell pellet resuspended in 6mL fresh Dulbecco's PBS (Ca^{2+}/Mg^{2+} free). The cells were centrifuged again for 3 minutes at 310g and the supernatant aspirated. The cells were resuspended in 4 mL- Stemline® II with cytokines (Table 2.4) and a 10 µL sample counted on a haemocytometer using the

trypan blue exclusion method. Cells were then seeded at 200,000/well in Stemline® II with cytokines (Table 2.4) in Costar 3516 6 well plates.

Table 2.4; Days 3-9 Cytokine mix

Factor	[Final]	[Stock]	1mL(1x)	1mL(6x)	2mL(6x)
BMP4	**20ng/mL**	50ng/µL	0.4µL	2.4µL	4.8µL
VEGF	**30ng/mL**	50ng/µL	0.6µL	3.6µL	7.2µL
FGFα	**10ng/mL**	50ng/µL	0.2µL	1.2µL	2.4µL
SCF	**30ng/mL**	50ng/µL	0.6µL	3.6µL	7.2µL
IGF2	**10ng/mL**	50ng/µL	0.2µL	1.2µL	2.4µL
TPO	**10ng/mL**	50ng/µL	0.2µL	1.2µL	2.4µL
Heparin	**5µg/mL**	5mg/mL	1µL	6µL	12µL
β-Estradiol	**0.4ng/mL**	0.4ng/µL	1.0µL	6.0µL	12.0µL
IBMX	**50µM**	100mM	0.5µL	3.0µL	6.0µL

2.4.2.6 Day 5

By this stage cells had become adherent with possible signs of budding. Fresh cytokines were added 0.5mL of x6 concentration cytokines/well as per table 2.4.

2.4.2.7 Day 7

A complete media change was required at this stage. Cells were harvested from wells and pooled into a centrifuge tube before centrifuging for 3min at 310g. Any adherent cells were left in the wells and 1mL fresh media/cytokine mix (Table 2.4) added. Supernatant from sedimented cells was discarded and cells resuspended in fresh media/cytokine mix (3ml/well final volume) according to table 2.4 but with half the dose (2.5µg/mL) heparin.

2.4.2.8 Day 9

Fresh cytokines were added x3 concentration (since only one day until media change) in 0.5ml Stemline® II media per well according to Table 2.4.

2.4.2.9 Days 10-17

By this stage cells were rapidly proliferating red suspension cells with very little budding (if any) remaining. Cells were harvested and pooled into a 15mL centrifuge tube then centrifuged at 310g for 3 minutes. The supernatant was discarded and the cells resuspended in 3mL/well Stemline® II with cytokines according to Table 2.5. The cells were supplemented every second day with 0.5mL Stemline® II with x6 concentration of cytokines.

Table 2.5; Days 10-17 Cytokine Mix

Factor	[Final]	[Stock]	1mL(1x)	1mL(6x)	2mL(6x)
Hydrocortisone	**1µM**	1mM	1µL	6.0µL	12.0µL
SCF	**50ng/mL**	50ng/µL	1.0µL	6.0µL	12.0µL
Flt3L	**16.7ng/mL**	50ng/µL	0.33µL	2.0µL	4.0µL
BMP4	**6.7ng/mL**	50ng/µL	0.134µL	0.8µL	1.6µL
IL3	**6.7ng/mL**	50ng/µL	0.134µL	0.8µL	1.6µL
IL11	**6.7ng/mL**	50ng/µL	0.134µL	0.8µL	1.6µL
EPO	**3U/mL**	10U/µL	0.3µL	1.8µL	3.6µL
IBMX	**50µM**	100mM	0.5µL	3.0µL	6.0µL

2.4.2.10 Days 17-24

Cells were counted using the trypan blue exclusion method before harvesting into a centrifuge tube and centrifuging at 310g for 3 minutes. The supernatant was discarded and cells washed in Dulbecco's PBS (Ca^{2+}/Mg^{2+} free) before resuspending in IBIT media (Table 2.6) supplemented with cytokine mix C (Table 2.7). Cell were seeded at

$1x10^6$ cells/well in Costar 3516 6 well plates. Cells were supplemented every 2 days with 0.5mL IBIT supplemented with 6x concentration cytokine mix C.

IBIT

Table 2.6 & 2.7; Days 17-24 Cytokine Mix

C

Component	[Final]	[Stock]	250ml	500ml
Iscoves Basal Media	**Base**	Base	240mL	474mL
BSA	**1%**	25% soln.	10mL	20mL
Insulin	**10µg/mL**	10mg/mL	250µL	500µL
Transferrin	**200µg/mL**	50mg/mL	1.0mL	2.0mL
β-mercaptoethanol	**0.1mM**	50mM	500µL	1mL
Lipid Mixture 1			1.25mL	2.5mL
Ethanolamine			10µL	20µL

Factor	[Final]	[Stock]	1mL (1x)	1mL (6x)	2mL (6x)
Hydrocortisone	**1µM**	1mM	1µL	6.0µL	12.0µL
SCF	**20ng/mL**	50ng/µL	0.4µL	2.4µL	4.8µL
IGF I	**20ng/mL**	100ng/µL	0.2µL	1.2µL	2.4µL
IL3	**6.7ng/mL**	50ng/µL	0.134µL	0.8µL	1.6µL
IL11	**6.7ng/mL**	50ng/µL	0.134µL	0.8µL	1.6µL
EPO	**3U/mL**	10U/µL	0.3µL	1.8µL	3.6µL

2.4.2.11 Days 24-31

Although the complete protocol is 31 days it was not necessary to continue differentiation beyond day 24 for the purposes of this research.

2.4.3 Haematopoietic differentiation of CD34+ cells

2.4.3.1 Day 0

Prior to cell thawing the appropriate volume of ISHIT medium was prepared (Table 2.8) with D0-D8 cytokines (Table 2.9) and pre-warmed to 37°C. A vial of CD34+ cord blood cells was removed from liquid nitrogen storage and warmed by hand until ice crystals had almost disappeared. The vial was then opened in the hood and the cell suspension transferred to a 50mL centrifuge tube. 9mL of pre-warmed ISHIT medium was added drop-wise until the cell suspension had been diluted 1:10. The cells were then centrifuged at 300g for 10 minutes and the supernatant aspirated to waste. The pellet was resuspended in 1mL of ISHIT medium and a sample taken for counting using the trypan blue exclusion method. Cells were then seeded at 1 x 10^4 cells /mL in prepared medium and incubated at 37^{o}C, 5% CO_2.

Table 2.8; ISHIT (Iscoves, Serum, Heparin, Insulin, Transferrin) Medium

Component	[Final]	[Stock]	500ml
Iscoves Basal Media	**Base**	Base	472mL
Serum (Human AB+)	**5%**	100%	25mL
Heparin	**3U/mL**	5000U/mL	0.3mL
Insulin	**10µg/mL**	10mg/mL	500µL
Transferrin	**200µg/mL**	50mg/mL	2.0mL

Table 2.9; Days 0-8 cytokines

Component	[Final]	[Stock]	1ml 1X	10ml 1x	1ml 10x
SCF	**60ng/mL**	50ng/µL	1.2µL	12µL	12µL
IL3	**5ng/mL**	50ng/µL	0.1µL	1µL	1µL
EPO	**3U/mL**	10U/µL	0.3µL	3µL	3µL
Hydrocortisone	**1µM**	1mM	1µL	10µL	10µL

2.4.3.2 Day 2

Cells were counted using the trypan blue exclusion method. Cells were pooled into a 50mL centrifuge tube and centrifuged at 300g for 5 minutes. The supernatant was removed and cells resuspended in 1-2mLof ISHIT medium with day 0-8 cytokines added (Table 2.8/2.9). An adequate volume of pre-warmed (37°C) ISHIT/Day 0-8 medium was added to a cell culture flask so that the final cell density would become 2 x 10^4 cells /mL upon addition of the cell suspension. Cells were incubated at 37°C, 5% CO_2.

2.4.3.3 Day 4

Cell density was adjusted to 4 x 10^4 cells /mL (using Day 2 protocol)

2.4.3.4 Day 6

Cell density was adjusted to 6 x 10^4 cells /mL (using Day 2 protocol)
NB. Cells were frozen at Day 6 for recovery and expansion at a later date (See freezing protocol below). Almost all experimental work was carried out using cell banks which were resuscitated at day 6.

2.4.3.5 Day 8

Cell density was adjusted to 1-3 x 10^5 cells /mL same with Day 8-11 cytokines (Table 2.10)

Table 2.10; Days 8-11 Cytokines

Component	[Final]	[Stock]	1ml 1X	10ml 1x	1ml 10x
SCF	**10ng/ml**	50ng/ □	0.2µl	2µl	2µl
EPO	**3U/ml**	10U/ □	0.3µl	3µl	3µl
Hydrocortisone	**1 □M**	1mM	1µl	10µl	10µl
Transferrin	**300µg/ml**	50mg/ml	6µl	60µl	60µl

2.4.3.6 Day 11

Cell density was adjusted to 5-10 x 10^5 cells /mL in ISHIT medium with Day 11-25 cytokines (Table 2.11)

Table 2.11; Days 11-25 Cytokines

Component	[Final]	[Stock]	1ml 1X	10ml 1x	1ml 10x
EPO	**3U/ml**	10U/ □	0.3µl	3µl	3µl
Transferrin	**300µg/ml**	50mg/ml	6µl	60µl	60µl

2.4.3.7 Day 15

Cell density was adjusted to 1-10x 10^6 cells /mL in ISHIT medium with fresh Day 11-25 medium (Table 2.11).

2.4.3.8 Days 18-22

Cell density was adjusted to 1-10x 10^6 cells /mL in ISHIT medium with fresh Day 11-25 medium (Table 2.11).

2.5 Haematopoietic Growth Factors

Table 2.12; List of growth factor manufacturers and reconstitution medium

Factors	Supplier	Mixing Agent
BMP4	R and D Systems	4mM HCl with 0.1% BSA
VEGF165	Peprotech	PBS/0.1% BSA
Wnt3A	R and D Systems	PBS/0.1% BSA
Activin A	Peprotech	PBS/0.1% BSA
Inhibitor VIII	Calbiochem	DMSO
FGFa	Peprotech	PBS/0.1% BSA
SCF	Invitrogen/clinical Biovitrum AB	PBS/0.1% BSA
b-estradiol	Sigma	Ethanol/Medium
IGF2	PeproTech	PBS/0.1% BSA
TPO	PeproTech	PBS/0.1% BSA
Heparin	Sigma	Water
IBMX	Sigma	DMSO
Hydrocortisone	Sigma	Ethanol/Medium
Flt3L	PeproTech	PBS/0.1% BSA
IL-3	PeproTech	PBS/0.1% BSA
IL-11	PeproTech	PBS/0.1% BSA
EPO	Roche	PBS
IGF1	PeproTech	PBS/0.1% BSA

The 18 growth factors listed were supplied and prepared as shown in the table. Although every effort was taken to keep conditions the same between laboratories it is suspected that medium preparation and variation in manufacturer lots could have had an impact on the differentiation process.

2.6 HL60 and J774 Cell Maintenance

J774/HL60 cells were cultured in cell culture flasks in RPMI 1640 cell culture medium supplemented with 10% Fetal Bovine Serum (FBS). Prior to subculture the appropriate volume of media was decanted into a 50mL centrifuge tube and pre-warmed to 37°C. In the case of J774 cells whereby the cells were adherent a cell scraper was used to separate cells from the cell culture flask surface. A sample of the cell suspension was then taken using a pipette and counted on a haemocytometer using the trypan blue exclusion method. The appropriate volume of cell suspension was then centrifuged in a centrifuge tube at 100g for 5 minutes and resuspended in cell culture medium at a volume of 3-5 $x10^5$ cells/mL. Cells were left in incubator at 37°C 5% CO_2 and subcultured every 3-4 days depending on confluency.

2.7 Cell Culture Analysis

2.7.1 Cytospin

Cells were centrifuged at 300g for 5 minutes and resuspended in Dulbecco's PBS (Ca^{2+}/Mg^{2+} free) to a concentration of 1 $x10^6$ cells/mL. The required number of cytospin slides were prepared (with slide, filter and funnel as specified) and 100µL aliquots transferred to the sample well of the funnel. Once loaded the rotor was balanced and the cytocentrifuge (Tharmac GMBH) run at 450 rpm for 4 minutes. The cytospin slides were removed and allowed to air dry for 1 minute. The slides were then stained using Rapid Romanowsky stain pack (TAAB) by first dipping into solution A ten times to fix. This was followed by immersion in Solution B for 1 minute 30 seconds and solution C for 15 seconds. The slides were rinsed in deionised water and allowed to air dry before mounting in DePeX Mounting medium (Sigma). The slides were then be analysed under a microscope.

2.7.2 Microscopy

Several microscopes were used during the project as follows;

A) Tissue Culture Microscope – A Nikon Eclipse with DS-Qi1Mc 12 bit camera was used to capture images of all cells grown in the tissue culture laboratory.
B) Colour Microscope – A Zeiss Axioscope fluorescence microscope with Canon EOS 60D digital camera was used to capture colour images of cytospin slides.
C) Experimental microscope A – A Zeiss AxioObserverD1 fluorescence microscope was used initially to capture images of the cell culture device and biosensors.
D) Experimental microscope B – Part-way through the project a Leica DMi8 was purchased and used with a Leica DFC camera for cell culture device images.

Leica LAS X software and ImageJ were used for image analysis

2.7.3 Flow Cytometric Analysis Preparation

A FACSCalibur™ flow cytometer (BD Biosciences) was calibrated using four colour BD CaliBRITE™ beads and BD FACSComp^{TM} software. BD CellQuest^{TM} Pro Software was opened and prepared for data collection (See BD FACSCalibur™ Instructions for Use). A cell count and viability analysis were performed using the trypan blue exclusion method. Then a sufficient number of cells (1 x10^5 per test) were centrifuged at 300g for 5 minutes and resuspended in a suitable volume (100µL per test) of FACSFlow™ sheath fluid (BD Biosciences). The cell samples were kept chilled/on ice throughout remaining steps.

2.7.4 Antibody Staining

In order to analyse antigenic markers micro centrifuge tubes were first labelled according to antibody/isotype stains and 100µL cell suspension decanted into each. Antibodies or isotypes were added so that antibody and isotype protein concentrations were equal (as obtained from BD Biosciences). The cells were then incubated in the dark at 4°C for 20 minutes. During this time flow cytometry tubes (BD Falcon™) were labelled according to antibodies/isotypes and filled with 200µL each of FACSFlow™ sheath fluid. Stained cells were removed from incubation and centrifuged at 300g for 5 minutes. The supernatant was discarded and the stained cells resuspended in 100µL FACSFlow™ before decanting into the labelled flow cytometry tubes. Each tube in turn was placed on the FACSCalibur™ sample injection port and run on high until 10,000 events had been collected for each sample. In depth analysis was completed using FlowJo software.

2.7.5 Apoptosis/Necrosis

Apoptotic Phosphatidylserine (PS), a hallmark of apoptosis, was stained using Apopoxin Green Indicator (Ex/Em = 490/525 nm) and for necrosis a membrane impermeable dye, 7-aminoactinomycin D (7-AAD, Ex/Em = 546/647 nm) was used (Abcam). For each test 1 x10^5 cells were centrifuged at 500g for 5 minutes and resuspended in 200µL assay buffer. 2µL of Apopoxin green and 1µL 7-AAD were added and the cell suspension vortexed before leaving in the dark at room temperature for 30 minutes. Prior to flow cytometric analysis 300µL of assay buffer was added to increase volume. Apopoxin green fluorescence was quantified on the FL1 channel and necrosis/7-AAD on FL3. Unstained cell samples were used as controls.

2.7.6 ROS

An ROS staining kit was purchased from Abcam. The deep red dye (Ex/Em = 650/675) reacts with ROS to generate deep red fluorescence which is detectable by flow cytometry. The ROS deep red dye was reconstituted by adding 40µL DMSO to the vial and mixing by pipetting. Cells (1 x10^5/test) were centrifuged at 300g for 5 minutes and

resuspended in 200µL assay buffer. 0.4µL of ROS stain was added (per 200µL sample) and the cell suspension vortexed before placing in a 37°C incubator for 30 minutes. The fluorescence intensity was then measured in the FL2 channel. Unstained cells were used as controls.

2.7.7 Mitochondria

A mitochondrial staining kit was purchased from Abcam. The kit uses a proprietary dye that selectively accumulates in mitochondria via the mitochondrial membrane potential gradient. A working stock was created by adding 20µL of the MitoGreen indicator to 10mL of assay buffer. The cells (2 x10^5/test) were centrifuged at 1000rpm for 5 minutes and supernatant removed to waste. The cells were resuspended in 100µL of prewarmed cell culture media with an equal volume of the working MitoGreen solution. The cells were vortexed and incubated at 37°C for 60 minutes. The cells were then washed twice in DPBS before flow cytometric analysis in the FL1 channel and/or microscopic analysis.
For microscopy cells were centrifuged onto slides using a cytocentrifuge (450 rpm for 4 minutes) and images captured immediately in a dark room at 100ms.

2.7.8 Hif-1-α

Alexafluor 647 mouse anti-human Hif-1-α was purchased from BD Biosciences. Prior to the antibody staining described cells were first permeabilized in 4% paraformaldehyde.

2.8 Flow Cytometry Analysis

2.8.1 CD Markers

In order to keep identical analysis methods between laboratories for data comparison the same methods were adopted at Heriot Watt University as those used at Glasgow University. As shown in Figure 2.1 the isotype population was first gated to separate live cells from dead cells and debris. The grid was then adjusted so that the population

was situated in the negative fluorescence (Lower Left) quadrant. These settings were then applied directly to the positively stained sample. The cells were considered positive/negative for the CD marker in question according to which quadrant the cells were situated. In the example shown the cells are 99.924% (0.024%+99.9%) positive for CD71, 99.965% (0.065%+99.9%) positive for CD235a and 99.9% positive for both CD71 and CD235a.

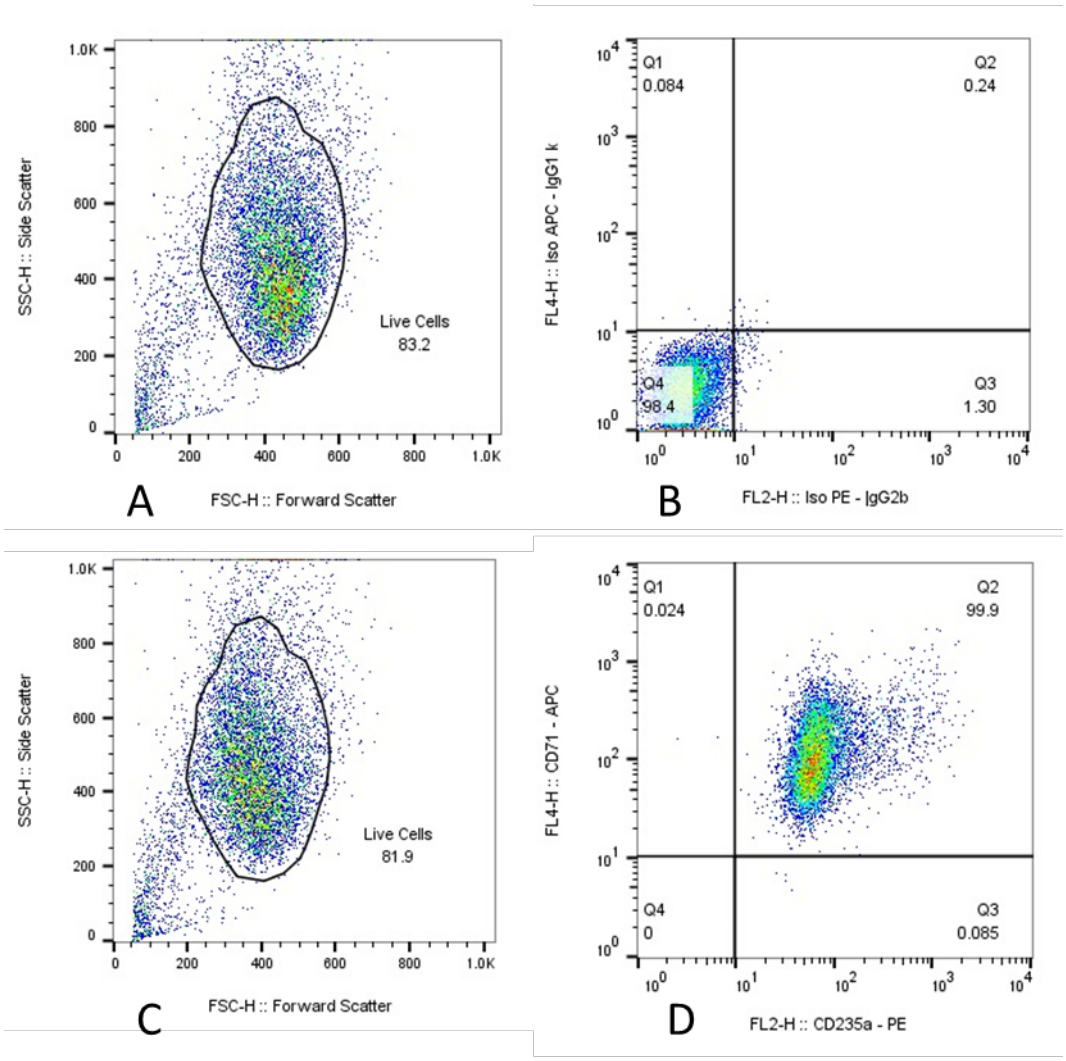

Figure 2.1 Flow Cytometric Analysis of CD Markers; (A) The isotype control cells were gated and then (B) the quadrant adjusted to contain the population in the negative. These parameters were then transferred to the positively stained population (C) and (D).

2.8.2 Apoptosis and Necrosis

The unlabelled (control) and apoptosis/necrosis stained cells were gated in the same way as the CD markers (Figure 2.2). Each gated sample was then assessed for mean fluorescence intensity (MFI) using the median as calculated by FlowJo (since flow cytometry samples do not exhibit normal distribution it is standard procedure to use the median). The positive samples were then normalised using the negative control (unlabelled) populations [78].

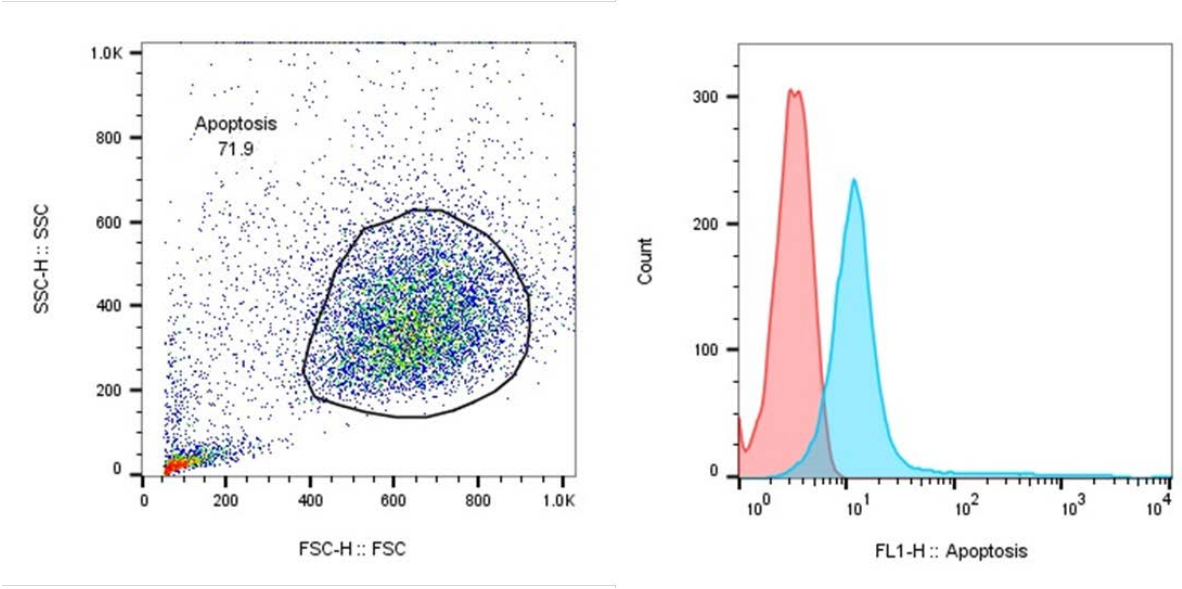

Figure 2.2 Flow cytometric analysis of Apoptosis. (Left) Cells were gated as before and the mean fluorescence intensity (MFI) was calculated using FlowJo Software. (Right) Histogram showing Unlabelled (Red) and Apoptotic (Blue) samples. The Positive MFI was normalised using the negative/unlabelled sample. Necrotic MFI values were calculated in the same way.

2.8.3 Enucleation

Since cytospin counts are not representative of whole populations of cells flow cytometry was also used as a secondary method to track enucleation. Since Forward and Side Scatter only account for size and complexity of particles (cells or otherwise) a nuclei stain DRAQ5™ (Abcam) stain was used to ensure the correct population was identified as nuclei (Figure 2.3).

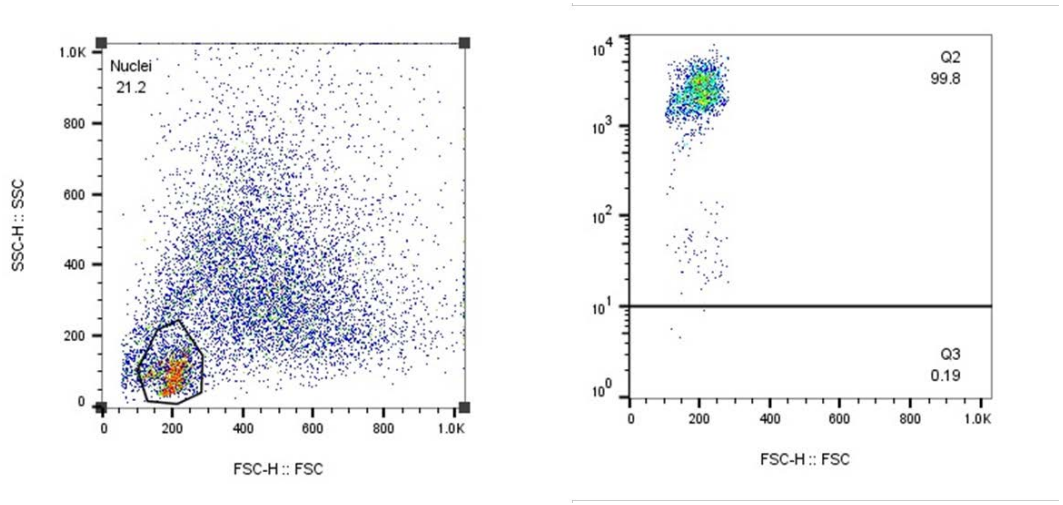

Figure 2.3 Flow cytometric analysis of enucleation. (Left) Nuclei were gated as before. (Right) Nuclei shown as positive for DRAQ5™ (PerCP) staining.

2.9 Statistics

Where appropriate students T-tests were performed using SPSS statistical Analysis software and results were considered significant at the level of $P \leq 0.05$ (*), $P \leq 0.01$ (**) or $P \leq 0.00$ (***). Unless otherwise stated all experiments were completed in triplicate.

Pearson's product moment correlation was also used where appropriate to gauge strength of correlations. Statistical significance was estimated as above and correlation strength according to the following;

	Coefficient, *r*	
Strength of Association	Positive	Negative
Small	.1 to .3	-0.1 to -0.3
Medium	.3 to .5	-0.3 to -0.5
Large	.5 to 1.0	-0.5 to -1.0

2.10 Computational Fluid Dynamics (CFD)

The flow environments of the cell culture device, capillary device, 500mL Integra Cellspin spinner flask and Celligen BLU Bioreactor were characterized by solving Navier-Stokes equations with specified boundary conditions using Comsol Multiphysics 4.4 package (Comsol, Hatfield, UK). The geometries were drawn directly into Comsol or in some cases in 2D in AutoCAD before importing. Two-dimensional axisymmetric models were selected for the capillary device since there are two planes of symmetry. Axisymmetric models were chosen over 3D since at the low Reynolds numbers calculated for these capillaries there should be no instabilities in laminar flow, pressure or velocity and the resultant simulations are mathematically in balance cylindrically. The advantages of modelling asymmetrically are three-fold. Firstly it allows for an increase in meshing density so that the viscous boundary layer has been resolved sufficiently to evaluate for shear forces in the flow. Secondly it would be difficult to produce an accurate 3D mesh over the centreline of the tube which supports the valid assumption of axisymmetric flow and finally it reduces solving time and memory [verbal communication, Alan McGuinn].

The minimum element size used was 0.0159 μm. The kinematic viscosity of cell culture media at 37°C was could not be determined experimentally and was assumed to be 7.8 $x10^{-4}$ Pa .s as obtained from literature [79]. The density of the media was obtained experimentally to be 991.348 kg/m^3 by weighing 500mL of cell culture media and subtracting the weight of the vessel.

Chapter 3 - Characterisation of Haematopoiesis

3.1 RC9b and SFC i55 iPS cells

The first step in the transformation of the haematopoietic differentiation protocol into an industrial bioprocess was to ensure the procedure was transferrable and could be run successfully across all laboratories in the consortium. The protocol was developed and performed efficaciously at Mountford Laboratories, University of Glasgow, hence initially all data produced at Heriot Watt University was analysed for equivalency. Aside from ensuring that cells were morphologically and physiologically identical it was paramount that the same proliferation (expansion) rates were attainable to ensure the robustness of the protocol prior to experimentation and eventually high volume bioreactor culture.

3.1.1 Morphology

Differentiation cultures were observed daily under a microscope to assess morphologic similarities/differences between laboratories. Pictures at Mountford Laboratories were taken using a Leica DMIL LED microscope and Nikon Digital Sight DS-L1 colour camera at x50 magnification (Figure 3.1) whilst those at Heriot Watt were taken using a Nikon Eclipse microscope with a DS-Qi1Mc monochrome camera at x100 magnification (Figure 3.2). Despite the contrast in imagery it is clear the cells are morphologically akin to one another.

At days 2-3 of the protocol stem cell ‘squares’ (cut from stem cell monolayers at day 0) had become more rounded/tubular and abundant (Figure 3.1 and 3.2 A/B) forming embryoid bodies (EBs). At Day 3 the EBs were mechanically separated and by day 5 some of the cells had begun to attach to the substrate surface (Figure 3.1 and 3.2 C) and branch out to form colonies (Figure 3.1 and 3.2 D). At day 8 proerythroblasts had begun to bud off from the colonies (Figure 3.1 and 3.2 E) and proliferate rapidly. By day 9/10 almost all cells were in suspension (Figure 3.1 and 3.2 F).

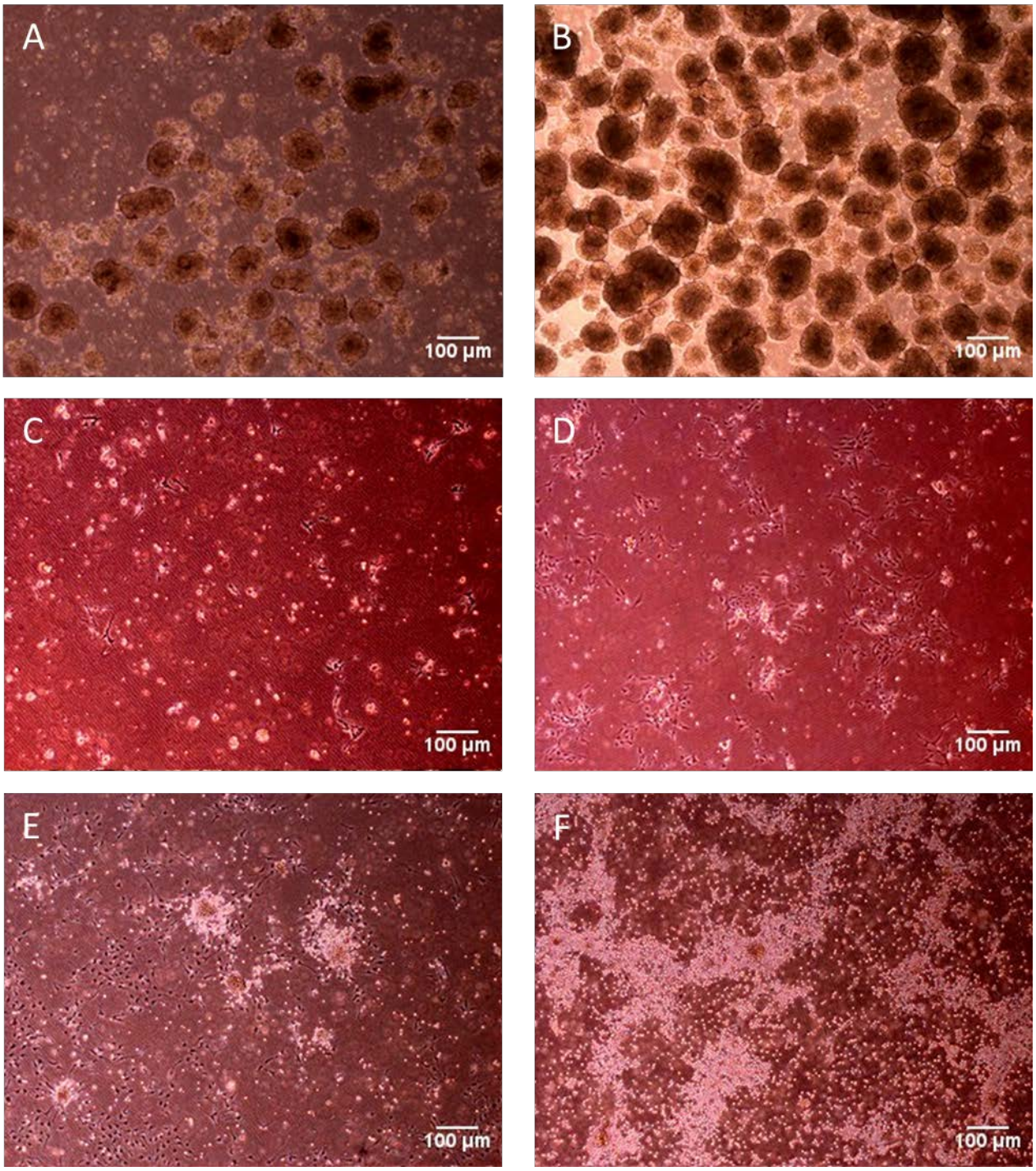

Figure 3.1; Cells at progressive stages in the haematopoietic differentiation protocol taken at Mountford Laboratories. (A) Day 2; Embryoid bodies are formed from 'squares' cut from stem cell monolayers at Day 0. (B) Day 3; EB aggregates become larger and more rounded/tubular. At Day 3 EBs are mechanically separated and reseeded. (C) Day 5; Separated cells begin to attach to substrate surface. (D) Day 7; Adherent cells branch out to form colonies/networks. (E) Day 8; Proerythroblasts bud off of colonies. (F) Day 9; Proerythroblasts begin to proliferate rapidly.

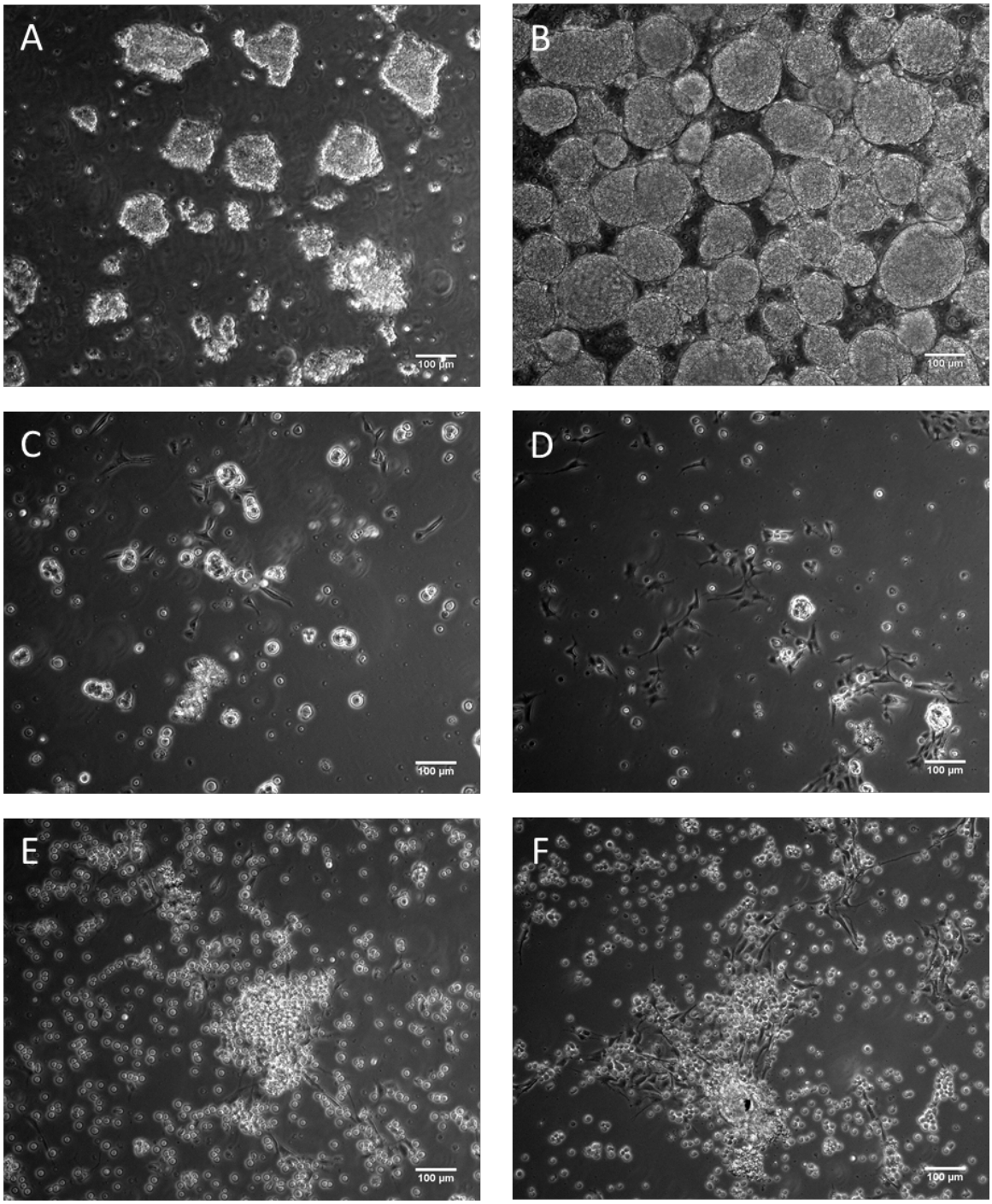

Figure 3.2; Cells at progressive stages in the haematopoietic differentiation protocol taken at Heriot Watt Laboratories. (A) Day 2; Embryoid bodies are formed from 'squares' cut from stem cell monolayers at Day 0. (B) Day 3; EB aggregates become larger and more rounded/tubular. At Day 3 EBs are mechanically separated and reseeded. (C) Day 5; Separated cells begin to attach to substrate surface. (D) Day 7; Adherent cells branch out to form colonies/networks. (E) Day 8; Proerythroblasts bud off of colonies. (F) Day 9; Proerythroblasts should begin to proliferate rapidly but appear unchanged from Day 8.

The main/only difference to be noted between the images for each laboratory is that at Heriot Watt Laboratories there was no observable proliferation, (Figure 3.2E/3.2F) the images for day 8 and 9 appear very similar. The interchangeable images for Mountford Laboratories (Figure 3.1E/3.1F) exhibit distinct proliferation.

3.1.2 Marker profile

A defined panel of pluripotent and haematopoietic antigenic markers were detected by flow cytometry at days 0 and 10 of the protocol to gauge whether cells were the correct phenotype prior to and in the midst of differentiation (in most instances cells did not expand enough to assess markers at later stages in the protocol). Day 0 pluripotency markers obtained at Heriot Watt Laboratories were erratic and frequently lower than those achieved at Mountford Laboratories (Figure 3.3).

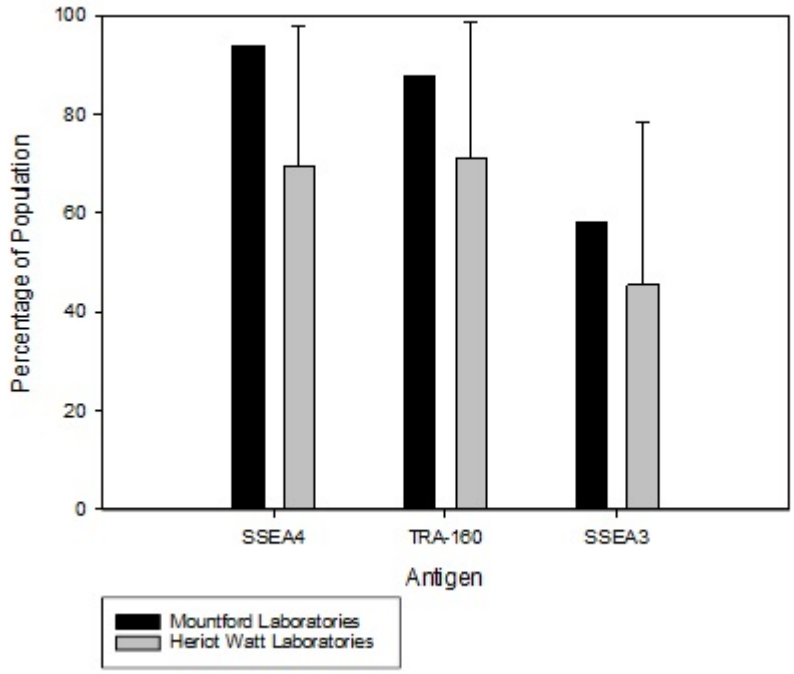

Figure 3.3; Comparison of average Day 0 pluripotency markers obtained for RC9b/SFC i55 cell lines at Heriot Watt University alongside a representative culture from Mountford Laboratories. Pluripotency markers tested at Mountford Laboratories were consistently higher and more reliable than those collected at Heriot Watt Laboratories which may have impacted on the differentiation process

It has been suggested that a deficiency in pluripotency markers denotes an inability to differentiate down a desired lineage. This may have impacted on cell phenotype later stages of the protocol and possibly proliferation/expansion. At Day 10 whilst most of the markers (CD235a/CD71/CD43/CD31) appeared stable and on target, immature cell markers CD45 and CD34 were significantly higher than those recorded at Mountford Laboratories (Figure 3.4).

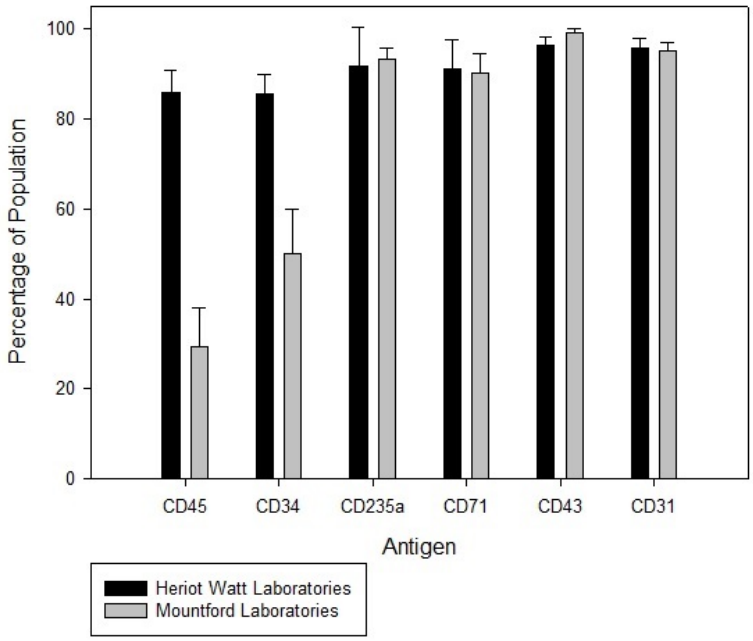

Figure 3.4; Comparison of average Day 10 antigenic markers obtained for RC9b differentiations at Heriot Watt University compared with a representative culture from Mountford Laboratories. Although CD43/CD31/CD235a/CD71 were constant, immature cell markers CD34 and CD45 remained high

Although microscopic observation suggested that cells were morphologically identical, the analysis of cell phenotype suggested a state of arrested development. This may have been the cause of insufficient proliferation/expansion levels achieved at Heriot Watt University.

3.1.3 Expansion

Training on the haematopoietic protocol was initially completed at Mountford Laboratories between November 2012 and June 2013 before attempting to transfer the process to Heriot Watt University. During this time, trials of the protocol were completed within the target expansion range routinely achieved by Mountford Laboratories (Figure 3.5).

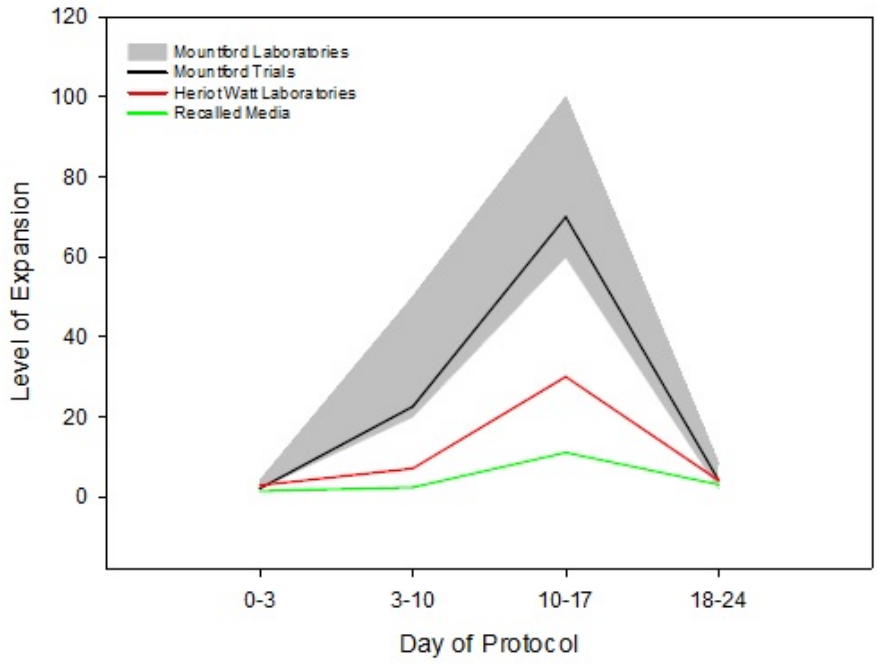

Figure 3.5; Typical expansion range (grey) at Mountford Laboratories compared with trials at Mountford (black) Heriot Watt Laboratories (red) and expansion achieved with Faulty/Recalled Media (green).

Following the transfer of the protocol to Heriot Watt University in July 2014, the same levels of expansion could not be achieved. Due to the inconsistencies in pluripotency markers replacement cells were recovered from Mountford Labs in January 2015 and new cell banks generated with improved pluripotency markers (SSEA4 >95%, TRA-160 >95%, SSEA3 >50%). Unexpectedly, expansion levels achieved using the fresh cell lines were inferior, particularly in the crucial embryoid body stage of development which had not been experienced prior. Large crystals were found residing in the media (Figure 3.6) and it was believed that these could have affected osmotic concentration.

Stem cells are extremely sensitive to environmental changes (be they biological or physical) and it was suspected that these crystals were the cause of further depreciated cell numbers. Consequently the specialized cell culture media (Stemline® II, ThermoScientific) was deemed unfit for use for the period January to June 2015 and recalled with no imminent replacement. One of the drawbacks of the project was that this specialized media was indispensable to the haematopoietic differentiation protocol and since its composition was unknown no replacement could be found.

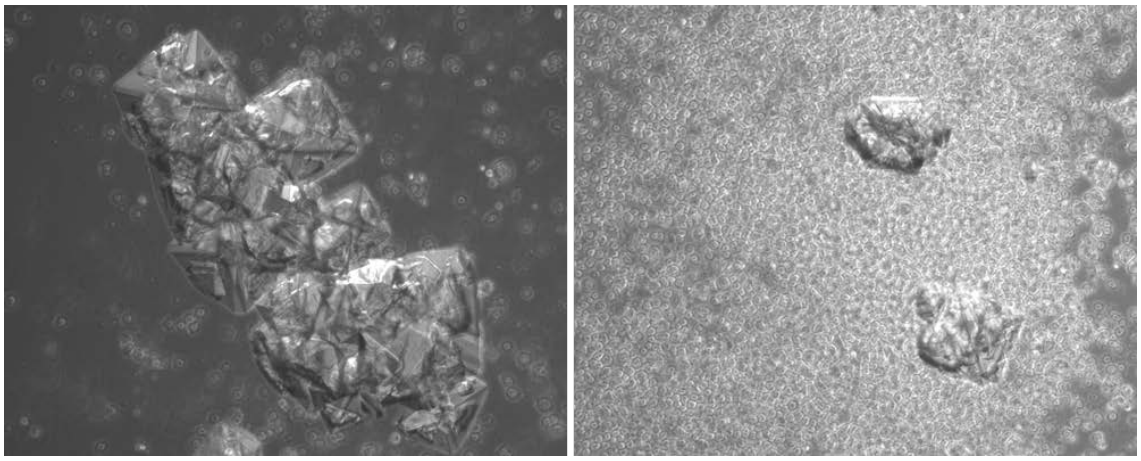

Figure 3.6; Large red crystals found in Stemline® II cell culture media

From July 2015 onwards, due to volatile reagents, the instability of the cell lines and the irreproducibility of the phenotyping/expansion data, work with RC9b and SFC i55 cell lines was halted in favour of CD34+ cord blood stem cells. It must be noted however that some of the preliminary data contained in this research was obtained using the RC9b cell line.

This preliminary work with pluripotent stem cells is deemed scientifically valuable since it emphasizes some common issues faced in making stem cell therapies clinically and commercially viable as shall be discussed in depth in Chapter 7.

3.2 CD34+ Cord Blood Cells

Similar to the RC9b and SFC i55 work, all data produced for CD34+ cells at Heriot Watt Laboratories was compared to that of Mountford Laboratories for equivalency. Since there were no significant differences between laboratory data in any category, only results for Heriot Watt Laboratories are listed. The following sections describe normal haematopoietic development of CD34+ cells prior to experimentation. Since CD34+ cells are banked at day 6 and must be resuscitated and cultured for 24h prior to use, all data begins at day 8 and ends at day 21, when cultures were terminated due to lack of further growth/expansion.

3.2.1 Morphology

CD34+ cord blood stem cells grow entirely in suspension since they are already germ layer specified Haemangioblasts. There is little distinction to be made at progressive stages of differentiation by microscopy (Figure 3.7) and so in order to improve and standardise imaging across laboratories, a cytocentrifuge was purchased and used in conjunction with Rapid Romanowsky staining. Below (Figure 3.8) are stained cytospin pictures taken using a Zeiss Axioscope and a Canon EOS 60D digital colour camera at x40 magnification.

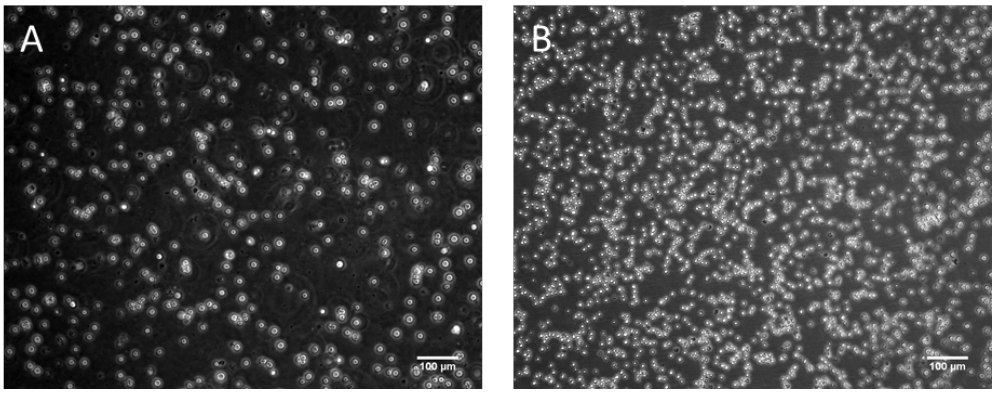

Figure 3.7; (A) Day 11 and (B) Day 18 of CD34+ Cord Blood Differentiation protocol taken with Nikon Eclipse microscope at x10 magnification. There were no discernible morphological differences between the images apart from cell size, which decreases over progressive days of the protocol

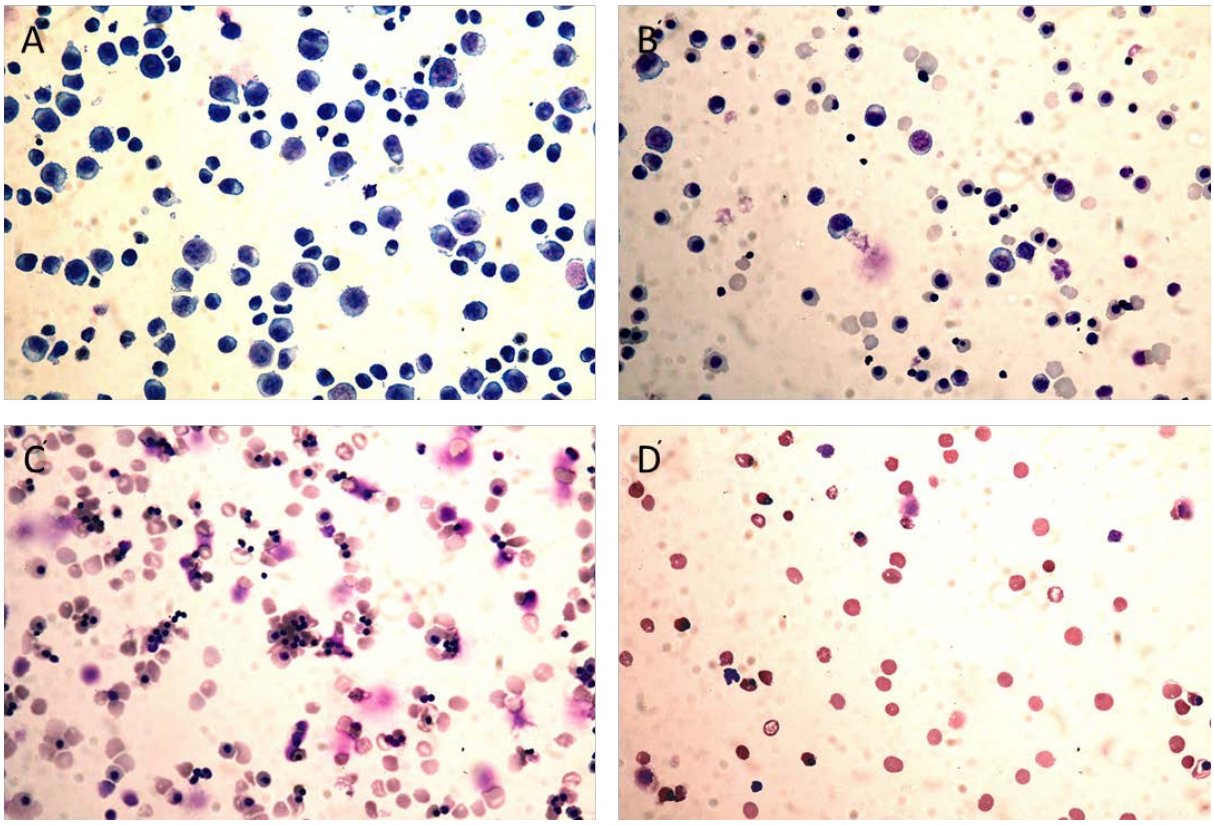

Figure 3.8; Cytospin pictures (x40 magnification) with genetic material (blue) and haemoglobin (red) staining. (A) Day 8-11; Cells are large and exhibit dark nuclear/mitochondrial staining. Blebbing can be seen at the edges of largest cells representing upregulated exocytosis. (B) Day 11-14; A mixed population of larger cells and smaller enucleated cells. Cells still appear blueish in colour representing retainment of mitochondrial genetic material. (C) Day 14-17; Cells become more uniform in appearance, enucleate further and begin to lose their blue hue. (D) Day 18-21; almost all cells have enucleated and have distinct colour and appearance of reticulocytes (immature erythrocytes). NB. Scale bars are not included for these images since the cytospin procedure stretches and distorts cells.

The cytospin images capture four observable stages of haematopoietic development. As well as morphological analysis, cytospin images were also used in combination with flow cytometry data to measure enucleation on each day of the protocol.

3.2.2 Enucleation

Flow cytometry images show that enucleation begins as early as day 11 (Figure 3.9) when for the first time, two distinct populations appear on the forward/side scatter plots (which signify 'event' size/complexity).

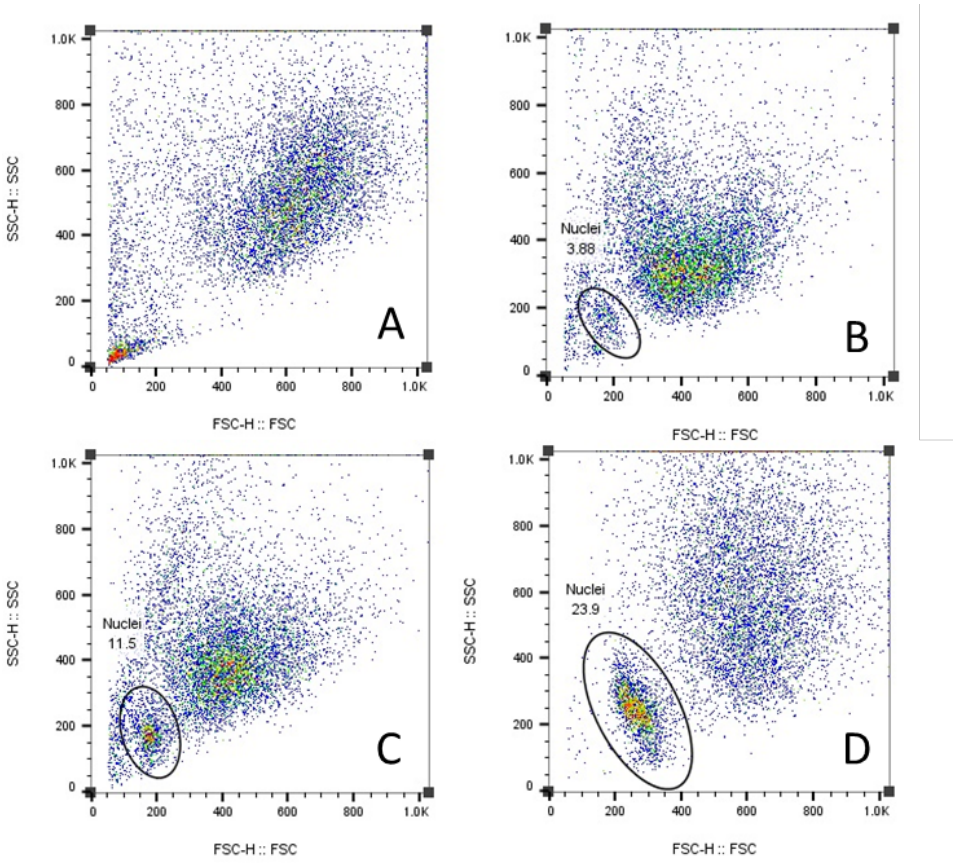

Figure 3.9; Forward and Side Scatter (FSC/SSC) images obtained by flow cytometry. (A) Day 10 of protocol, cells appear as a single population. (B) Day 11 of protocol, ordinarily two populations are visible as 0-4% of cells have enucleated. (C) Day D12 of protocol, 6-12% enucleation and D16, 20-30% enucleation

Over the following days the nuclei population increases gradually and plateaus at day 16 at approximately 25% of the population (Figure 3.10A). Cytospin pictures confirm that enucleation is at its' height between days 15 and 18, peaking at day 16 (Figure 3.10B).

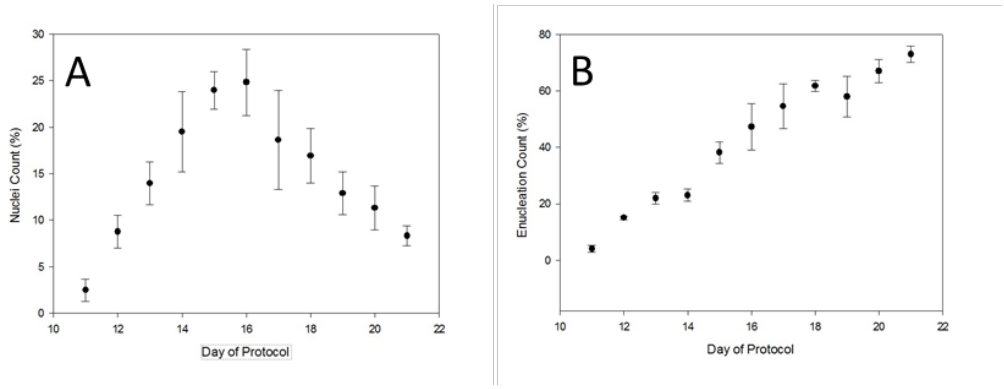

Figure 3.10; (A) Nuclei population counts for each day of the protocol obtained using FSC/SSC flow cytometry plots. (B) Enucleation counts for each day of the protocol using cytospin images. Both methods confirm that enucleation is at its' height between days 15 and 18, peaking at day 16. By day 21 75% of cells have enucleated.

Despite the sustained increase in enucleation post day 16 the mean nuclei population remained <25%. This was due to the population being marked for apoptosis by exposure of phospatidylserine (PS) on the nuclear membrane (Figure 3.11) showing that nuclei are marked for apoptosis in the same way as cells and are continuously degraded throughout the protocol

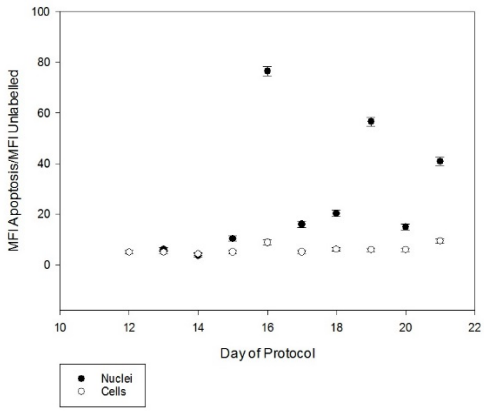

Figure 3.11; Apoptosis measured by Mean Fluorescence Intensity (MFI) of cells/nuclei marked with green (Ex490/Em525) PS sensor/MFI of unlabelled nuclei/cells. Nuclei exhibit elevated apoptosis levels in comparison to cell population, peaking at days 16, 19 and 21

3.2.3 Apoptosis and Necrosis

The general cell population was evaluated for apoptosis and necrosis to assess cell health for the duration of the protocol, particularly post day 16 when cell number begins to decline.

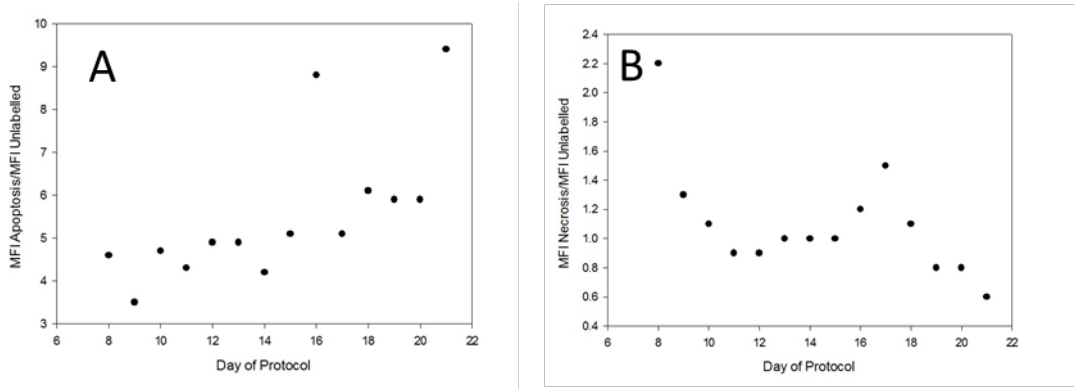

Figure 3.12; (A) Cellular apoptosis was labelled by apopoxin green (Ex490/Em525) PS sensor and detected by flow cytometry. A normal apoptotic rate of 2-6% is observed until day 16 when apoptotic cells more than double. (B) Necrotic Cells were labelled by membrane impermeable red dye 7-aminoactinomycin D (Ex/Em 546/647 nm). Necrosis is high post thaw but remains low throughout the protocol. Typically cells necrose at a rate of <1%, necrosis increases slightly post day 16.

Normally 2-6% of a cell population are apoptotic at any given time, as is the case for the entirety of the protocol, other than two peaks at days 16 and 21. Necrosis is usually ≤1% however it is characteristically high at day 8 post-thaw and there is also a peak at day 17 which marks the degradation of apoptotic cells from the day previous.

The apoptotic/necrotic peak at day 16/17 coincides with the enucleation peak and these events could conceivably be connected. It is possible that cells that do not enucleate are marked for apoptosis or that enucleation itself can be damaging to cells if not executed correctly.

3.2.4 Mitochondria

Human embryonic stem cells contain mitochondria but their immaturity and paucity mean that they chiefly rely on glycolysis for energy. Fully developed red blood cells are devoid of mitochondria and similarly switch to glycolysis as their metabolic pathway. Theoretically both the RC9b and CD34+ cord blood cells should have less/underdeveloped mitochondria and therefore require less oxygen.

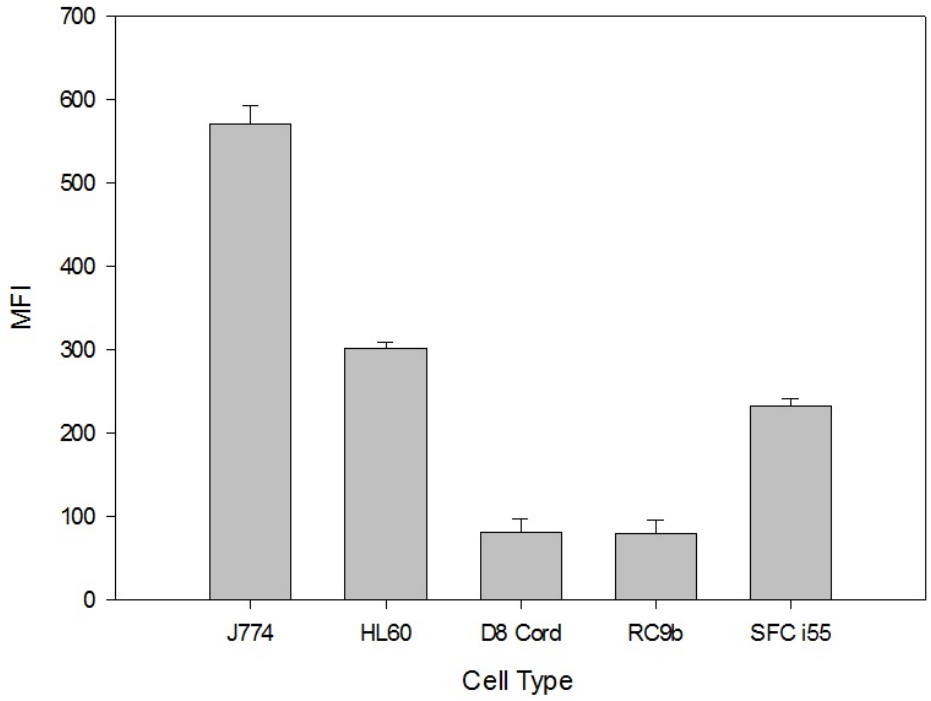

Figure 3.13; Mean Fluorescence Intensity (MFI) of different types of cells stained with apopoxin green indicator (Ex/Em 490/520 nm) captured using flow cytometry. Cell lines J774 and HL60 exhibit the highest MFIs and RC9b and D8 cord blood cells have the lowest as predicted.

Figure 3.13 shows that as predicted, the RC9b and CD34+ cells have lower mean fluorescence intensity of mitochondrial staining and therefore should require less oxygen than model cell lines J774 and HL60. Interestingly the SFC i55 cell line have more mitochondria than either of the other types of stem cell. This implies that although iPS cells are supposedly phenotypically the same as hESCs, metabolically they are not. The generation of iPS cells involves the manipulation of adult somatic cells to

transcribe embryonic genes and effectively become embryonic themselves but it is unclear what happens to their adult cellular machinery during this transition. Some very recent studies have shown that mitochondria experience DNA deletions during the modification and are hence mutated [64]. It is for such reasons that few (and none until 2015) clinical trials involving iPS cells have been sanctioned and further investigation should be taken into their genetic and metabolic differences from embryonic stem cells in order to ensure their safety in cellular therapies.

It was also important to note at which stage in the protocol mitochondria are extruded to evaluate whether oxygen concentration should be decreased over the duration of the protocol.

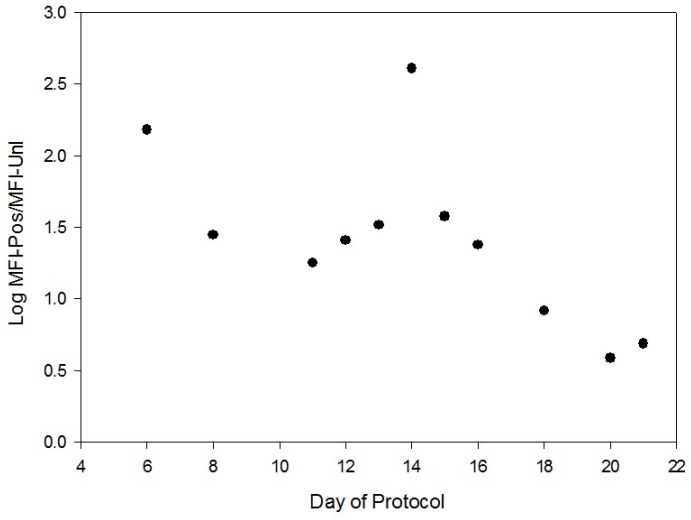

Figure 3.14; MFI of cells stained with green mitochondrial label apopoxin (Ex/Em 490/520 nm)/MFI of unlabelled cells as captured by flow cytometry. MFI decreases from day 8-12 before peaking at day 14 and then declines further. It is believed that this peak represents mitochondrial extrusion.

Figure 3.14 shows that the mitochondrial MFI depreciates between day 8 and 12 before a peak at day 14. Following day 15 the mitochondrial signal diffuses further. Pictures taken of the cells at Day 8 and day 12 (Figure 3.15, below) show that mitochondria do indeed grow dimmer on progressive days of the protocol. However pictures taken at day 14 show that mitochondria are almost extinguished and following this it is virtually

impossible to capture them by fluorescence microscopy. Therefore it is suggested that the peak MFI observed at day 14 is in fact a mass extrusion event and cells should require markedly less oxygen from this stage onwards in the protocol.

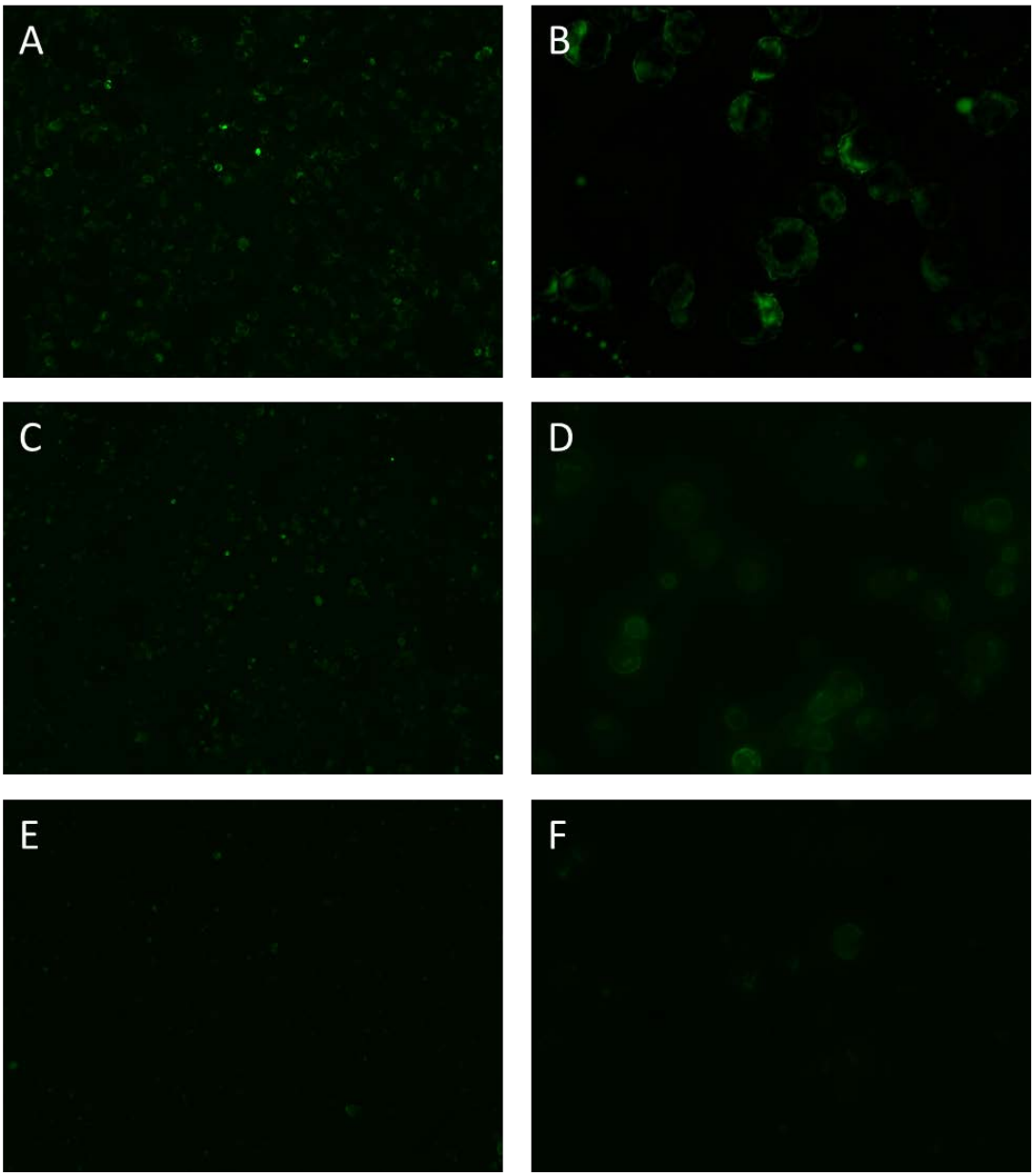

Figure 3.15; Mitochondria captured using a Leica DMi8 fluorescence microscope and DMC camera using x10 (left) and x40 (right) magnification. Cells were labelled with apopoxin green (Ex490/Em520nm) at days 8 (A&B), 12 (C&D) and 14 (E&F) of the protocol. Images show the fluorescence signal becoming weaker as the protocol progresses.

3.2.5 Marker profile

CD34+ cells were analysed by flow cytometry at days 11, 15 and 18 of the protocol to coincide with media changes and conform to experimental design.

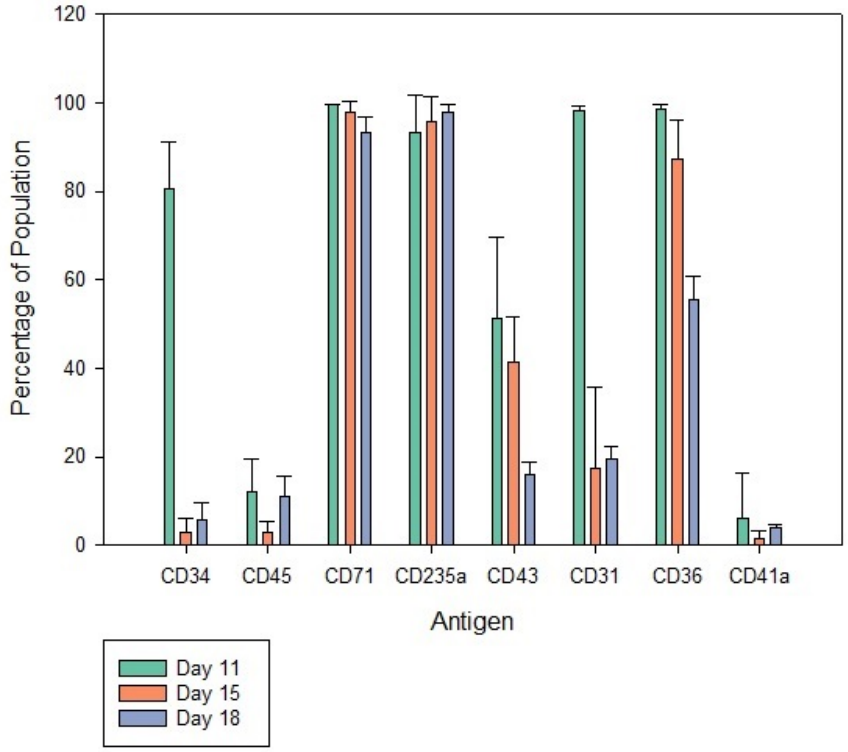

Figure 3.16; Average haematopoietic cell markers for day 11, 15 and 18 captured by flow cytometry. CD71 and CD235a remain >90% throughout the protocol. Immature cell marker CD34+ is elevated at day 11 but drops off completely by day 15/18. CD43/CD31/CD36 are in gradual decline. Platelet marker CD41a remains low.

Figure 3.16 shows that at day 11 CD34+ remained high but had plummeted by day 15/18 indicating maturation to haemangioblasts. CD43 and CD31 are transient haemangioblast markers which predictably drop off upon progression to the erythroid series whereby CD36 peaks signifying early erythroid cells. CD71 and CD235a remained high throughout the protocol since these are expressed by erythroid precursors and erythrocytes themselves. CD41a remains low throughout cord blood differentiation since it is an early haemangioblast marker which has already diminished by day 11 but

it should be noted that this is also a platelet marker. CD45 is a leukocyte marker and marks some residual unsolicited differentiation to white blood cells.

3.2.6 Expansion

CD34+ fold-expansion was not as great that obtained for RC9b/SFC i55 at Mountford Laboratories (cumulative fold-expansion x320000) however it was much more reproducible and the protocol was easily transferred to Heriot Watt University. Figure 3.17 shows that the average expansion level achieved with CD34+ cells at Heriot Watt Laboratories was within the defined range achieved at Mountford Laboratories.

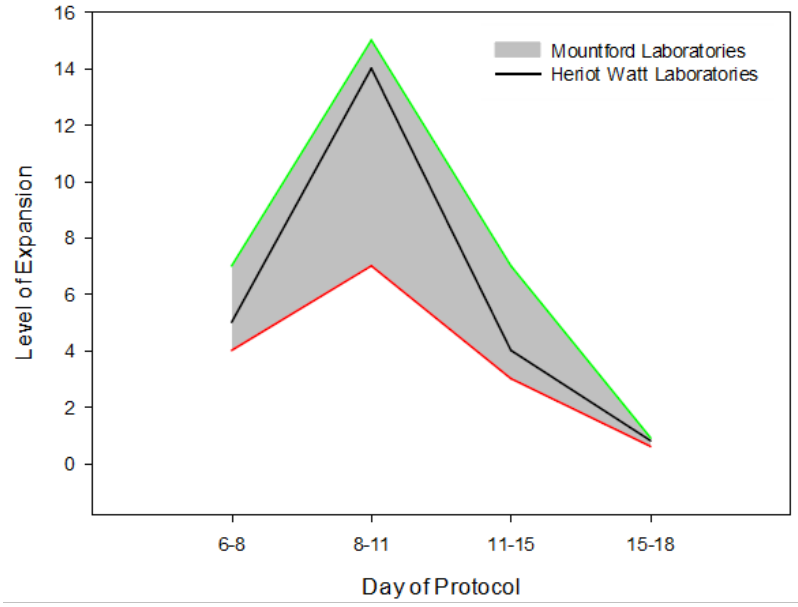

Day	Fold-Expansion
0-6	2-12
6-8	4-7
8-11	7-15
11-15	3-7
15-18	0.6-0.9
Total	**7940**

Figure 3.17; typical expansion range at Mountford Laboratories (in grey) compared with Heriot Watt Laboratories (black). Red and green are minimum and maximum ranges respectively

Cumulative fold-expansion for CD34+ cells was at a maximal value of x7940, around 40 times less than for RC9b/SFC i55 cells yielding only 7.94×10^6 cells per 1×10^4 cells/mL seeded at day 0. However these figures suggest that the Celligen BLU bioreactor could still produce a unit of blood, especially since CD34+ cells are suspension cells more amenable to scale-up

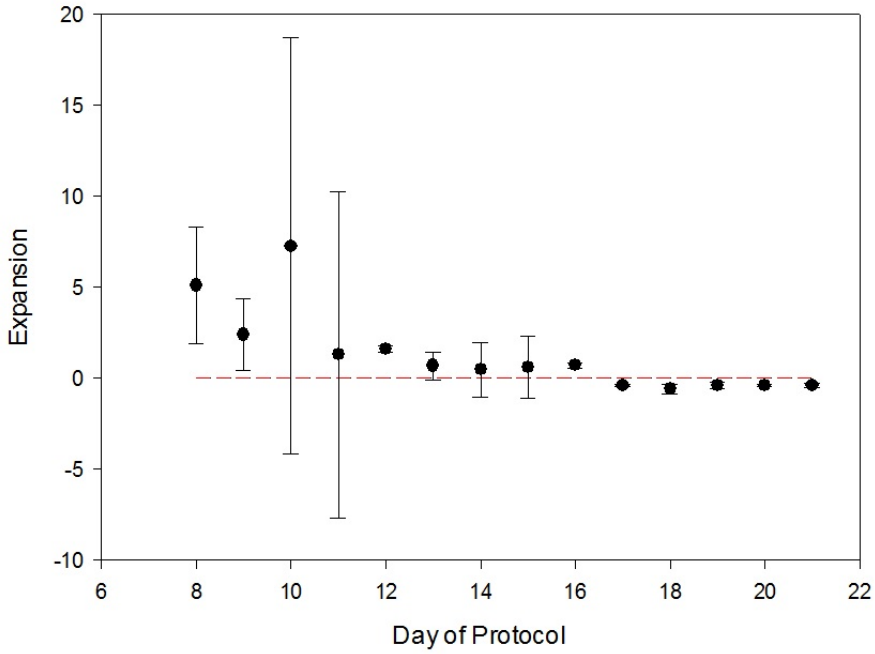

Figure 3.18; Average expansion levels of CD34+ cord blood stem cells during haematopoietic differentiation protocol. Cells characteristically decline post-thaw but recover to form expansion peak day 9-11. Following day 16 the cells decrease in number since enucleated cells lose their capacity to proliferate.

Figure 3.18 is a more in depth analysis of expansion at Heriot Watt using CD34+ cells. The cells are characteristically in lag phase post-thaw but then enter an expansion peak day 8-11 of the protocol with an overall average expansion of x14. This is also the most variable stage of the protocol as indicated by the error bars. Following this between days 12 and 15 is a second lesser expansion peak. From day 16 onwards the cells go into decline, the main reason being that they lose their capacity to replicate once they have enucleated.

3.3 Summary

At the beginning of the project red blood cells were being generated from hESCs with a view to moving to iPS cells from carefully selected donors. This chapter has shown that unexpectedly, neither the RC9b nor SFC i55 cell lines were ideal candidates for a manufacturing process since the data collected was not reproducible between laboratories. It was also shown that SFC i55 cells were not metabolically similar to RC9b which yields further investigation.

Cord blood stem cells seemed to pose a solution to this problem since their expansion and marker profile could be replicated although their fold-expansion was not as great. For the purposes of this research it was reasonable to move forward with CBS cells to find if they were ideal candidates for a GMP-compatible scalable process and yielded cells which were safe and compatible for blood transfusion.

Chapter 4 - Development of device

4.1 Introduction

Although the aim of the project was to scale-up production of red blood cells from human pluripotent stem cells, the reagent/materials cost to recurrently test a bioreactor or spinner culture vessel was so great that this was unfeasible. Instead an ultra-scale-down (USD) approach was taken to reduce cost, gain precise control over the cell microenvironment and for its potential to be integrated into a sensing platform. A microfluidic cell culture device was proposed which was amenable to both adherent and suspension cells and could be used for online continuous monitoring of differentiating cells in response to a range of oxygen concentrations. It was also hoped that the device could be used to screen for other prolific metabolites such as carbon dioxide and glucose.

Following the successful design and fabrication of the microfluidic device, it was acknowledged that the RC9b cell line did not expand enough (at Heriot Watt) to consume detectable volumes of the analyte (namely oxygen) and also that the cells were not plentiful enough for flow cytometric analysis. Hence a second, ‘mesofluidic’ device was also fabricated and is described in this chapter.

4.2 Microfluidic cell culture device

The preliminary design proposed for the microfluidic device was a simple straight channel with biosensor ‘microtrenches’ flanking a central cell culture chamber (Figure 4.1). A number of more specific considerations of the design were made based upon methods described by Beebe et al. 2002 [80] and the successful differentiation of the RC9b cell line at Mountford Labs, Glasgow.

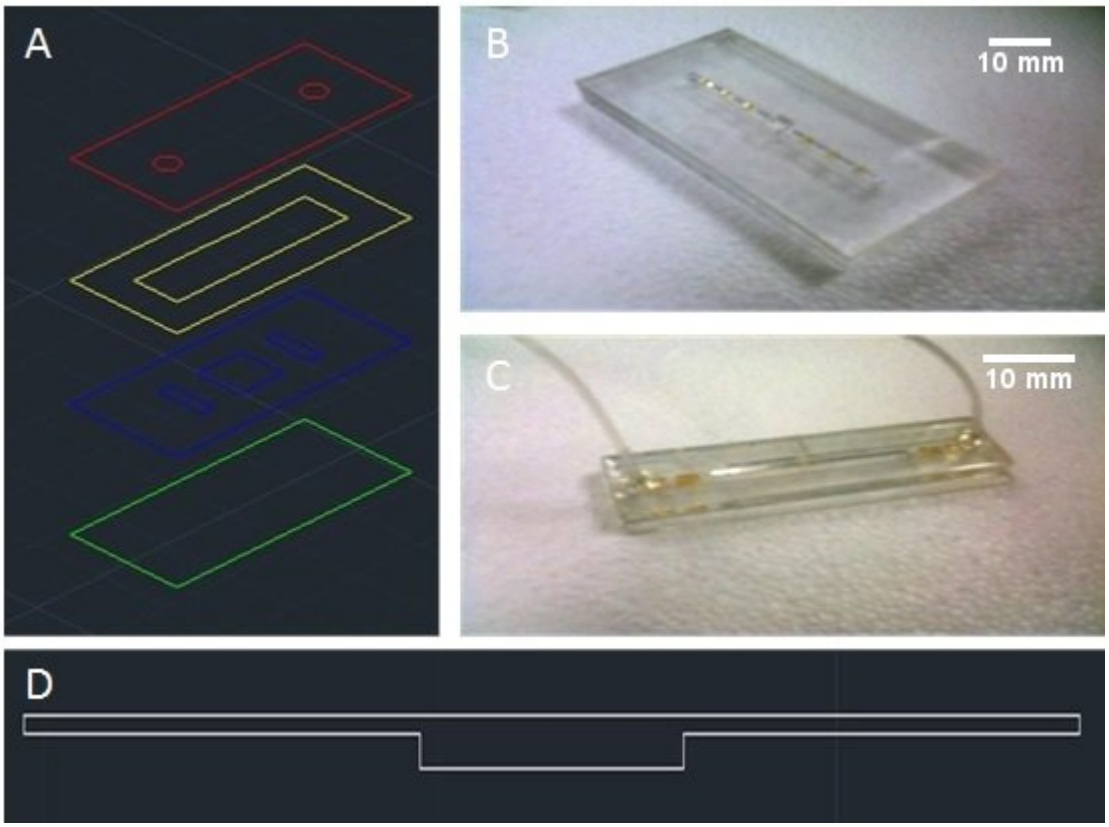

Figure 4.1; (A) Isometric view of the multilayer device as drawn into AutoCAD for laser cutting. Device top (red) with 1.58mm diameter inlet and outlet, compatible with common tubing sizes. Device Channel (yellow) which flowed over cell culture chamber and biosensor microtrenches (blue) and base (green). All pieces were laser cut into PMMA using an Epilog laser cutter and then stacked to form the device (B), which was then thermal bonded using ethanol. Inlet/Outlet holes were drilled and tubes attached using silicone sealant (C). A third hole was drilled in the side of the device for addition of cells. (D) The side view (bottom, white) shows a 0.6mm chamber height with 0.2mm channel height. Once laminar flow is developed in the channel cells in the chamber area should be protected from displacement.

4.2.1 Cell culture chamber surface area

Average cell counts of RC9b differentiated in 6-well plates designated that during the adherent stage cells grew to approximately 4.5 $x10^5$ cells/cm^2 and for the suspension stage, 3.16 $x10^6$ cells/cm^2. Since it was necessary to analyse cells by flow cytometry to allow comparison with data from other labs in the research consortium and this required a bare minimum 1.4 $x10^6$ cells, the proposed surface area for the cell culture device was 0.44 cm^2.

4.2.2 Channel height

RC9b differentiation was routinely carried out in 3mLs of media in 6-well plates with a surface area of 9.5cm^2 giving a culture height *h,* of 3.1mm. For microscale culture *h* is typically 5-10 times smaller than macroscale, resulting in a channel/chamber height range of 310-620µm [80]. For ease of fabrication and to allow for cell expansion, a chamber height of 600µm was selected with 200µm height channels flanking either side.

4.2.3 Effective culture time and critical perfusion rate

Since the device had to be amenable to adherent and suspension cells, a central cell culture chamber (6.67 mm x 6.67 mm) with raised channels either side was proposed so that laminar flow would prevent the cells from being washed out of the device. With the channel width, length and height set as 6.67mm, 6.67mm and 0.6mm respectively the ECT was calculated as 14 hours by applying the channel height ratio (5.1) to the macroscale culture time (72 hours). Since the media should be replaced every 14 hours the Critical Perfusion Rate (CPR) was estimated as 3.8µL/hour, a velocity of 7.88 $x10^{-7}$ m/s [80].

4.2.4 Channel length

One of the advantages of microfluidic devices is that diffusion is the governing force of mass transport, speeding up reaction times. The *Péclet number* (Pe) was calculated to

ensure that diffusion would dictate transport of oxygen in the device (rather than convection) using the following equation;

$$\mathrm{Pe} = \frac{N_{\mathrm{conv}}}{N_{\mathrm{diff}}} = \frac{c_i|\mathbf{u}|}{D\nabla c_i} = \frac{LU}{D}$$

Where *L* is a characteristic length scale, *U* is the velocity magnitude, and *D* is the characteristic diffusion coefficient. In order for the effects of diffusion to exceed the effects of convection, the *Péclet number* must be <1. Since the diffusion coefficient of oxygen at 37°C is approximately 2.52 x10^{-5} cm^2/s and the velocity calculated as 7.88 x10^{-5} m/s;

$$Pe = 1 = \frac{L * 7.88 \times 10^{-7}\ cm/s}{2.52 \times 10^{-5}\ cm^2/s}$$

Hence the maximum channel length which upholds diffusive action would be 32mm. It was therefore decided that a channels of 12mm ((*12mm**2) +6.67mm= 30.67mm) would be placed either side of the cell culture chamber to allow room for microtrenches, while upholding diffusive transport [80].

4.2.5 Maintaining laminar flow

The Reynolds number was calculated as <1 typical of microfluidic devices. This ensured that laminar flow would prevail inside the device.

4.2.6 Material selection

It was of paramount importance that the device be fabricated from a gas impermeable material (to conserve oxygen) which was biocompatible, hence poly-methyl methacrylate (PMMA) was chosen over polydimethylsilonane (PDMS). Materials were also selected based on affordability, biocompatibility, durability, chemical inertness and sterilization method.

4.2.7 Fabrication method

Based on the device design and material specification, laser cutting into Poly-methyl methacrylate (PMMA, purchased from Easter Road Plastics) was chosen as the most suitable fabrication method. The device design was drawn as multilayer into AutoCAD 2014 design software and then cut into layers of PMMA using an Epilog laser cutter as shown. The device layers were aligned and bonded on a hot plate with ethanol at 79°C for 30 minutes.

4.2.8 Fittings and fixtures

PEEK tubing, fittings and filters (IDEX health and Science) were purchased and used as supplied. A waste reservoir was fabricated from a Nalgene jar with a PEEK tubing inlet and a syringe filter vent, which were fastened using silicone sealant. A heat mat with a thermostat set to 37°C was placed underneath the culture chamber. A platform was constructed from aluminium angle bars and PMMA which held the device, biosensors, media/waste reservoirs and heat mat in place so that the device could be transferred easily from hood to microscope.

4.2.9 Mass flow rate controllers and pump

Three mass flow rate controllers were purchased from AliCAT Ltd and set up for CO_2, O_2 and N_2 according to the user manual. The cell culture media was continuously sparged with a predetermined air mix and the media withdrawn from the reservoir using a MilliGAT microfluidic pump.

4.2.10 Experimental set-up

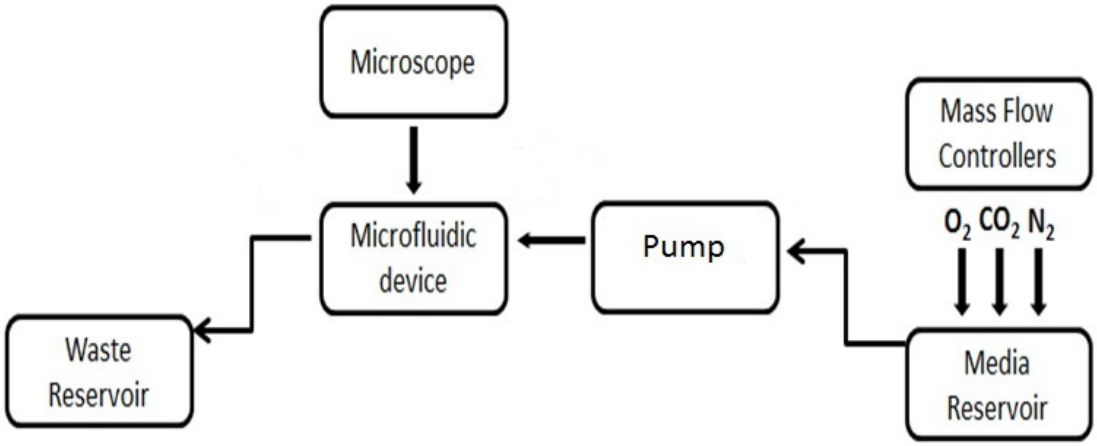

Figure 4.2; Schematic of experimental apparatus for microfluidic device. AliCAT mass flow controllers continuously sparged the media reservoir with a predetermined gas mix. The media was perfused using a MilliGAT microfluidic pump at a rate of 3.8µL/hour through the microfluidic device with in-house biosensors. The waste reservoir was connected downstream of the device. The apparatus was placed under a Zeiss Axioscope for in-situ image capture during cell differentiation.

4.2.11 Experimental method

The microfluidic device was placed in a laminar flow hood and attached to the MilliGAT microfluidic pump and media reservoir (upstream) and waste reservoir downstream. Ethanol was then perfused for >40 minutes followed by sterile DPBS and then air. Once sterile, media which had been warmed to room temperature was placed in the media reservoir and cells inserted by syringe at the designated inlet. The apparatus was removed from the hood and placed under the Zeiss Axioscope. The media reservoir was attached to the mass flow controllers for continuous gas sparging. After an hour, at which time the media/gas had equilibrated, the microfluidic pump was started.

4.2.12 Complications with device

As prior mentioned the device was based upon the maintenance/differentiation of RC9b cells cultured at Mountford Laboratories, Glasgow. When the process was transferred to Heriot Watt University the cells did not proliferate well and the protocol was deemed non-transferrable. The device however was developed successfully for use with J774 and HL60 cells with the possibility for use with other cell types.

A new device was developed which was compatible with RC9b/CD34+ cord blood cells and it was decided to base the device design on 6-well plates to ensure analyte concentration/cell expansion. The rationale for continuing with a ‘mesofluidic device’

(rather than well-plates) was the continued use of the biosensors and in-situ imaging, with the cost effectiveness of a reusable device/equipment. The PMMA microfluidic devices had reoccurring problems with contamination and so it was devised that the new device be fabricated entirely from autoclavable materials. As was discussed previously due to time constraints and the high volume of laboratory and manufacturing work required on the project alternative polymers were not suitably researched at the time. It was also felt that alternative fabrication methods may take too much development hence every effort was taken to persist with the existing methods of fabrication. The MilliGAT pump was also prone to contamination during long-term use and was replaced with an AL-2000 Syringe Pump (WPI, Europe).

4.3 Mesofluidic cell culture device

The proposed design of the mesofluidic cell culture device was again a simple straight channel flowing over a central cell culture chamber. The surface area ($9.5cm^2$), height of media (3.1mm) and ECT were all kept concurrent with a 6-well plate. The CPR was calculated as 43µL/hour

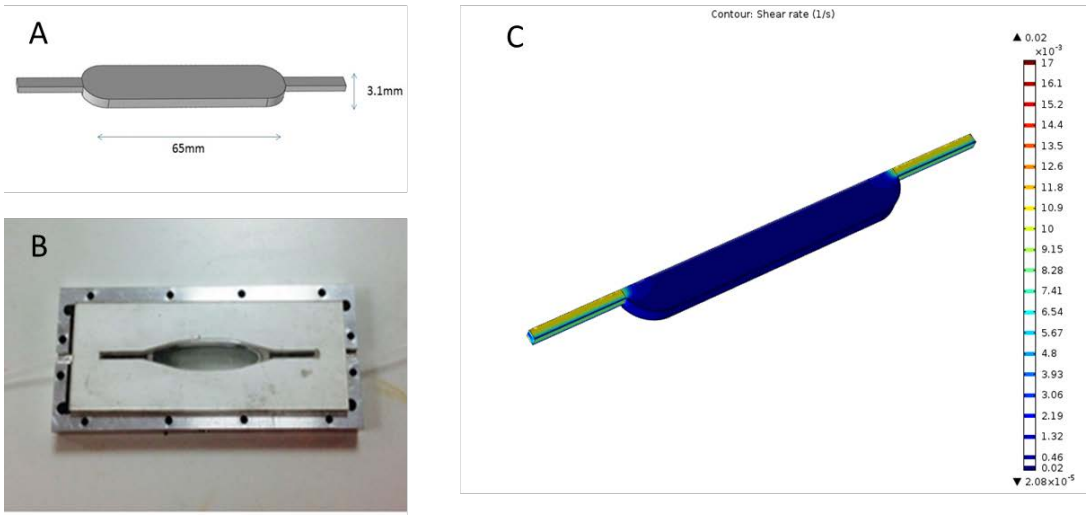

Figure 4.3; (A) Schematic of cell culture device chamber and channel. The surface area of the cell culture chamber was 9.42 cm^2 and media height 3.1mm, closely resembling that of a 6-well plate. Channel depth was 2mm to accommodate tubing. The design was cut into Stainless Steel using a milling machine, as was the clamp. The top and bottom of the device were cut from borosilicate glass and the gaskets cut from silicone sheet. Once all parts were assembled inside the clamp (B) the lid was fastened using M4 hex bolts and nuts which were tightened to 1 Nm using a torque wrench. (C) Is a CFD simulation of shear stress inside the device. It was ascertained cells would not be susceptible to shear stresses exceeding 3 x10^{-4}/s which is far below physiological shear stress.

4.3.1 Material selection

The mesofluidic device was fabricated from borosilicate glass (Newcastle Glass Ltd), stainless steel (The Metal Store) and silicone sheets (Silex Ltd). The Clamp had an aluminium base, stainless steel lid (The Metal Store) and stainless steel bolts/screws/gaskets purchased from Screw Fix. All materials were biocompatible and sterilisable by autoclave. Fittings and fixtures were as before.

4.3.2 Fabrication method

The device chamber and channel were cut into stainless steel using a Bridgeport Milling machine. A 2mm hole was drilled into the side of the chamber so that cells could be injected and sealed with a M2 stainless steel hex screw. The inlet/outlets were 10-32 coned ports so that IDEX health and Science fittings with PEEK tubing could be screwed directly into the device. The aluminium clamp base was also milled and 3.6mm holes for M4 screws were cut using a drill. Initially the clamp lid was made from aluminium but it warped under autoclave/screw pressure and so a stainless steel replacement was laser cut. Top and bottom glass pieces were made to measure and used as supplied from Newcastle Glass Ltd. The bottom glass piece was permanently attached to the stainless steel chamber using silicone sealant. Silicone sheeting was cut to size using a scalpel for use as a gasket to seal the glass lid. All parts were rinsed in acetone followed by deionised water to clean before assembly and autoclave to sterilise.

4.3.3 Experimental set-up

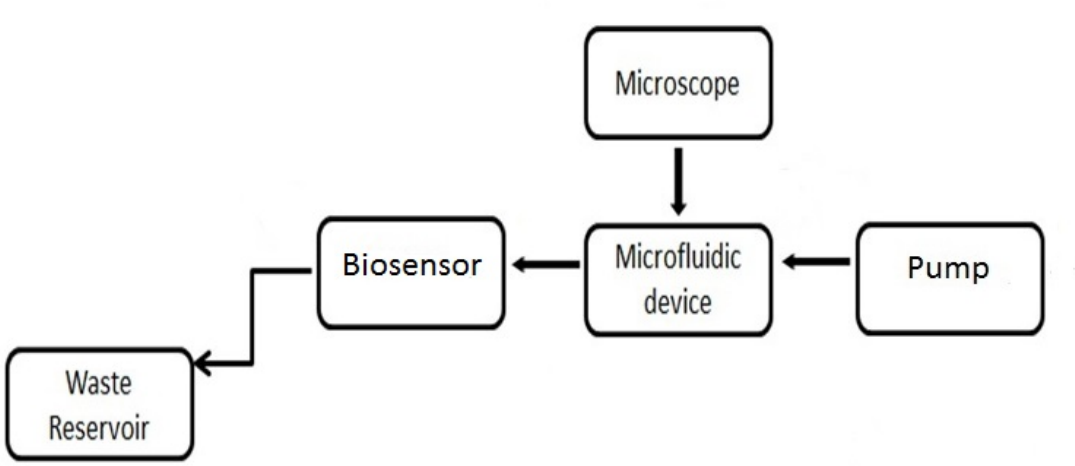

Figure 4.4; Schematic of mesofluidic experimental set-up. Media was pre-sparged with gas of pre-determined concentration and then loaded into an SGE gas tight syringe under sterile conditions. The syringe was placed on the AL-2000 syringe pump and perfusion through the device set at 43µL/hour. The biosensor was placed downstream of the device and was connected to the waste reservoir. The apparatus was left under a Leica Dmi8 microscope for in-situ imaging

4.3.4 Experimental method

The apparatus was assembled (Other than the gas tight syringe and biosensor) and autoclaved for 15 minutes at 121°C. The gas tight syringe was sterilised by UV and the biosensor by passing ethanol for 40 minutes followed by sterile DPBS. Once all parts were sterile they were assembled in a laminar flow hood. Media (at room temperature) was drawn into the syringe and connected to the inlet tubing. Cells were added to the device by syringe/needle via the M2 inlet which was then screwed shut. Following assembly the apparatus was moved to the Leica DMi8 microscope and the AL-2000 pump set to 43ul/hour.

4.4 Biosensors

4.4.1 Oxygen

Ruthenium-tris (4,7-disphenyl-1, 10-phenanthroline) dichloride Ru (dpp) was purchased from Sigma-Aldrich (now Merck) its fluorescence is strongly reduced by molecular oxygen due to dynamic quenching. The complex was dissolved in ethanol to final concentration of 1mg/ml. The ethanol dissolved ruthenium was then mixed with PDMS polymer base and curing agent in volume ratio of 1:10:1 then stirred until evenly distributed. In the beginning the mixture was applied to ‘microtrenches’ but was later spin-coated onto circular coverslips. Once formed the biosensors were degassed for 30 mins and cured over 3 hours at 65°C. Although the biosensors were developed successfully Sigma-Aldrich discontinued Ruthenium-tris (4,7-disphenyl-1, 10-phenanthroline) dichloride Ru (dpp) mid-way through the project and despite every effort a good quality, affordable replacement could not be found. For the latter part of the project biosensors were instead purchased from Ocean Optics.

4.4.2 Glucose

ConA-TRITC and FITC-dextran were prepared in DPBS at a mass ratio of 100:1 and then added to 4% (w/v) low melting agarose solution at 48°C to a final concentration of 500:5 mg/mL. The microtrenches were then filled and allowed to solidify for 1 hour. Eight alternating coats of poly-allyl-amine hydrochloride (PAH) and poly-sodium 4-styrenesulfonate (PSS) were then applied alternately (four each) allowing 30 minutes for drying between each application. Although this biosensor was effective in detecting glucose the PAH/PSS film could not be sterilized and hence this biosensor needs further development and was not used for experiments.

4.4.3 Carbon Dioxide

8-Hydroxypyrene-1,3,6-Trisulfonic Acid, Trisodium salt (HPTS) is a highly water-soluble pH indicator which can be immobilized in hydrogels. Although it does not detect carbon dioxide per se it can be used to monitor the pH of the media which is a product of the fusion of carbon dioxide with the media (although cell metabolism also affects pH). Although several attempts were made to encapsulate HPTS in PDMS its fluorescence properties were lost during fabrication. Since HPTS requires ratiometric detection its use would have necessitated the purchase of an additional filter cube. Hence it was decided not to progress further with this biosensor although recently successful HPTS biosensors have been produced using other matrix materials.

4.4.2 Chambers

Initially biosensors for the microfluidic device were situated either side of the culture area in microtrenches however they were later housed in separate chambers. Biosensor chambers were drawn as multilayers in AutoCAD and cut into PMMA using an Epilog laser cutter. The biosensor was applied to the chamber base and the layers bonded using dichloromethane. Tubing was applied to inlets/outlets using silicone sealant.

4.5 Summary

Two devices were successfully developed for use on the project (micro and mesofluidic) The microdevice encompassed all of the benefits that USD has to offer with significantly reduced media costs, easy integration into a microscopy platform and shortened reaction times (ECT). However laser cutting proved more difficult than anticipated, since considerable trial and error was necessary to optimise the microstructures, particularly when cut into thin (200µm) PMMA. Several months were also spent on bonding these devices using thermal bonding, UV adhesive, sheet adhesive, biocompatible wax and silicone sealant. Many of these methods were not compatible with ethanol which was necessary to sterilise the PMMA. Unfortunately information on bonding in microfluidics is scarce and is usually acquired through personal recommendations. Upon successful bonding of the device with ethanol and heat the leak-proof device was prone to serial contaminations, which was the rationale for switching to autoclavable materials in the mesofluidic device. This second device was successful from the onset armed with knowledge and experience from the failures of the microfluidic device. However many of the microfluidic advantages were lost since reagent usage and ECT remained unchanged. It was however amenable to use with biosensors and in-situ microscopy.

In hindsight the development of three biosensors (in light of other difficulties experienced during the project) was overly ambitious, particularly since they were not amenable to sterilization methods. Again although there is abundant information on the development of biosensors, few of these mention sterilization methods or indeed compatibility to cell culture devices. [64][65][67]. This could be considered for future work in the development of microfluidic devices and biosensors.

Chapter 5 - Oxygen Experiments

5.1 Introduction

Oxygen is usually the principal limiting factor in the scale-up of bioprocesses. Industrial scale bioreactor cultures require constant oxygenation by sparging with mechanical mixing to ensure all gasses and nutrients are mixed homogenously. Since the majority of cell death and damage is incurred through bubble damage, a reduction in sparge rate which does not limit oxygen would certainly be advantageous. There is evidence to suggest that human embryonic stem cells require less oxygen due to the paucity and immaturity of their mitochondria and that in some instances hypoxia is in fact beneficial since it reduces oxidative stress. It is unknown whether this is true of the RC9b or CD34+ cell lines but as shown in Chapter 3 their mitochondria are indeed subsidiary to more conventional cell lines. It was therefore anticipated that a reduction in oxygen concentration might improve culture health and expansion and it was hoped that by finding the respiration rate of cells at successive stages of the protocol it would be possible to calculate the critical oxygen concentration for scale-up to bioreactor culture.

5.2 Ruthenium biosensor calibration

A calibration was performed for each biosensor prior to use by flushing 37°C cell culture media through the chamber at 0 and 5, 10 or 21% oxygen (dependent on experiment) and recording fluorescence intensity at 100ms.

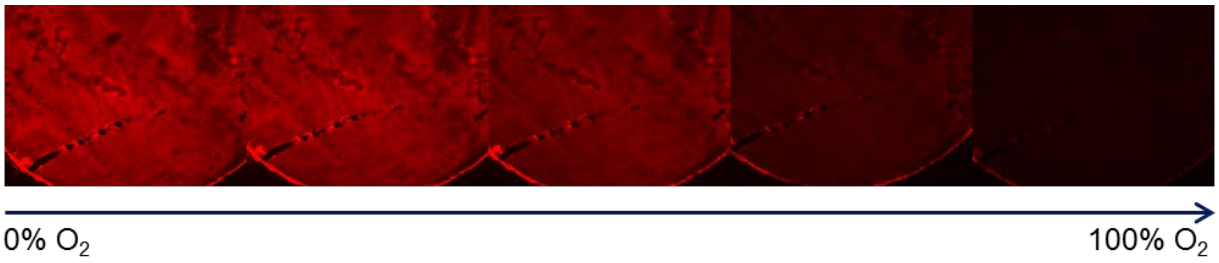

Figure 5.1; Ruthenium biosensor at increasing oxygen concentrations from 0 to 100%. Since the Stern-Volmer Equation becomes less reliable at high quencher concentrations the biosensor was calibrated at 0 and the maximum value (5, 10 or 21% oxygen) as determined for each experiment.

Since ruthenium fluorescence is dynamically quenched by oxygen its fluorescence intensity diminishes with increased oxygen concentration (Figure 5.1)
The *I/Io* ratio (as described previously) was then plotted against oxygen concentration (µg/mL) to find the Stern-Volmer constant. This could then be used to calculate how much oxygen was consumed during each experiment.

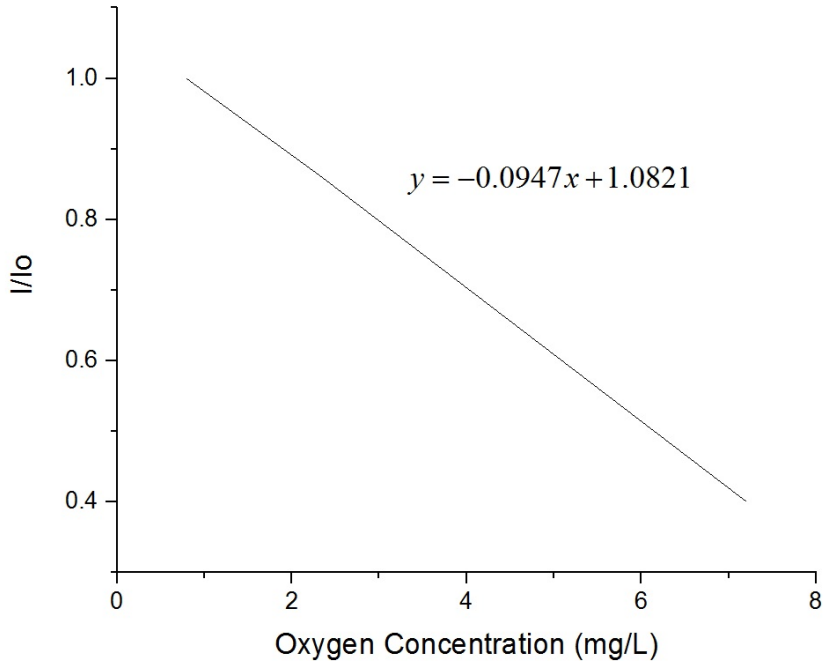

Figure 5.2; Oxygen concentration (mg/L) with fluorescence intensity in presence of quencher (I) over fluorescence intensity in absence of quencher (Io) to gain Stern-Volmer constant, in this instance -0.0947. This was calculated prior to each experiment and used to find the corresponding oxygen concentration for its duration

5.3 Preliminary device experiments

Prior to and following each experiment the biosensors were tested for accuracy using a series of media with known oxygen concentrations. Device apparatus were set up as specified in Chapter 4. Images of biosensors and cells were captured at the beginning (T0) and the end of each experiment (T*n*) as a minimum but where possible were taken every 24 hours. Cells were counted at the end of each experiment and experimental pictures were used for cell counting using ImageJ. For the J774 and RC9b trials cell counting was the only form of analysis but once experiments began with CBS cells they were removed from the device post-experiment and analysed for cell markers, apoptosis/necrosis, Hif-1-α, mitochondria, ROS and enucleation using flow cytometry.

5.3.1 J774 Trials

Preliminary tests with the cell culture device and biosensor were conducted with model adherent cell line J774 at ambient (21%) oxygen to ensure that the device was in good working order prior to use with RC9b cells.

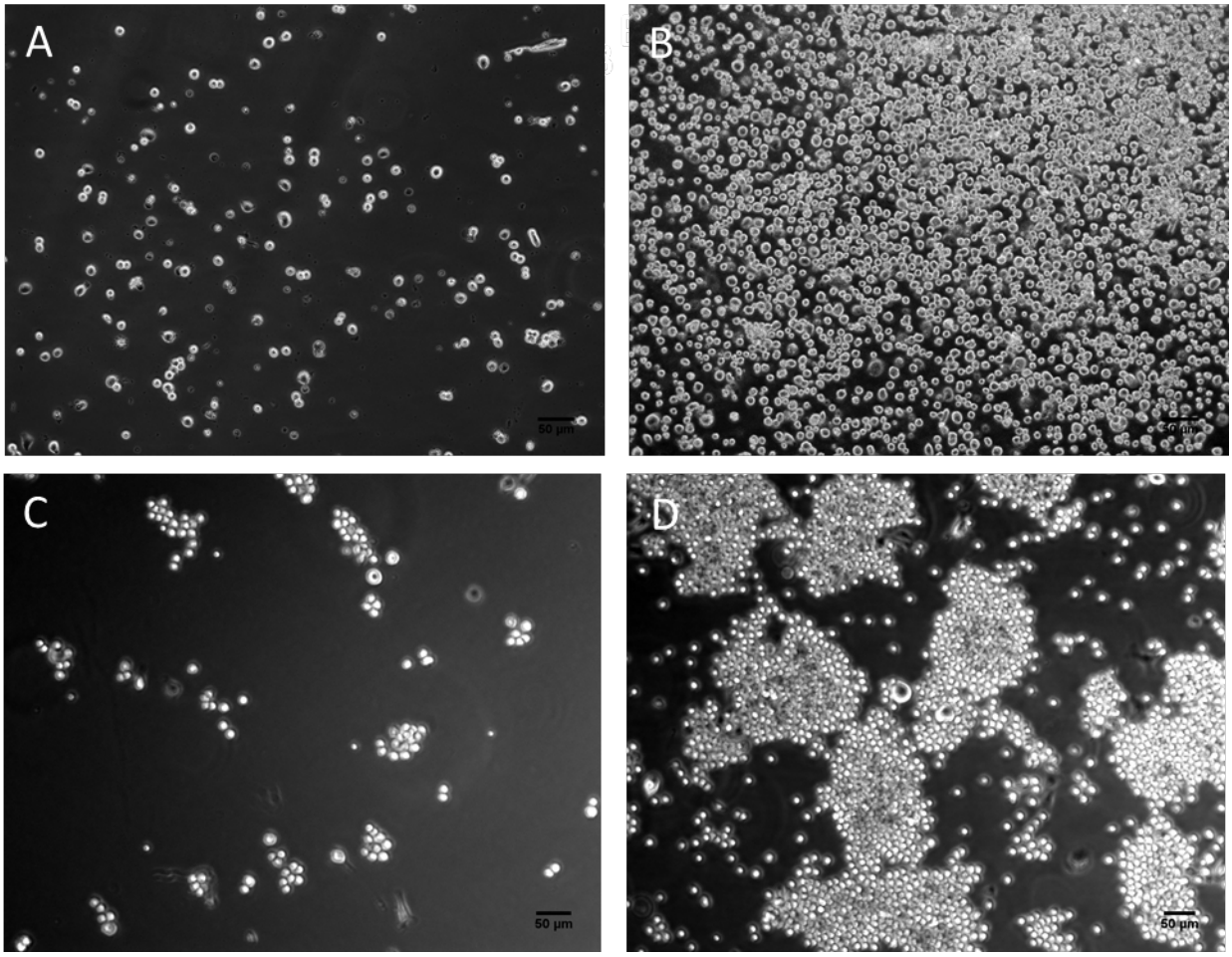

Figure 5.3; J774 Murine macrophage cells grown in mesofluidic cell culture device at 21% oxygen captured at (A) 24 and (B) 48 hours with comparative cultures grown in a 37°C 5% CO2 incubator (C&D). Although cells differ in growth pattern (cells grow in patches on treated cell culture flask surface) the cultures demonstrated similar rates of expansion

Images captured at 24 and 48 hours (Figure 5.3) confirmed that adherent haemocytic cells were compatible with the culture device and could be cultivated over the extended periods of time required for RC9b differentiation (>48 hours). Cells were counted every 24 hours throughout the culture period and compared with control cultures which were grown simultaneously in 37°C 5% CO_2 incubators. There were no significant differences to be found between the cell counts and furthermore the ruthenium biosensor was used to successfully obtain an estimation of oxygen consumption per cell (between 13 and 92 amol $cell^{-1}$ sec^{-1}) which was within range of the literature value

recorded for J774 cells (31 amol $cell^{-1}$ sec^{-1}). Also of note is that the cells use markedly more oxygen during log phase than the stationary phase of growth

The only perceptible difference between the culture images was the growth pattern, as J774 cells grew in patches on treated cell culture flask substrates rather than randomly. This was not considered a concern for RC9b cells since cells had been successfully grown on a number of substrates including glass.

Table 5.1; Cell counts/doubling times for J774 cells grown in the device and incubator were markedly similar. The ruthenium biosensor was also used to successfully calculate oxygen consumption at 24 and 48 hours. Following the success of this experiment it was decided to trial the device with RC9b cells

Hour	**0**	**24**	**48**
I	50.43	55.76	57.19
I/Io	0.378399	0.418382353	0.429089136
O2 (ug/mL)	7.20	6.78	6.67
Cell Count			
Device	1000000	1650000	3000000
Doubling time	-	33.22	27.83
Cell Count			
Incubator	1000000	1600000	3060000

5.3.2 RC9b trials

Following the success of the J774 trials RC9b cells were cultured in the device from day 3-7 of the protocol in hypoxic conditions (3% oxygen). Images taken at Days 3, 4, 6 and 7 show that growth in the device was far more expansive than in the incubator control cultures (Figure 5.4). At day 7 the cells were harvested and counted. Cell doubling time under hypoxic conditions was more than halved from 106.2 to 42.34 hours.

Table 5.2; Cell counts/doubling time for RC9b cells grown in the device was more than halved in comparison to the control incubator culture. The ruthenium biosensor was also used to successfully calculate oxygen consumption at 72 hours following the experiment which indicated an oxygen consumption rate of 2.04 amol cell^{-1} sec^{-1}

Hour	0	72
I	120.83	121.07
I/Io	0.9112	0.913
O2 (µg/mL)	1.71	1.65
Cell Count Device	1000000	3250000
Doubling time	-	42.34
Cell Count Incubator	1000000	1600000
Doubling time	-	106.2

Biosensor readings were taken at 0 and 72 hours. This experiment was only completed once due to aforementioned problems with the RC9b cell line and serial contaminations in the microfluidic PMMA device. The overall oxygen consumption rate of differentiating RC9b cells was calculated as 2.04 amol cell^{-1} sec^{-1} which is close to the experimental value for CBS cells (2-3.5 amol cell^{-1} sec^{-1}, Figure 5.4). This result coupled with the amplified fold-expansion were considered very encouraging in terms of scale-up and await further investigation once the cell lines/reagents are more established.

As described earlier the device was proposed for use with CD34+ cord blood cells and prior-tested with the model haemocytic suspension cell line HL60.

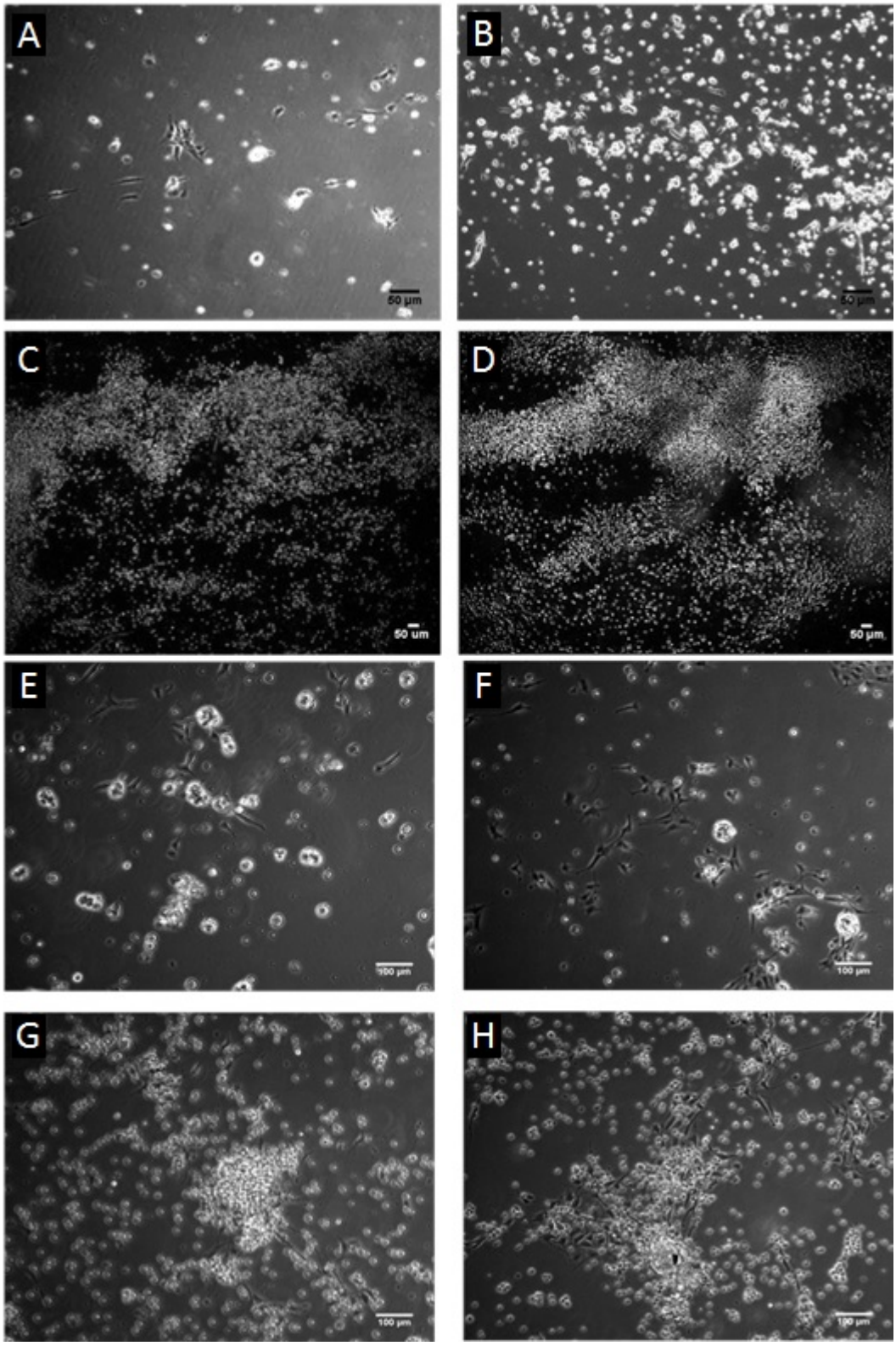

Figure 5.4; (A) Cells (At day 3 of protocol) in device 4 hours post-seeding (B) at 24 hours and then 56 (C) and 72 (D) hours with comparable pictures of incubator cultures (E, F, G and H)

5.3.3 HL60 trials

Since the device had already been established for long-term use with adherent J774 and RC9b cells, the main/only issue was to ensure it would work with suspension cells i.e. they would not wash out under flow conditions. Briefly, the device was trialled for 24 hours with HL60 cells and it was found that cells remained in the device and proliferated normally.

5.4 Cord blood device experiments

5.4.1 Rate of oxygen utilization

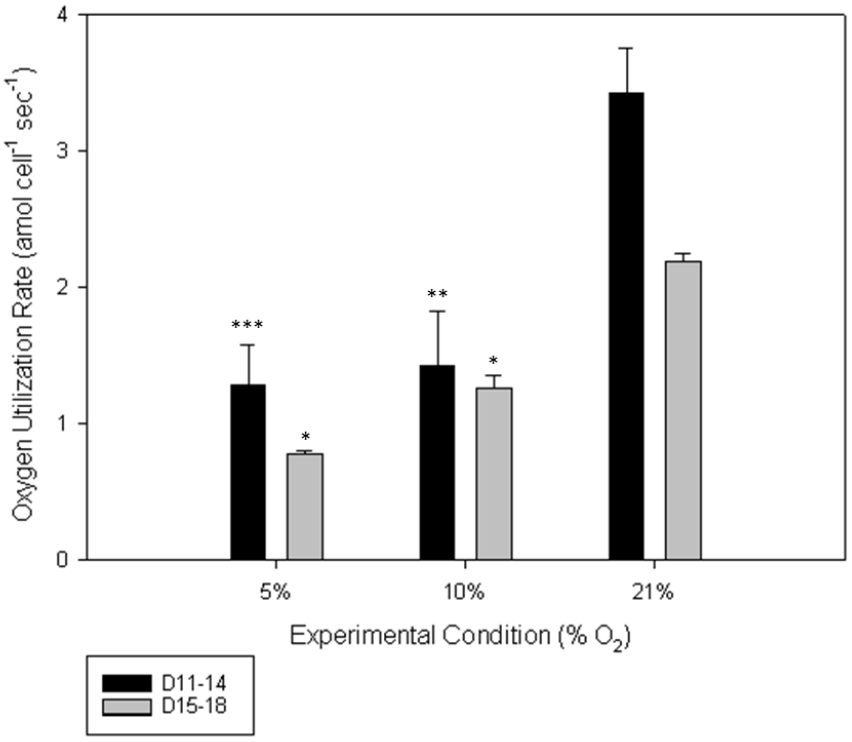

Figure 5.5; Oxygen Consumption Rates (amol cell^{-1} ml^{-1}) of Differentiating CD34+ Cord Blood Cells at D11-14 and D15-18 at 5, 10 and 21% O_2 in cell culture device. As predicted cells consumed more oxygen in the early stages of development as opposed to the latter stages. Oxygen consumption rate was significantly lower at 5 and 10% oxygen when compared with 21% as indicated by asterisks.

As predicted CD34+ differentiating cells consumed less oxygen than the average for haemocytic cell types. Of the two time frames tested, D11-14 had the highest oxygen consumption, most likely due to their conserved mitochondria at this stage in the differentiation process. At 10% and especially 5% oxygen the cells consume markedly less oxygen and should have switched to anaerobic glycolysis as a main energy source. The D15-18 cells however seem less affected by hypoxic conditions since they should already have switched to glycolysis as their main energy pathway.

5.4.2 Expansion

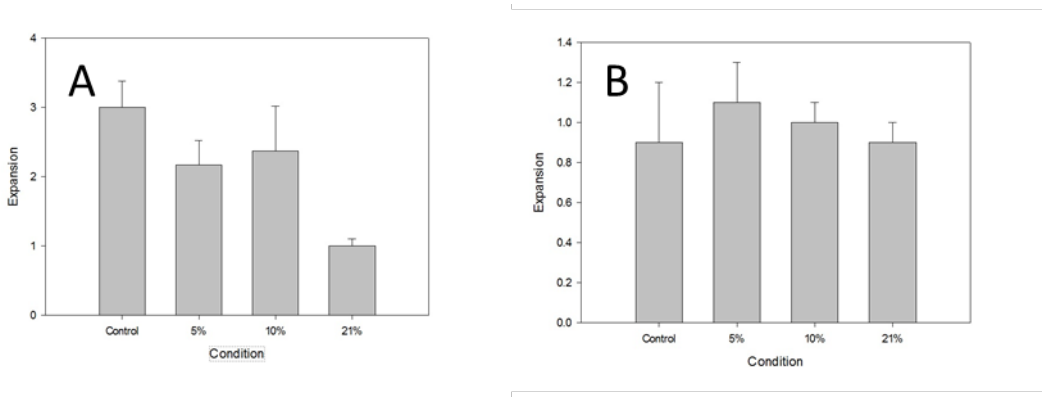

Figure 5.6; Expansion for (A) D11-14 and (B) D15-18 at 5, 10 and 21% oxygen in cell culture device compared with incubator control cultures. Encouragingly D11-14 cells grew marginally better in 5 and 10% oxygen in the device when compared with 21% oxygen. However none of the cultures grew as well as the incubator control cultures. D15-18 cells were less effected by oxygen level but similarly showed some improvement in expansion at 5 and 10%

As anticipated CD34+ cells showed greater expansion at 5 and 10% oxygen tensions in comparison to 21% cultures carried out in the device. The marker profile was also experimentally interesting (next section) however the device cultures did not grow so well as the control incubator cultures, even at ambient oxygen. A large -80°C freezer which was placed next to the device apparatus was the expected cause of the lacklustre expansion since its substantial vibration caused the cells to shudder for prolonged periods. Following two rounds of experiments (from which Figures 5.5-5.8 are formulated) the apparatus was moved away from the -80°C freezer. Following this the

third round of experiments showed reduced expansion under hypoxic conditions in comparison to control cultures and hence the experiments were repeated in static conditions (Section 5.5)

5.4.3 Marker profile

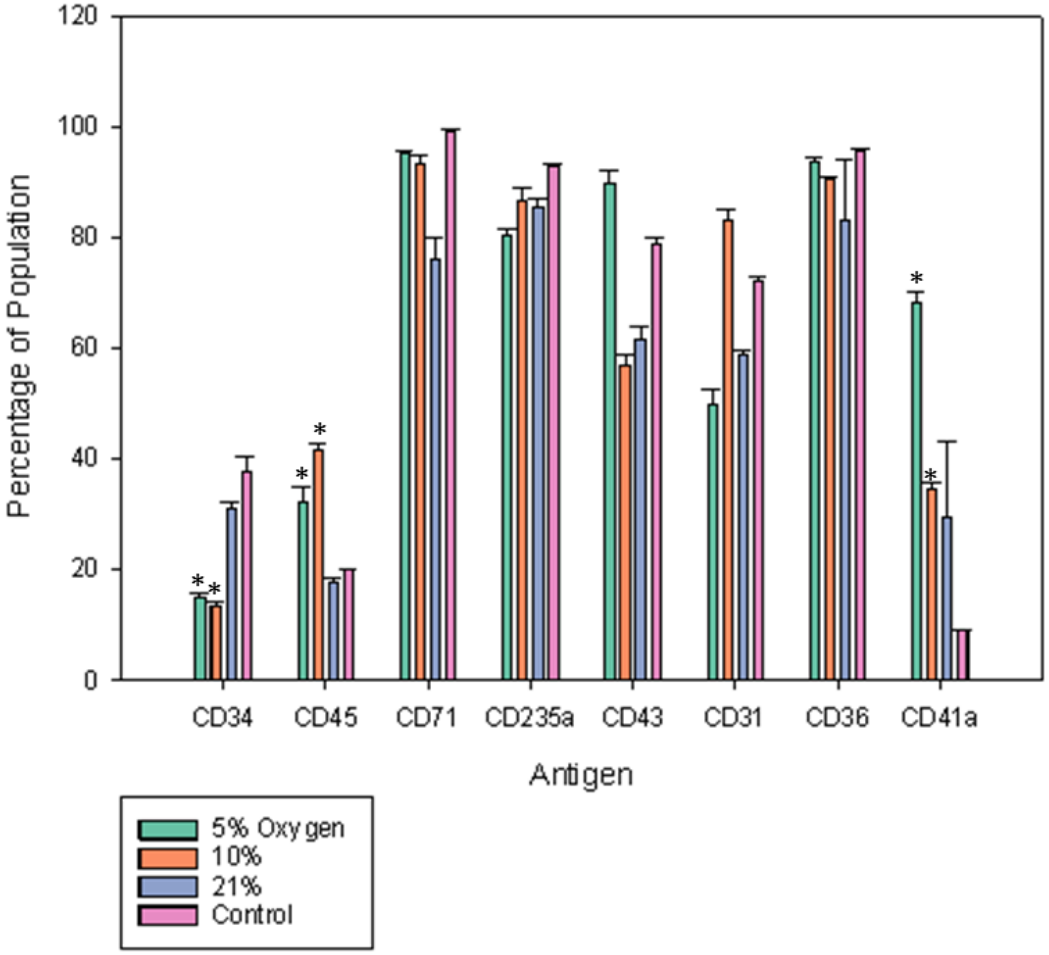

Figure 5.7; Mean antigenic markers recorded following D11-14 experiments with 5, 10 and 21% oxygen in device alongside control Incubator cultures. Most of the markers appear unaffected however CD34 and CD45 immature cell markers are significantly lower and higher respectively, for 5 and 10% oxygen. Additionally the CD41a platelet marker was significantly higher for 5 and 10% oxygen suggesting that hypoxia induces cells to produce platelets. However this effect was also observed in the device for 21% indicating that this effect could be a product of the device conditions, not necessarily oxygen concentration.

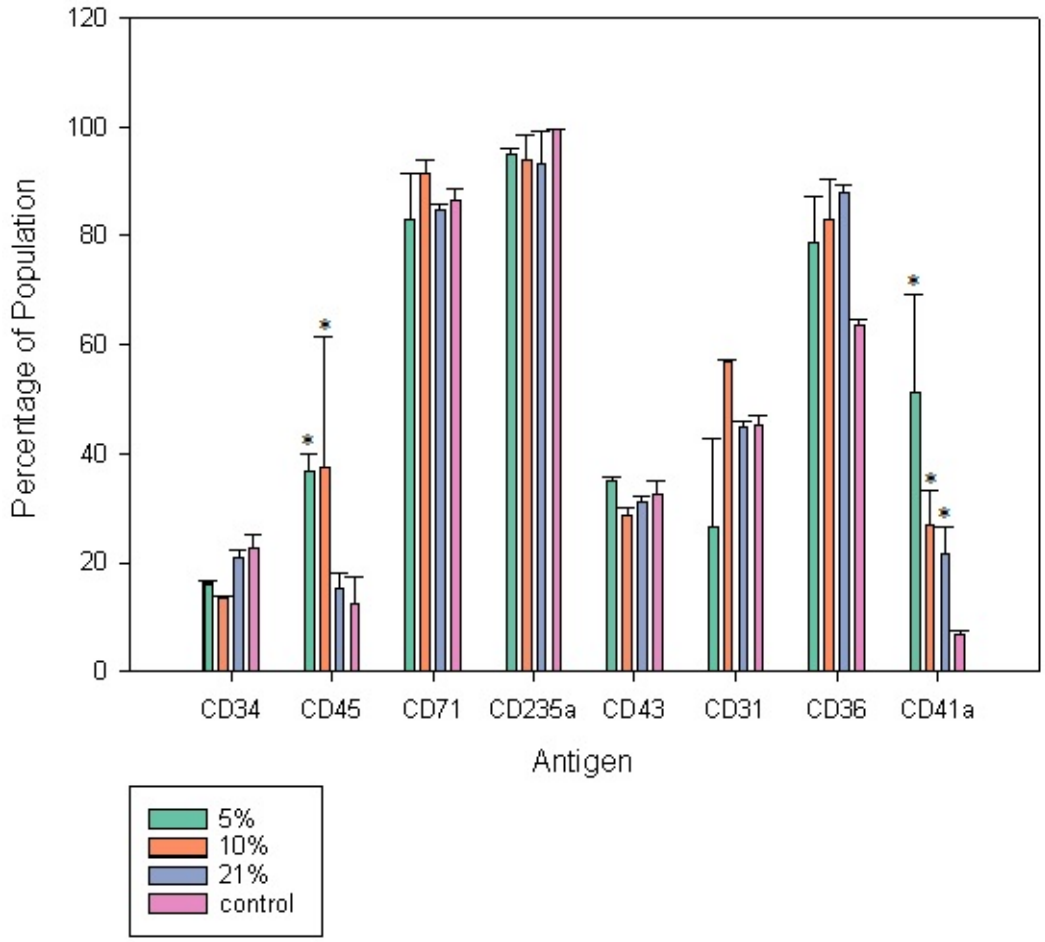

Figure 5.8; Mean antigenic markers recorded following D15-18 experiments with 5, 10 and 21% oxygen in device alongside control Incubator cultures. As for D14 most of the markers appear unaffected however CD34 markers are marginally lower and CD45 cell markers are higher for 5 and 10% oxygen. The CD41a platelet marker was significantly higher for 5 and 10 and 21% oxygen suggesting that either hypoxia, device conditions or both induce cells to produce platelets.

Since the differences in the CD41a platelet marker were also observed in the ambient condition it was supposed they were attributed to either (a) differences in media imposed by perfusion system (b) mild long-term shear effects inflicted by the vibration of external equipment and/or perfusion system or (c) the combination of shear and hypoxia. It was also possible that the device conditions were having an effect on expansion and other antigenic markers. In order to investigate this further 5, 10 and 21% oxygenated cultures were run as static cultures in cell culture flasks in a 37°C incubator.

5.5 Cord blood static cultures

Since the device experiments yielded some unexpected results a secondary static culture experiment was devised to discover whether the platelet markers were a true product of hypoxia or whether they were induced by the mild shear environment of the device. These cultures were treated the same way as the control cultures only they were placed inside a closed chamber inside an incubator set at 37°C. The mass flow controllers (described previously) were set at the desired gas blend and the line led into the chamber with a vent at one side to allow for pressure.

5.5.1 Expansion

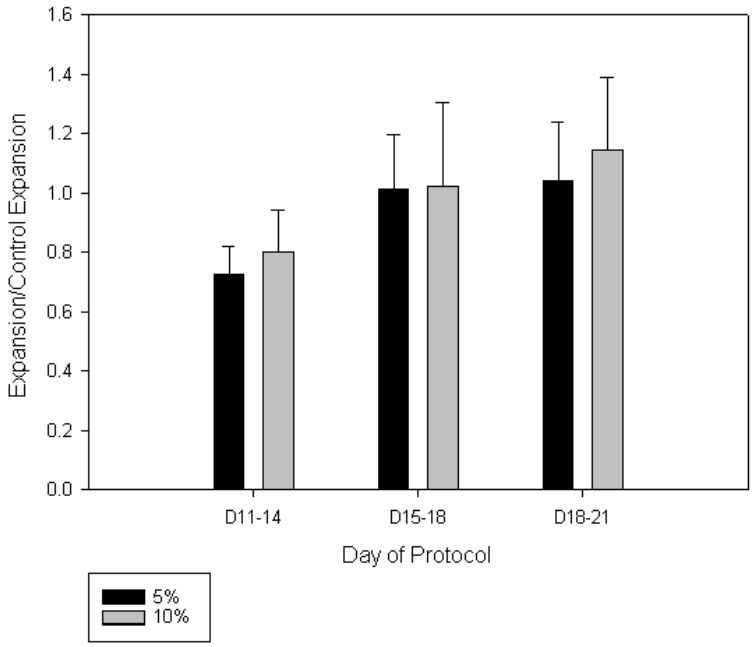

Figure 5.9; Experimental expansion/Control expansion i.e. levels >1 indicate that proliferation is not affected by low oxygenation. D11-14, typically the peak expansion period, exhibited remissive proliferation for both 5 and 10% oxygen. However for Day 15-18 following mitochondrial expulsion, expansion was similar to control cultures. By D18-21 expansion is improved in comparison to control cultures

In conflict with device cultures (and anticipated results) the CD34+ cells did not proliferate so well in hypoxic conditions as in the ambient. It was therefore deduced that expansion data for the device was unreliable and that the CD34+ cells do not proliferate well under hypoxic conditions before Day 14. These results were surprising since mitochondrial profiling had shown similar levels between RC9b and Day 8 CD34+ CBS cells and it was hoped that hypoxia would increase cell yield for both types of stem cell. However since these cells are isolated from different environments *en vivo* and are maintained differently *in vitro* perhaps too many assumptions have been made about the interchangeability of stem cells and their abilities to generate functionally identical cells. Encouragingly though in terms of scale-up, the cells did proliferate well in hypoxia from day 15 onwards, supporting the case that sparge rate can be substantially reduced at this stage.

5.5.2 HIF-1- α

All cells were analysed for Hypoxia-inducible-factor 1-alpha (HIF-1- α), however the results came back inconclusive. One explanation is that the oxygen tensions used during experimentation were not low enough although this seems unreasonable since it was shown that oxygen utilization was downregulated in response to both 5 and 10% oxygen, a hall-mark of the Hif-1 response. Another explanation is that CD34+ cells do not induce this response to hypoxia. This also seems unlikely since Hif-1 is highly conserved and moreover all nucleated cells in the human body are known to induce this response to hypoxia. The most likely explanation is that flow cytometry is not a suitable analysis method for Hif-1-α as was initially thought. This would be better assessed by Western blot should the experiment be repeated.

5.5.3 ROS

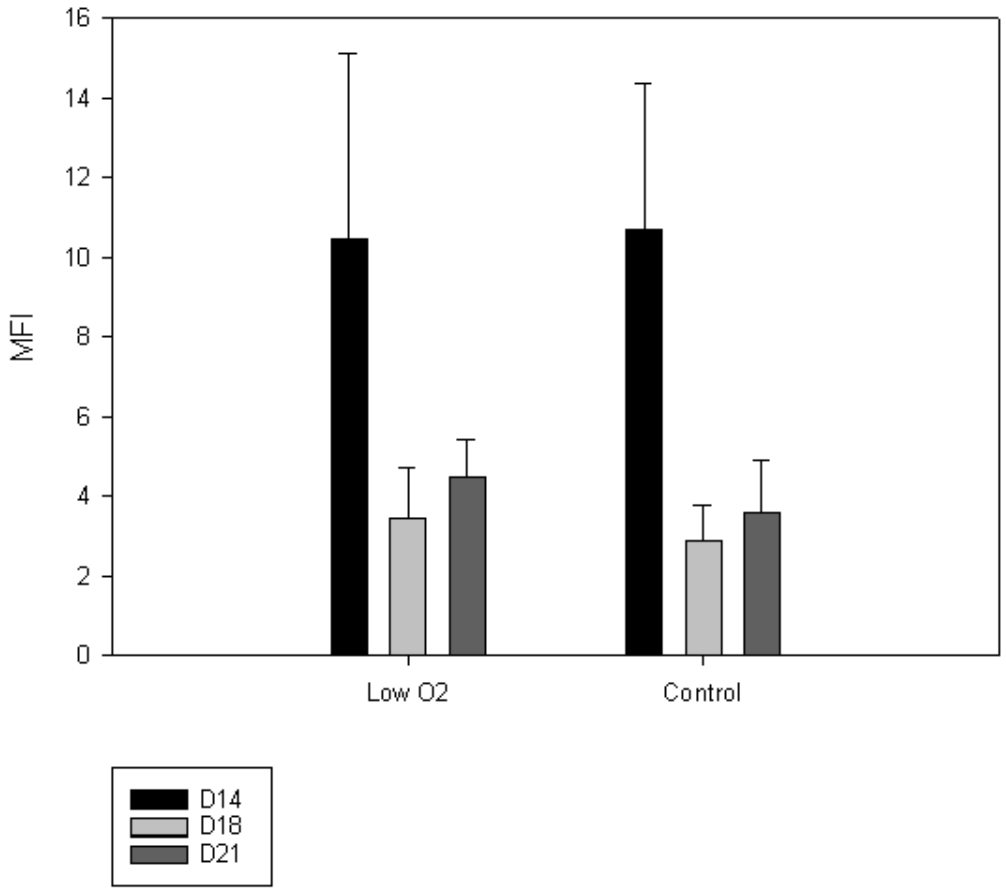

Figure 5.10; Reactive Oxygen Species Recorded by flow cytometry at Day 14, 18 and 21 for CD34+ differentiating cells in low (5% and 10% combined) and ambient oxygen. Contrary to the hypothesis that cells in ambient oxygen have higher instances of reactive oxygen species, the profiles were very similar for each condition. Up to Day 14 Cells have a higher inclination for ROS

It was conjectured at the beginning of this research that cells in hypoxic environments may benefit from lower occurrence of Reactive Oxygen Species (ROS). However there were no apparent differences in ROS for any of the conditions tested. It was of note that before day 14 cells have higher incidence of ROS which may be due to retainment of mitochondria and/or nuclei. The similarities in ROS between the low and high samples may explain why there was little impact on expansion.

Initially it was anticipated that ROS would be naturally elevated in all ambient (control) cell cultures as a residue of cellular metabolism, able to diffuse in and out of cells in culture. However it would seem that ROS only accumulate inside cells as direct product of mitochondrial action. It is unclear what happens to mitochondria under hypoxia, some journals report downregulation of action and others biogenesis and upregulation. The experimental results are contradictory since it was shown that oxygen utilization was downregulated under hypoxic conditions however Figure 5.11 shows that the mitochondrial MFI was higher which would indicate upregulation/biosynthesis. Since it was earlier shown that mitochondria are extruded on day 14 of the protocol perhaps the increased MFI is a result of upregulated mitochondrial expulsion in response to hypoxia. It is hence difficult to speculate on the similarities of ROS between control and hypoxic conditions. As before perhaps the analysis method was not sensitive enough since the difference in oxygen utilization (approximately 2 amol $cell^{-1}$ sec^{-1}) between hypoxic and control cultures is markedly small and may not accumulate detectable differences of ROS.

5.5.4 Mitochondria

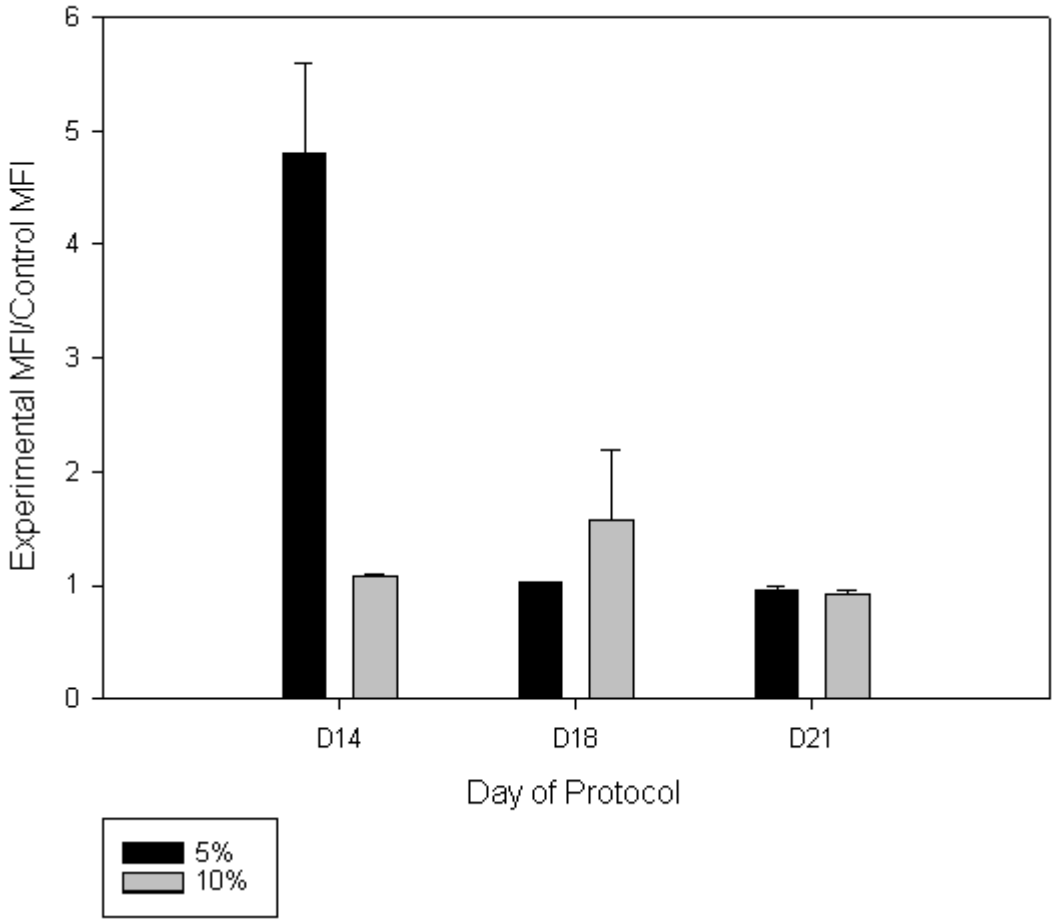

Figure 5.11; Mitochondrial MFI for Day 14, 18 and 21 of cells treated with 5 and 10% oxygen in comparison to control cultures. The mitochondrial MFI of cells at day 14 cells grown in 5% oxygen was almost 5 times higher than control cultures

The mitochondrial MFI of Day 14 cells grown in 5% oxygen was almost 5 times higher than that of control cultures. This could mean that more mitochondria are produced in response to hypoxia or that mitochondria work at a higher rate since the assay works by accumulation. Since it was found to the contrary that oxygen utilization is lower under hypoxic conditions that the mitochondrial signal peaks on day 14 prior to mitochondrial expulsion and since early-onset enucleation has been recorded under hypoxic conditions (next section) it is supposed that the elevated MFI is a symptom of mitochondrial

clearance. Since there was no recorded upregulation HIF-1-α it is not sure by which mechanism cells produce this response.

5.5.5 Marker profile

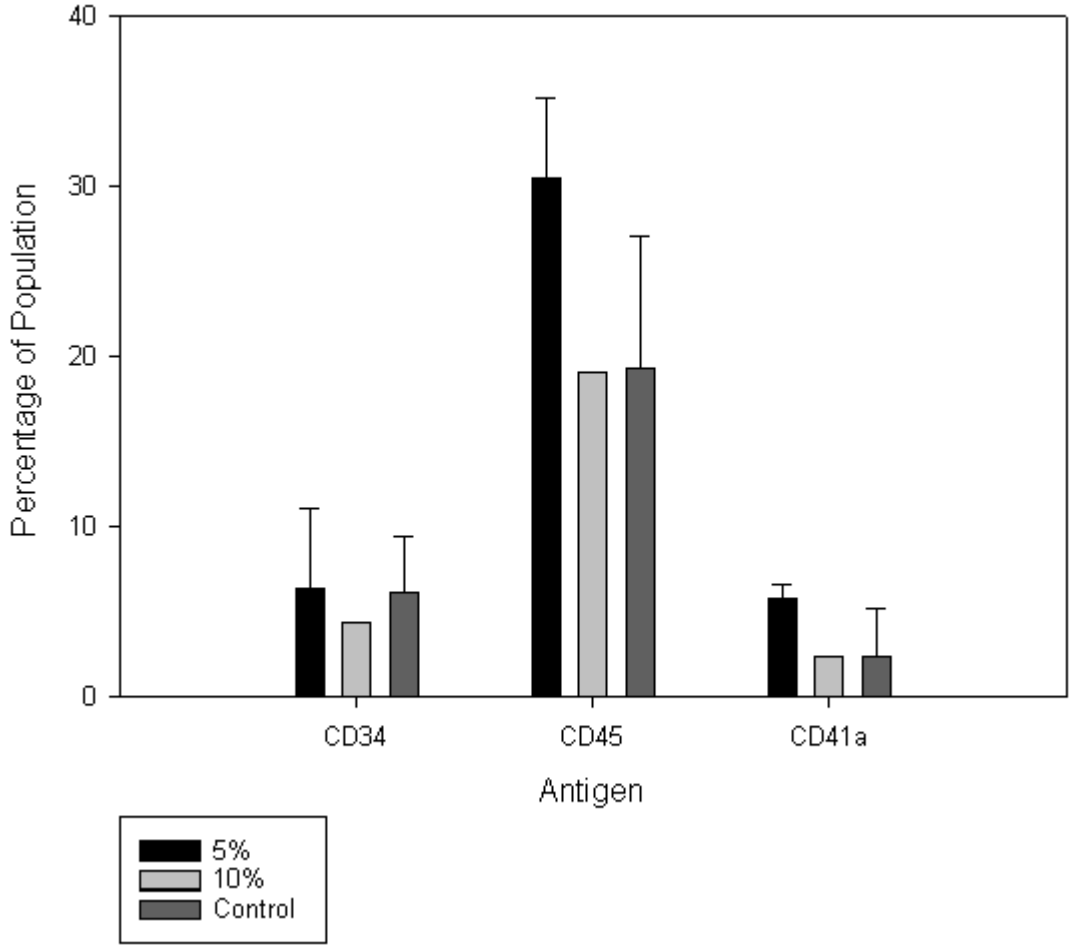

Figure 5.12; Markers of interest (as specified during device cultures) for Day 14 cells grown in static cultures at 5, 10 and 21% (control) oxygen. Cells did not exhibit the same fluctuations as shown in the device cultures, leading to speculation that the mild shears experienced within the device were the causation

The predisposed markers of interest (CD34, CD45 and CD41a) which showed a significant response hypoxia in the cell culture device did not show an effect for the static culture conditions leading to the supposition that the mild long-term shears experienced during culture were the cause of these diversions.

5.5.6 Enucleation

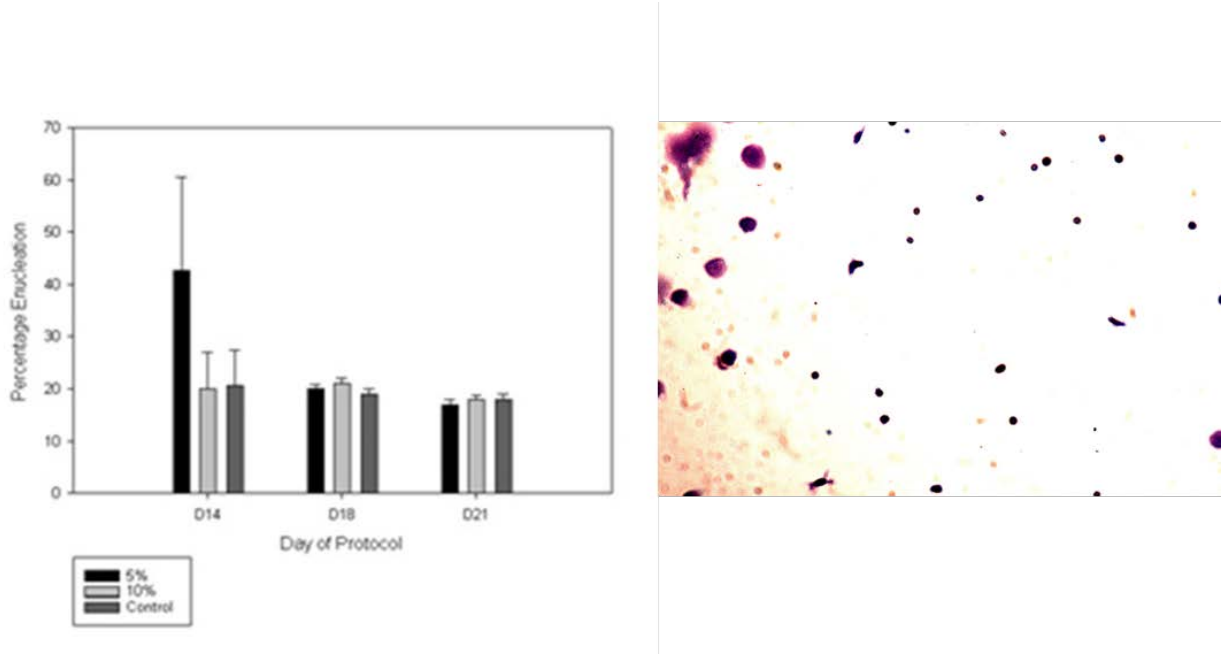

Figure 5.13; Percentage of enucleation exhibited by cells at days 14, 18 and 21 of the protocol grown in 5, 10 and 21% (control) oxygen. Cells grown in 5% oxygen exhibited higher enucleation than those grown in 10 or 21% oxygen. Cytospin images recorded of these cultures showed patches of extruded nuclei. NB. Scale bars are not included for these images since the cytospin procedure stretches and distorts cells (x40 magnification).

As was shown earlier (Section 3.2.2) cell nuclei are continually extruded from day 12 onwards but they are continually marked for apoptosis so that even at the peak of enucleation only a maximal 35% is recorded on flow cytometry plots. FSC/SSC flow cytometry images showed Day 14 CD34+ differentiating cells which were grown in 5% oxygen presented much higher rates of enucleation than those grown in 10 or 21% oxygen indicating early-onset enucleation under hypoxic conditions. This was confirmed by cytospin images which revealed large areas of extruded nuclei. The cells themselves appeared diffused, possibly due to imaging method (cytospin procedure distorts cells and the g-force causes the cells to lyse) and these factors combined could perhaps be part of a stress response to hypoxia. It might be that hypoxia is a trigger for enucleation which has been an issue for the *in vitro* generation of red blood cells using

pluripotent stem cells (not shown). Since hypoxia was also found to decrease the doubling time of pluripotent RC9b cells two-fold it may be that oxygen concentration is a key regulator (and enhancer) of haematopoietic development. This is something which should be investigated further.

5.6 Summary

Encouragingly device/ruthenium biosensor trials with J774 cells returned similar results to those found in literature, however many of the cited values do not express differences in the lag and log phases which were found experimentally to be very different. As this Chapter has shown oxygen utilization is dynamic throughout the life of the culture dependent on both biological and physical factors, therefore it should be monitored continuously.

Although results are shown here for one trial with RC9b cells the microdevice was used several times in hypoxic conditions. Prior to contamination cells always appeared to proliferate wildly in comparison to incubator cultures. This is very exciting in terms of scale-up. As anticipated erythropoiesis was upregulated under hypoxic conditions and yielded more than double the number of cells. This is definitely something which should be revisited once the RC9b/SFC i55 cell lines have been stabilised. The oxygen consumption rate of 2.4 amol $cell^{-1}$ sec^{-1} was very similar to that found for cord blood cells (2-3.5 amol $cell^{-1}$ sec^{-1}) which was encouraging since both these cell types expressed similar levels of mitochondria. It also reinforces metabolic similarity which is promising in terms of producing equivalent erythroid cells using different types of stem cells.

Disappointingly CBS cells did not exhibit the same upregulation of erythropoiesis. However since erythropoiesis is upregulated by erythropoietin and this is added from day 0 of the CBS protocol (for RC9b this was not added until day 10) perhaps the signal was superseded. Given this and the results of the ROS there is no reason why CBS cell expansion should be improved under hypoxic conditions.

It was however encouraging in terms of scale-up that following mitochondrial clearance oxygen concentration can be reduced significantly. This should prevent augmented bubble damage in bioreactor culture and ROS which have been shown to age red blood cells *en vivo.*

Chapter 6 – Shear Stress Results

6.1 Introduction

Under physiological conditions cells are subjected to a wide range of shear stresses due to persistent changes in local pressure and viscosity. This is particularly true of haematopoietic cells of which many types are mobile in the blood stream and therefore additionally exposed to changes in arterial and venous morphologies. Additionally CD34+ cells are of fetal origin and it is unclear at which stage in their development differentiated cells are released to the fetal blood stream or indeed the shear stresses imposed by fetal circulation. Hence in this chapter differentiating CD34+cord blood cells were subjected to a range of shear stresses at progressive stages in their development in order to discover whether there was any observable effect on morphology, physiology, expansion and all-round cell health.

6.2 Determining shear stress values

Aside from exposing cells to physiological shear stresses (0-5000/s) it was important to also represent *in vitro* systems which were being used for (or projected for use on) the project. Small scale cultures were being carried out in 6-well plates or T-flasks under static conditions and therefore shear was considered as 0/s. Two scale-up vessels were purchased for use on the project; an Integra Cellspin with 500mL spinner flask and a 5L Celligen BLU bioreactor. Prior to experimentation both were analysed for shear stress levels using Comsol Multiphysics 4.4 computer fluid dynamics (CFD) software package. This work was completed with the assistance of Dr Alan McGuinn who worked as PDRA on the project and completed most of the drawings and mathematical modelling for the simulations. Experimental design, some drawings/simulations and data analysis were carried out personally.

6.3 Agitation rates

In order to model shear stress inside the scale-up vessels it was necessary to estimate the agitation rate. At the time of experimentation the Integra Cellspin was already in use for CD34+ cord blood cells with agitation rate set at 15rpm however the Celligen BLU rate had to be estimated by traditional means.

The ideal agitation rate should ensure turbulent regime and for stirred tank cultures this transitional Reynolds number is 10^4, yielding an agitation rate of 47 rpm $(10,000*0.00078)/(991.348*(0.1)^2)$. For sparged cultures this figure should then be reduced by 20%, leaving a final agitation rate of 37.5 rpm [40].

Since the Integra Cellspin was already running successfully a second more experimental approach was taken to estimate the agitation rate inside the Celligen BLU Bioreactor which reflected the Reynolds number calculated (2034). This was then applied to the Celligen BLU and the equation solved to find the agitation rate, which was calculated as 9.56rpm.

6.4 CFD modelling

6.4.1 Integra Cellspin and Celligen BLU

The Integra Cellspin 500mL spinner flask was measured accurately and its' geometry copied into Comsol (Figure 6.1A&B). The model was then run using the following settings; Element size: Max 0.00532m, Min 0.001m, Growth rate 1.13, 2 Boundary layers, 132,530 elements, Viscosity 0.00078 N.s/m^2, Density 991.348 kg m^{-3} at 15rpm for 30 seconds to ensure steady state was reached. The simulation was assessed for shear stress and the prevalent output calculated as 50-60s.

The Celligen BLU Bioreactor was also measured accurately and its' geometry copied into Comsol (Figure 6.1 C&D). The model was then run using following settings; Element size: Max 0.00795m, Min 0.0015m, Growth rate 1.13, 5 Boundary layers, 645,056 elements, Viscosity 0.00078 N.s/m^2, Density 991.348 kg m^{-3} at 37.5rpm for 10 seconds to ensure steady state was reached. The simulation was assessed for shear stress and the prevalent shear rate output was calculated 140/s. The model was run a second

time at an agitation rate of 9.56rpm which gave an output of 50-60s, the same as the Integra Cellspin.

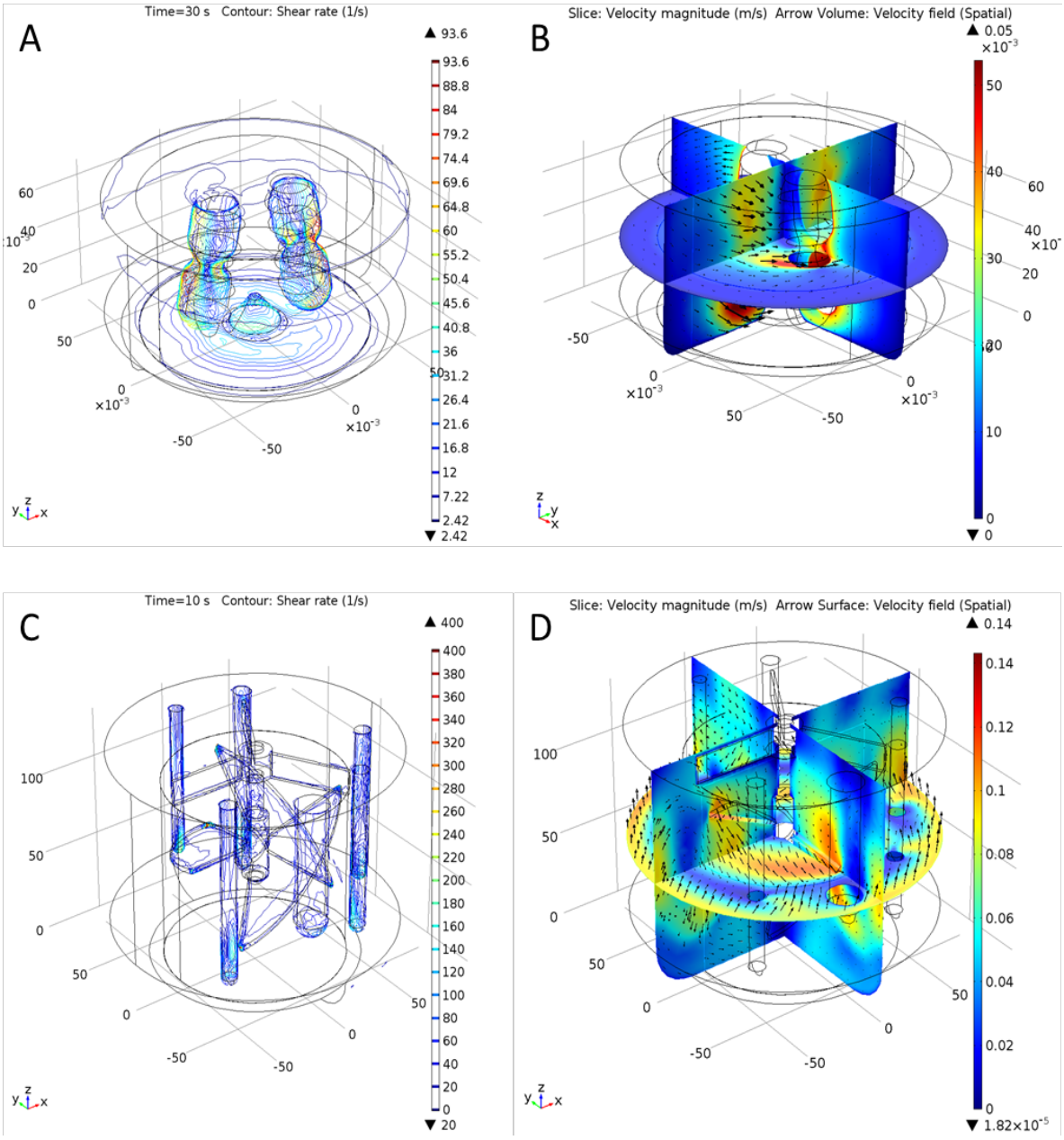

Figure 6.1; CFD outputs for Shear Stress (A) and Velocity (B) in the Integra Cellspin as calculated by Comsol with the specified settings. Simulations were also completed for the Celligen BLU Bioreactor (C&D). The outputs were used in the experimental design of the capillary experiment

In addition to physiological shear stresses, the mean shear stress levels (60 and 140/s) for the scale-up vessels as calculated by Comsol were added to the experimental profile

6.4.2 Capillary Tubes

Optimum shear rate for mammalian cells is usually within the range of 0.2 and 3 N m^{-2} but can be as high as 4 N m^{-2} in the blood stream. Since differentiating CD34+ cells change in size and elasticity over the duration of the protocol and are intended for blood circulation, it was important to test up to the maximum rate. The following shear rates were chosen for assessment; 0/s, 60/s, 140/s, 250/s, 500/s, 1000/s, 2000/s, 3000/s, 4000/s, 5000/s, incorporating *en vivo, in vitro* and optimum shear rates (obtained by dividing by viscosity). A series of flow rates and diameters of PEEK capillary tubing were assessed by CFD to find corresponding internal mean shear rates. Since capillaries are axisymmetric only half of the capillary was drawn into Comsol to increase solving power (Figure 6.2).

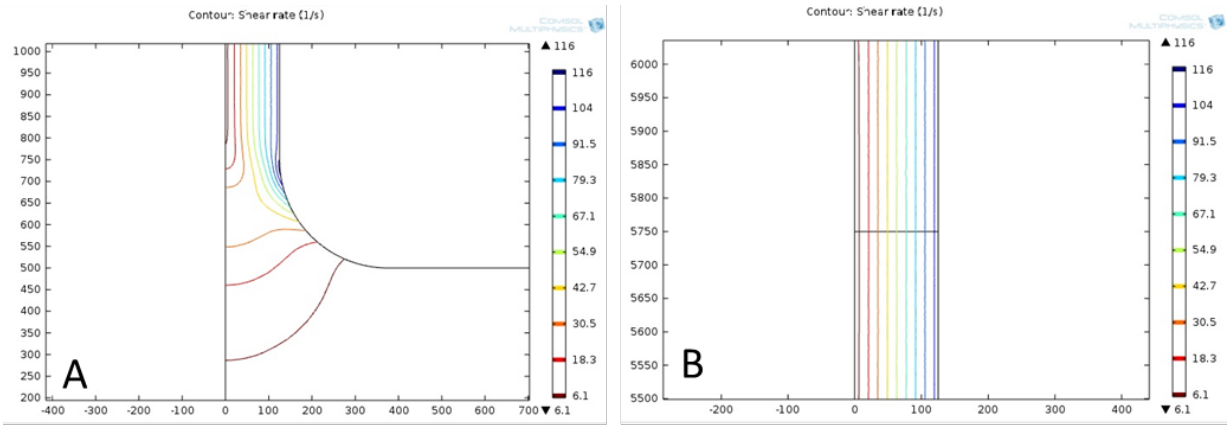

Figure 6.2; Example of a CFD simulation showing top view shear stress contours inside 250µm ID tubing at a flow rate of 10µl/min. Image A shows that shear is variable at the entry region so a trajectory was drawn across the capillary (B) where flow was fully developed and the resultant data was averaged to gain a mean shear for each tubing size/flow rate.

Following the analysis two tubing sizes were chosen; 250µm and 500 µm. Reynolds numbers were then calculated to ensure laminar regime.

Table 6.1; Summary of conditions found within 250µm tubing for selected flow rates. As flow rate increases so does the minimum to maximum shear range

Flow rate (uL/min)	Capillary ID (um)	Mean Linear Velocity (m/s)	Reynolds Number	Minimum Shear (s)	Maximum Shear (s)	Average Shear (s)
10	250	0.003395	1	6	116	60
23.5	250	0.007979	3	14.5	275	140
43	250	0.0146	5	26.9	511	250
85.5	250	0.02903	9	60	1059	500
171	250	0.05806	18	121	2298	1000
341	250	0.11578	37	276	5249	2000
515	250	0.17486	56	464	8817	3000
675	250	0.22918	73	658	12500	4000
855	250	0.2903	92	897	17000	5000

Table 6.2; Summary of conditions found within 500µm tubing for selected flow rates. There is a much higher/wider range of shear with increasing flow rate than for 250 µm

Flow rate (uL/min)	Capillary ID (um)	Mean Linear Velocity (m/s)	Reynolds Number	Minimum Shear (s)	Maximum Shear (s)	Average Shear (s)
77	500	0.006536	4	6	114	60
180	500	0.015279	10	15	280	140
325	500	0.027587	18	29	543	250
650	500	0.055174	35	65	1240	500
1300	500	0.11035	70	157	2984	1000
2600	500	0.22069	140	395	7505	2000
3950	500	0.33529	213	701	13300	3000
5305	500	0.4503	286	1057	20100	4000

6.5 Tubing Length

JP Martinez et al. [81] found that tubing length had little/no effect on cells subjected to progressive shear stresses inside capillary tubing. Prior to experimentation this concept was tested using 3 lengths of tubing (0.5, 1 and 1.5m) and perfusing cell suspensions (2mL suspensions of $2x10^6$ cells/mL) at a constant speed of 25µL/min. Suspensions were transferred to 6-well plates and left for 48 hours before counting and analysis by flow cytometry. No significant differences were found between any of the samples and only one tubing length (1m) was taken forward for the experiment proper.

6.6 Experimental Set up

As described previously a 2mL suspension of $4x10^6$ cells ($2 x10^6$/mL) was drawn into 10mL BD Plastipak syringe and connected to tubing using Upchurch Scientific connectors. The dispensing end of the tubing was attached to a T25 flask. Once all sterile connections were made the loaded syringe was removed from the hood and mounted onto the Aladdin syringe pump. The flow was started at the desired rate and stopped only once the entire cell suspension had been discharged. 1.5mL of the final

cell suspension was then removed by pipetting (the rest discarded) and transferred to a 6-well plate. Each well was topped up with 1.5mLs to a final volume of 3mL/well. The process was repeated for each flow rate before transferring the 6-well plate to a 37°C 5% CO_2 incubator and leaving for 48 hours before analysis. The cells were counted at T0 and again at T48 at which point they were also analysed by flow cytometry (for antigenic markers, apoptosis, and necrosis) and cytospin.

6.7 Expansion

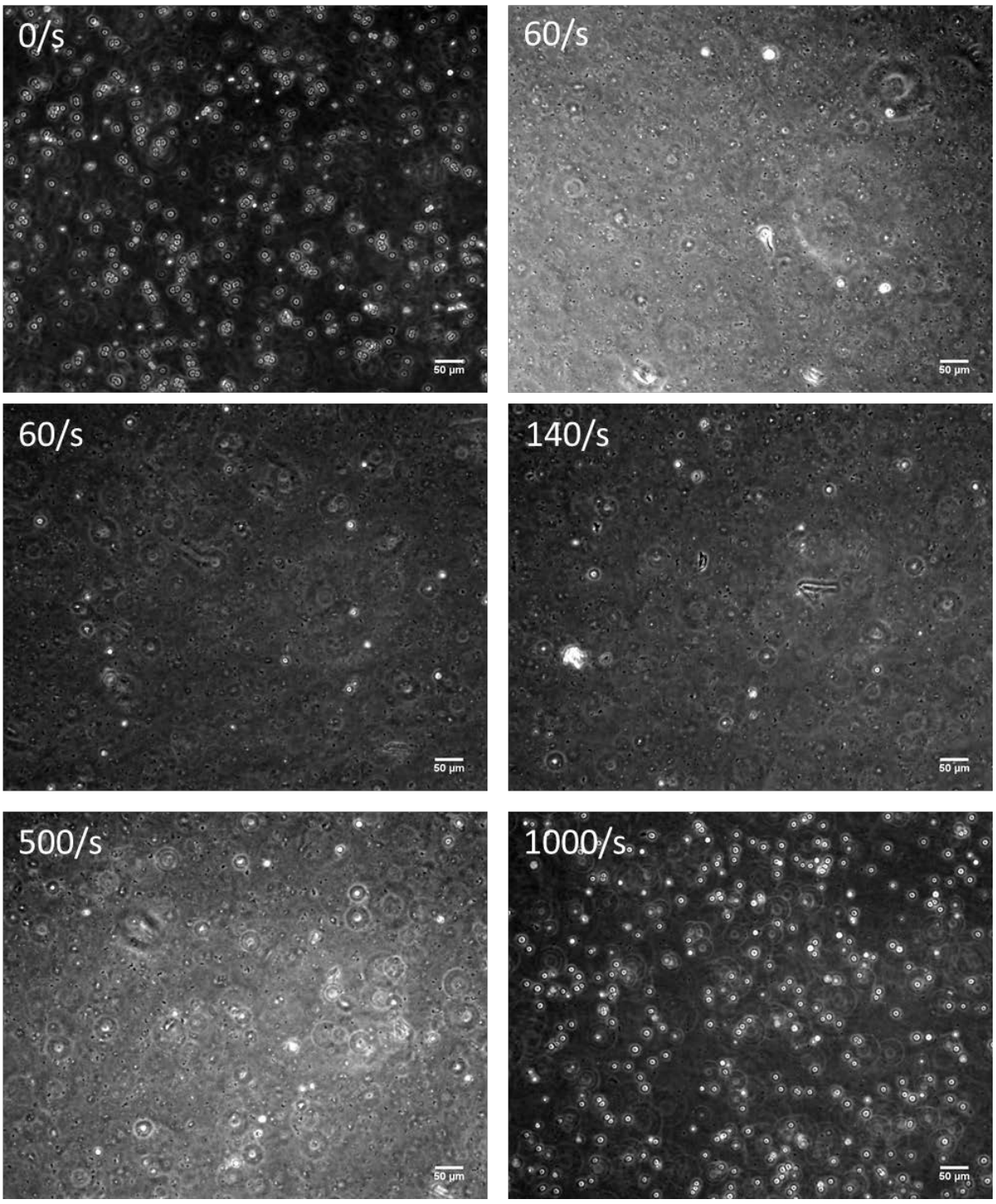

Figure 6.3; D11 cells exposed to consecutive shear rates in 250µm capillary tubing. Unexpectedly cells were prone to lyse at shears <1000/s. It was supposed that this was due to entry effects

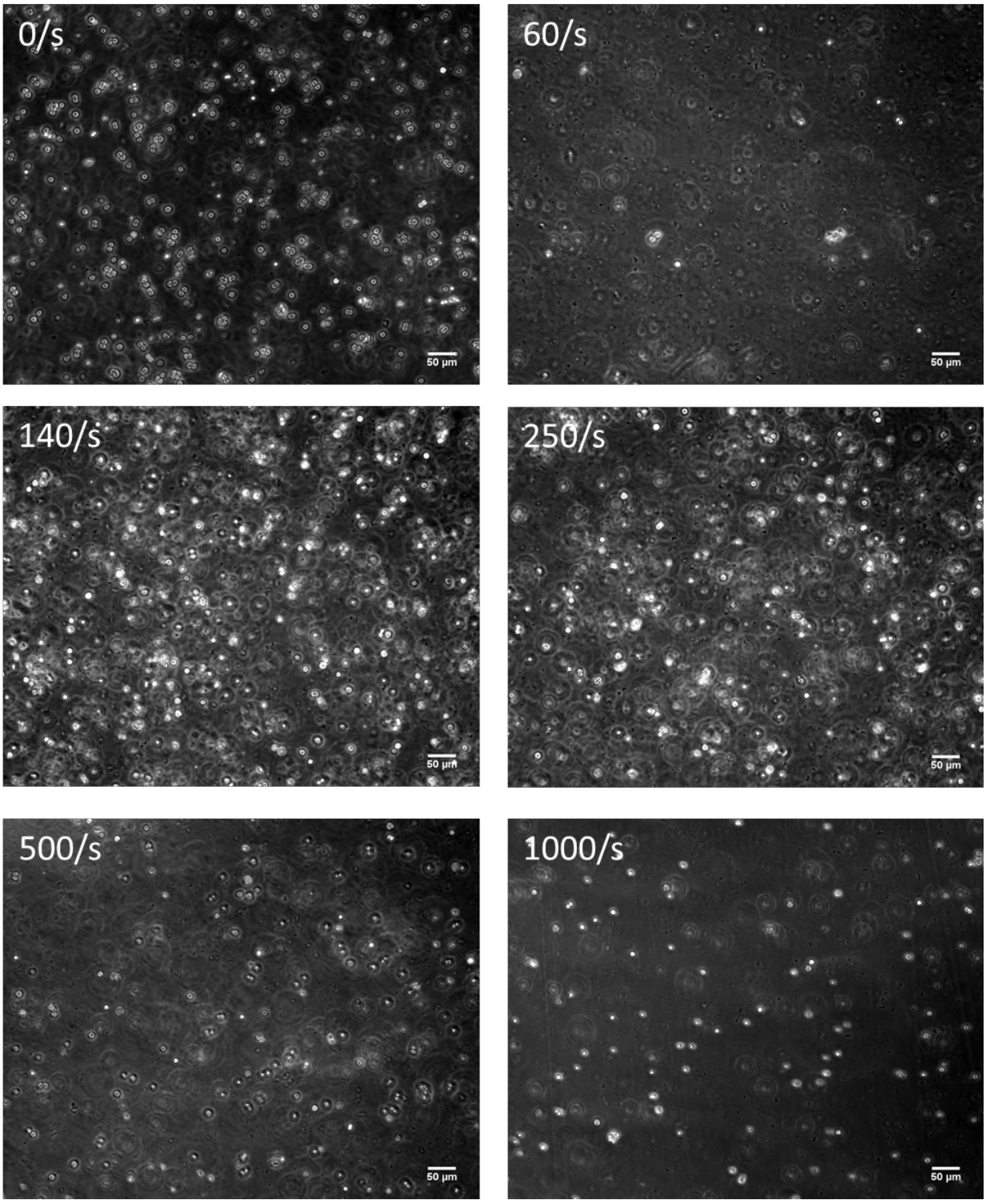

Figure 6.4; D11 cells exposed to consecutive shears in 500µm tubing. Cells were less prone to entry effects. Peak shear appeared to be 140/s immediately following the experiment

At this stage in the protocol cells are large (11-12µm diameter), mostly nucleated and low in elasticity. Images captured immediately following the experiment for 250µm tubing revealed that unexpectedly, cells were prone to lyse at shears <1000/s (Figure 6.4). It was supposed that this was due to 'entry affects' since CFD profiles had shown that narrow capillaries exhibit concentrated areas of elevated shears near the entry region. In order to compensate for this effect a second larger tubing size (500µm, Figure 6.5) was used and as shown cells appeared improved for 140-500/s.
Cell counts for 60-500/s in 250µm tubing were hence disregarded in terms of expansion although the marker profiles were still experimentally interesting (Section 6.8).

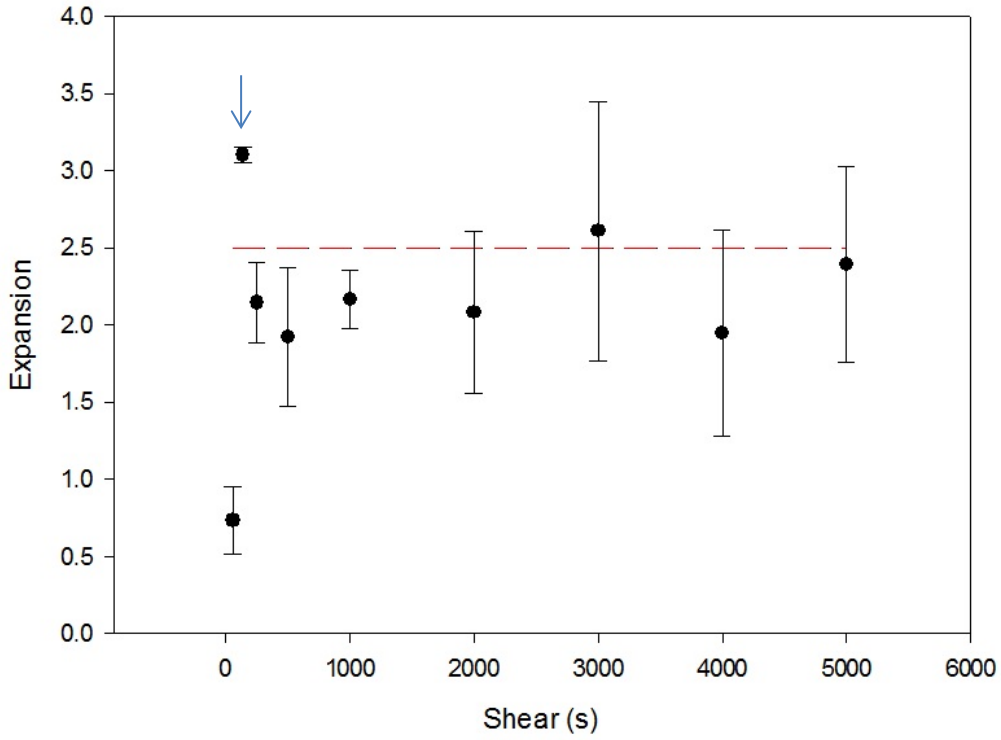

Figure 6.5; Cell expansion of Day 11-13 cells subjected to progressive shears (60-5000s) inside capillary tubes in triplicate. The red line indicates the average cell expansion for static cultures (0s). Almost all shear conditions resulted in reduced expansion, particularly 60/s. The optimum shear was 140/s as indicated by the arrow

Ordinarily day 11-13 fold-expansion is 2-3.5 and encouragingly most of the cultures lie within this range. The cells showed marginally improved expansion at 3000 and in particular, 140/s.

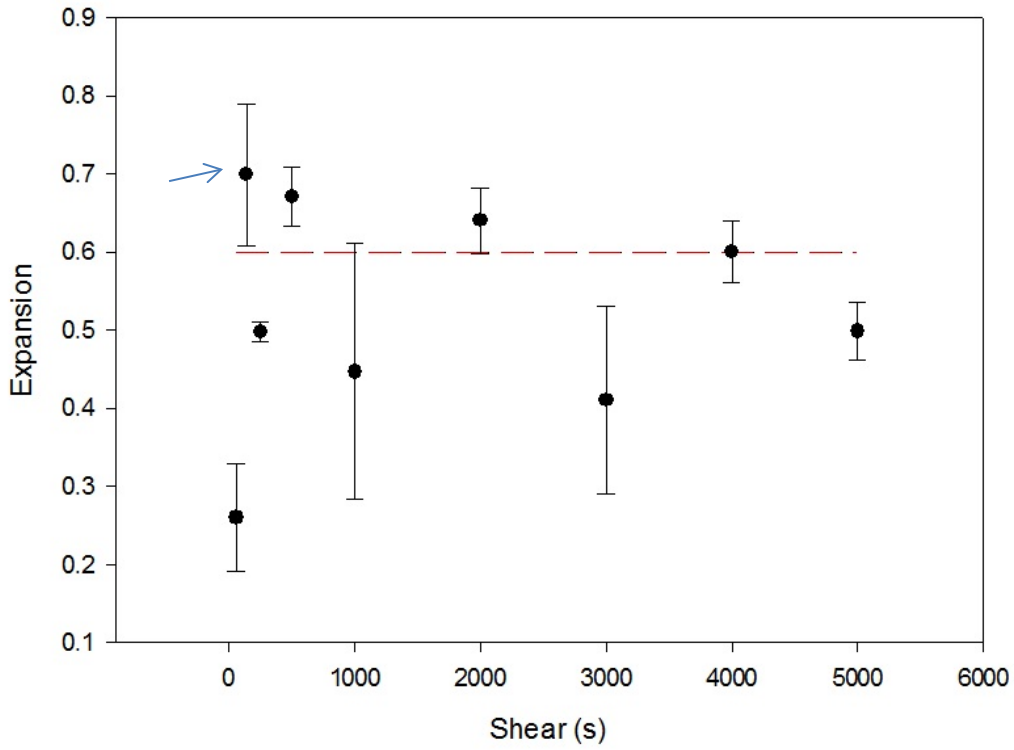

Figure 6.6; Cell expansion of Day 15-17 cells subjected to progressive shears (60-5000s) inside capillary tubes in triplicate. The red line indicates the average cell expansion for static cultures (0s). Almost all shear conditions resulted in reduced expansion, particularly 60/s. The optimum shear was 140/s as indicated by the arrow

Day 15-17 showed similar patterns of expansion to day 11-13 with almost all cultures negatively affected by shear and 140/s as the optimum. Expansion during this period is usually 0.6-0.9 and cultures show a lesser capacity to recover, most likely due to enucleation.

Day 18-20 perhaps shows the most candid effect of shear on cells in terms of abundance since by this point 65-75% of cells have lost the ability to proliferate. The optimum shear is again 140/s with the range of 140-500s also reasonable. Expansion seems to

increase gradually from 1000-4000s showing that cells are also amenable to high shears experienced in the blood stream.

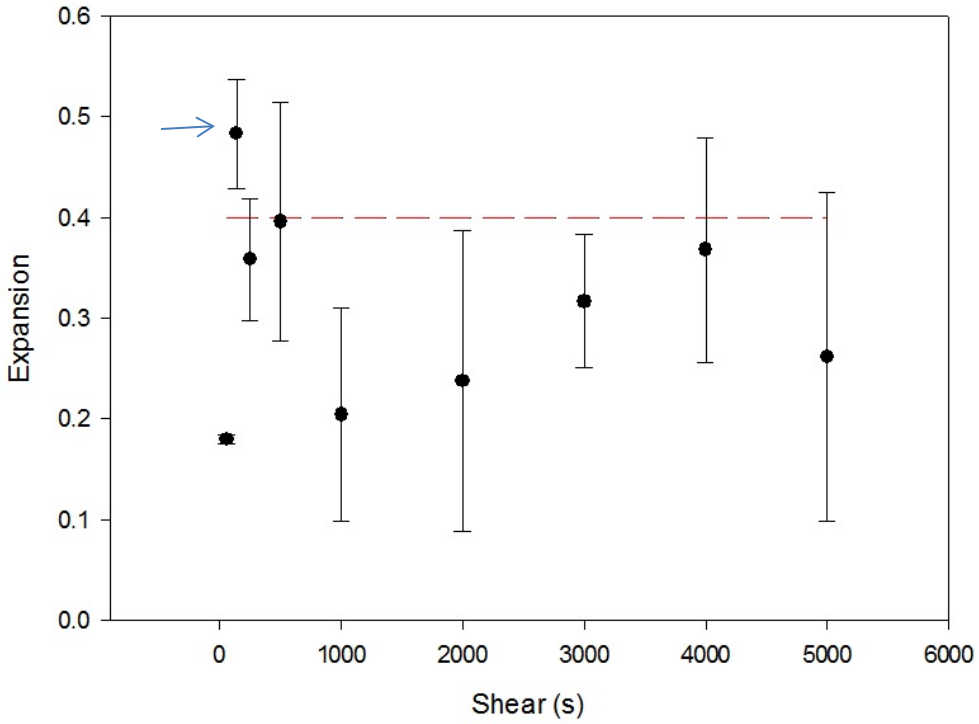

Figure 6.7; Cell expansion of Day 18-21 cells subjected to progressive shears (60-5000s) inside capillary tubes in triplicate. The red line indicates the average cell expansion for static cultures (0s). All shear conditions resulted in reduced expansion, particularly 60/s. The optimum shear was 140/s as indicated by the arrow.

Based on this data there is a strong case for 140/s (0.11 N m^{-2}) as the optimum shear for stirred tank bioreactor culture. However it was also necessary to see if shear had an adverse effect on differentiation.

6.8 Marker profile

6.8.1 Platelet markers

As was shown in earlier sections it was suspected that mild shears induced synthesis of platelets. The relationship between CD41a and shear stress appeared well-defined on flow cytometry plots (Figure 6.8) however only 28% of samples presented a correlation at the $P \leq 0.05$ (*) level.

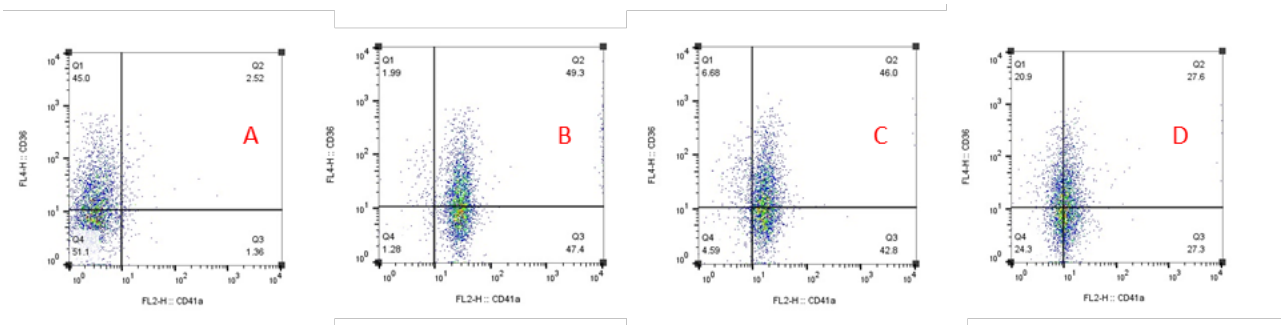

Figure 6.8; Flow cytometry dot plots of day 17 CD36/CD41a stained cord blood cells which had been (A) untreated or 0/s (B) subjected to 500/s (C) 1000/s (D) 2000/s of shear stress. It is clear from the plots that while CD36 seems unaffected CD41a decreases as shear increases. This relationship was significant at the $P \leq 0.00$ (***) level, correlation value -0.941

Nevertheless there is a visual correlation between CD41a and shear stress. Since CD41a is also an early stage haemangioblast marker CD42b and GPVI were added to the panel in order to confirm presence of platelets. Figures 6.9-6.11 show that for each of the time-scales tested (D11-13, D15-17 and D18-20) there is a noticeable increase in platelet markers in comparison to the control cultures. At D11-13 the increase is minor, with a maximal 11% of the cell population. The most affected stages of the protocol are D15-17 and D18-20 with average populations of 38% and 31% respectively.

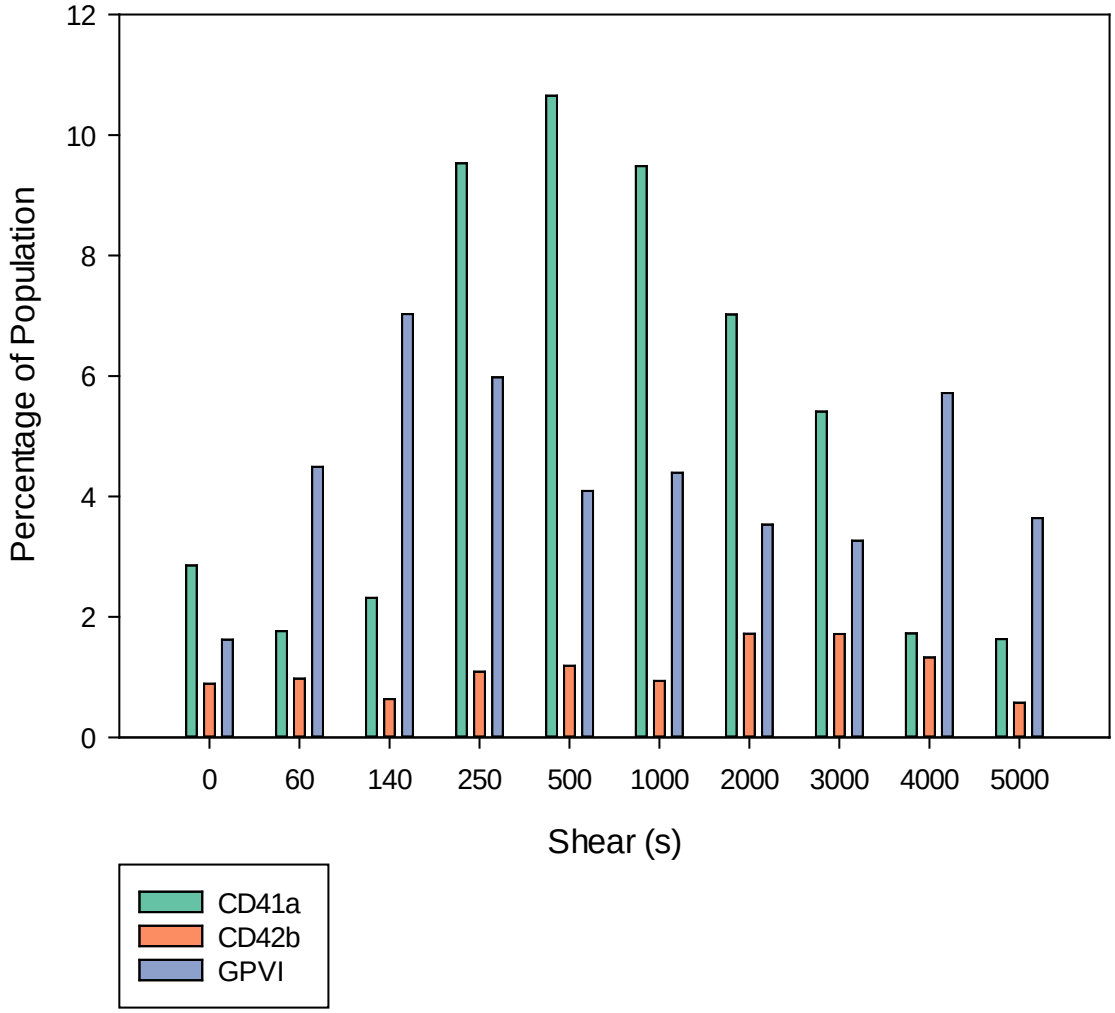

Figure 6.9; Average platelet marker profile following day 11-13 experiments. CD41a and GPVI are elevated in comparison to the control (0/s) peaking at 500 and 140s respectively. CD42b remains relatively low.

Since platelets markers only rise to 11% for day 11-13 of the protocol it is proposed that either megakaryocytes necessary to produce platelets are in precursor form and not able to produce platelets or that these cells are more robust/better able to regenerate. Day 15-17 and day 18-20 cells exhibited much higher platelet marker peaks as shown in Figures 6.10 and 6.11.

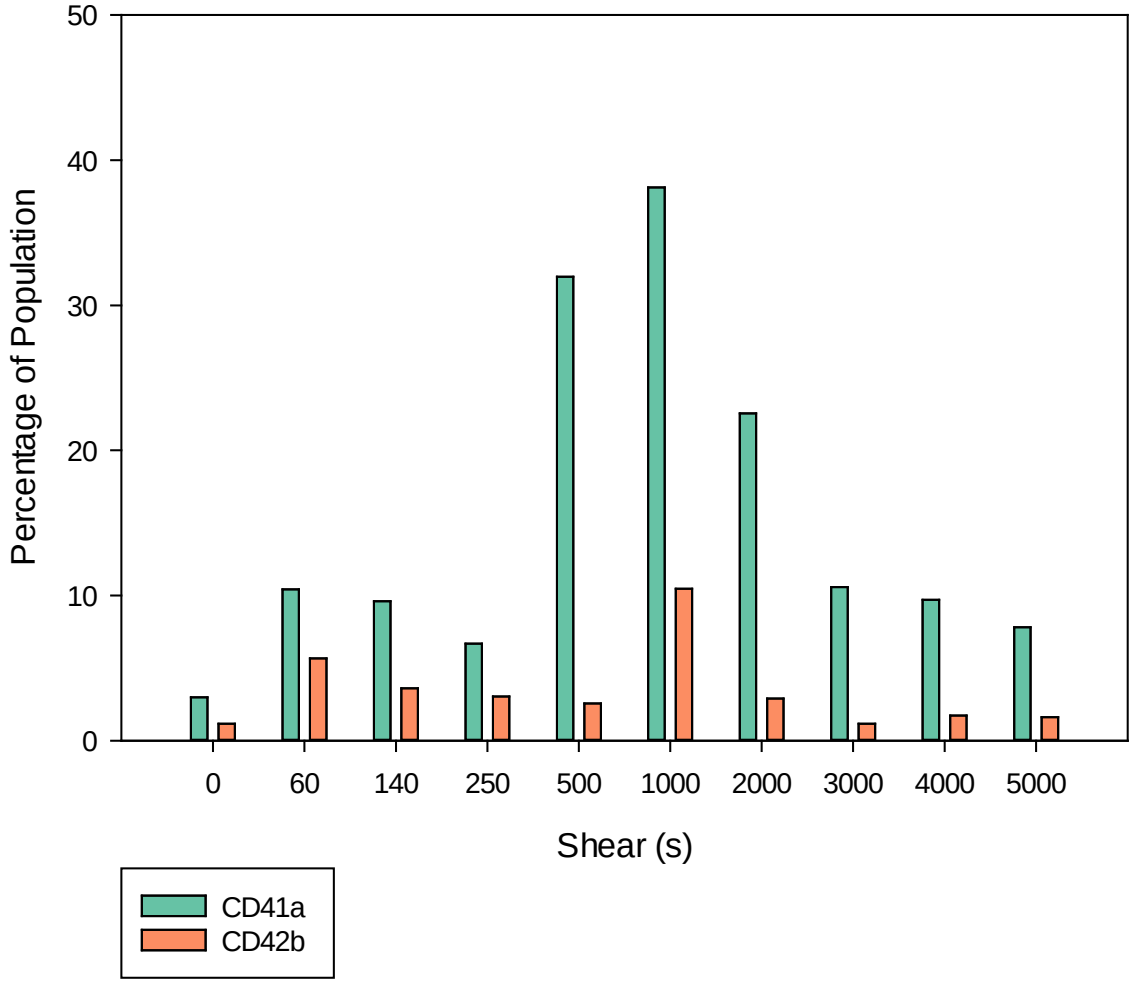

Figure 6.10; Average platelet marker profile following day 15-17 experiments. CD41a and GPVI are elevated in comparison to the control (0/s) peaking at 1000s. CD42b remains relatively low. GPVI data is not available for day 15-17 experiments since this was only added to the panel mid-way through experimentation

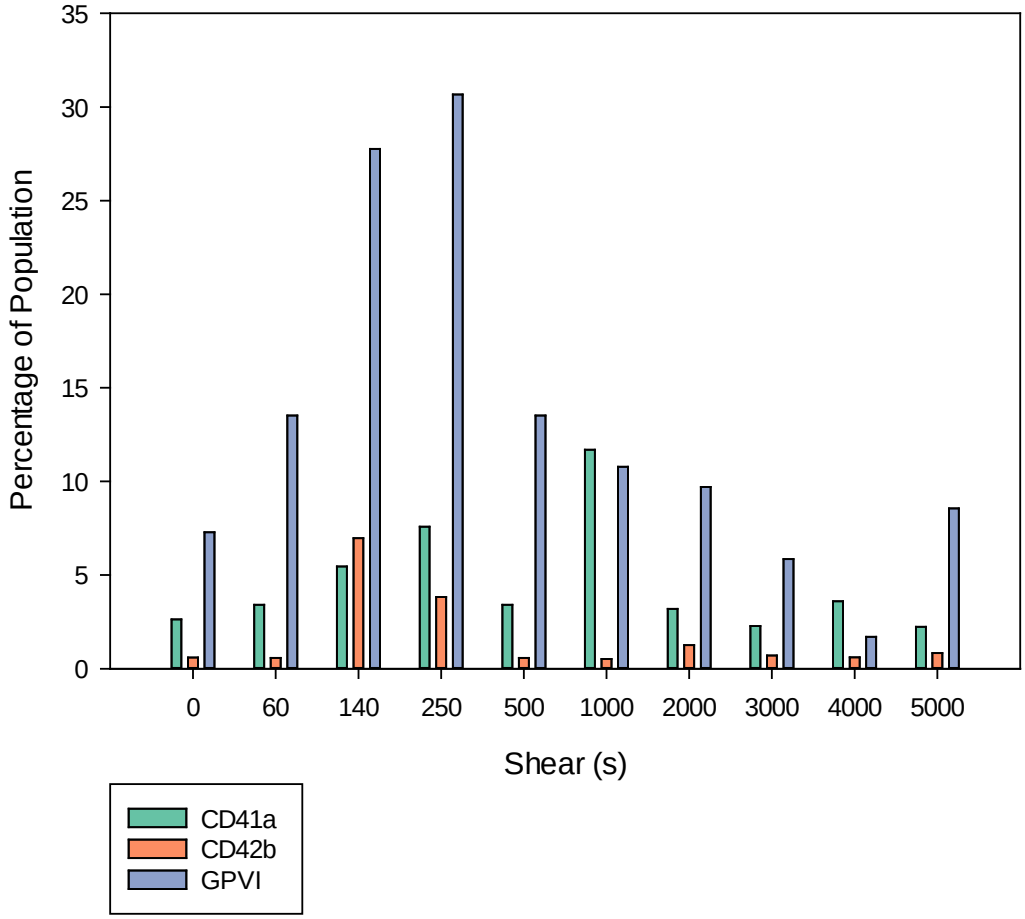

Figure 6.11; Average platelet marker profile following day 18-20 experiments. GPVI is elevated in comparison to the control (0/s) peaking at 250s. CD41a is less prolific but nevertheless elevated in comparison to control cultures peaking at 1000s. CD42b has a marginal peak at 140s.

Higher platelet markers would indicate presence of platelets and it was hoped that this would be confirmed by the cytospin images. It is feasible that platelets should be released in response to shear stress and cellular damage as is their action *en vivo.* However curiously, as was shown in figure 6.8, in some instances whole cell populations expressed platelet markers and which seemed unrealistic. Moreover, platelets 2-3µm in diameter, are much smaller than erythrocytes 8-10µm and hence two cell populations should have been visible on the flow cytometry images. It was hypothesized that the platelets could become adhesive to damaged erythrocytes as is shown in Section 6.10.

6.8.2 Other markers

The rest of the panel (CD45, CD34, CD31, CD43, CD71, CD235a and CD36) were also tested using the Pearson method however no correlations were found. Hence it can be assumed that shear stress has no effect on haematopoietic development, only it induces megakaryocytes to generate platelets.

6.9 Apoptosis and necrosis

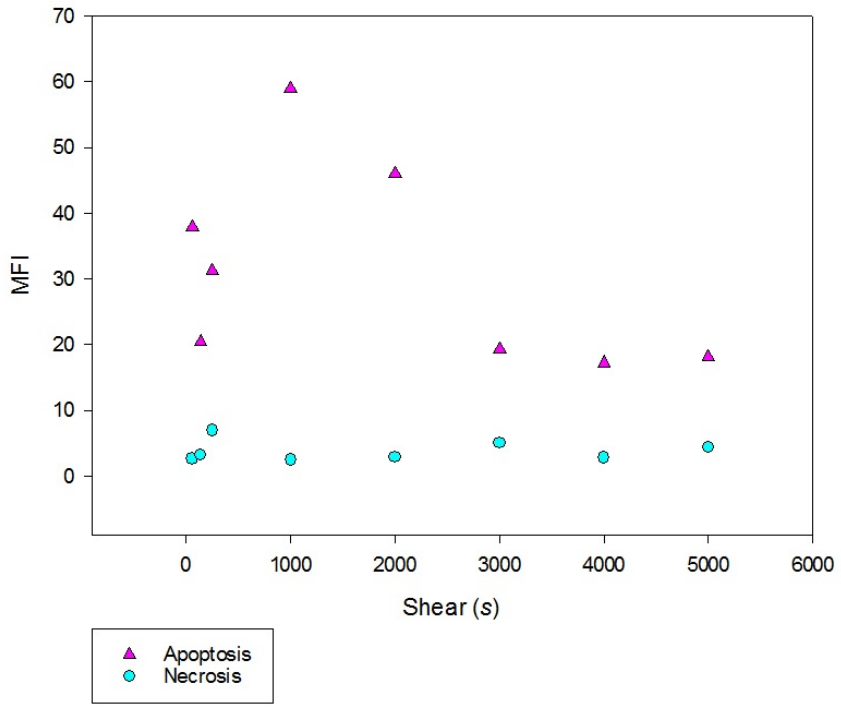

Figure 6.12; Apoptosis and necrosis profiles of cells exposed to increasing shear stress. There is a dip in apoptosis at 140/s which makes a strong case for optimum shear. Apoptosis peaks at 1000s coinciding with peak platelet synthesis

Apoptosis and necrosis were recorded at progressive shear stress using flow cytometry. There was a marked dip in apoptosis at 140s which reinforces the case that this may be the optimum shear for scale-up culture. Following this there was a peak in apoptosis which corresponded to platelet synthesis. Apoptosis dropped off from 3000-5000s which was unexpected but perhaps this is due to erythrocytes being adapted to high

shear stresses such as those found in the blood steam. This could also be a product of experimental design as shall be discussed in Section 6.12.

6.10 Enucleation

No correlations were found between shear stress and enucleation. Although this could be seen as a disadvantage since enucleation cannot be mechanically manipulated, it could also be advantageous since it would be unaffected by scale-up. This result was surprising since others have implicated mechanical shear stress as a stimulus, it may be that only long term shears affect enucleation and this should be investigated further.

6.11 Morphology

Day 11-14 cells which were subjected to increasing shear stresses showed no discernible morphological differences. This was surprising since at this stage in the protocol cells are larger, rounder and less elastic than the latter, however they show a greater capacity to regenerate as was shown in the expansion data. There were several discernible morphological effects of shear stress on latter stage (post day 15) differentiating CBS cells which are shown in figure 6.13. Many of the cells appear elongated (6.13A) which is most likely a result of the flow profile inside capillary tubes.

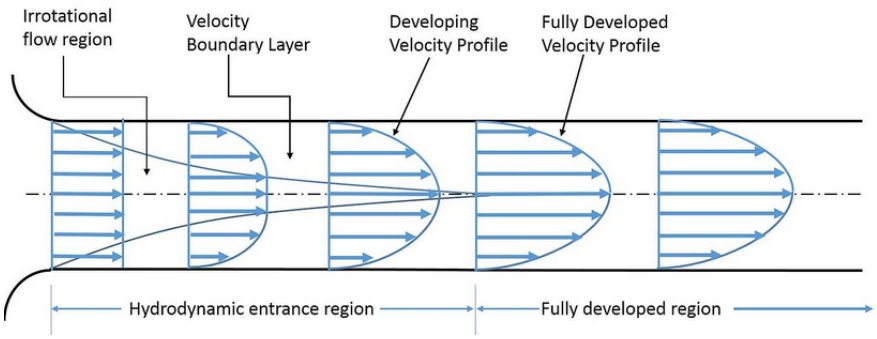

Figure 6.13; Velocity profile inside capillary tubing. Under laminar flow conditions a parabolic velocity curve develops where flow is static at the capillary wall and increases toward the tubing centre. Shear stress is highest at the capillary inlet

since before flow becomes fully developed cells can come into contact with the no-slip condition at the capillary wall

Since mature red blood cells are known to be elastic and slip through blood capillaries with diameters 5-10µm at shear stresses up to 4 N m^2 it is surprising that CBS derived erythroid precursors show elongation 48 hours post-experiment. Of course since they have lost their nuclei they have lost their ability to regenerate however it would seem that CBS derived erythroid cells are not as malleable as adult erythroid cells and are more susceptible to damage by shear stress. This may be grounds for further investigation since it is important that manufactured erythrocytes are suitability characterized and their properties well-known prior to clinical trials

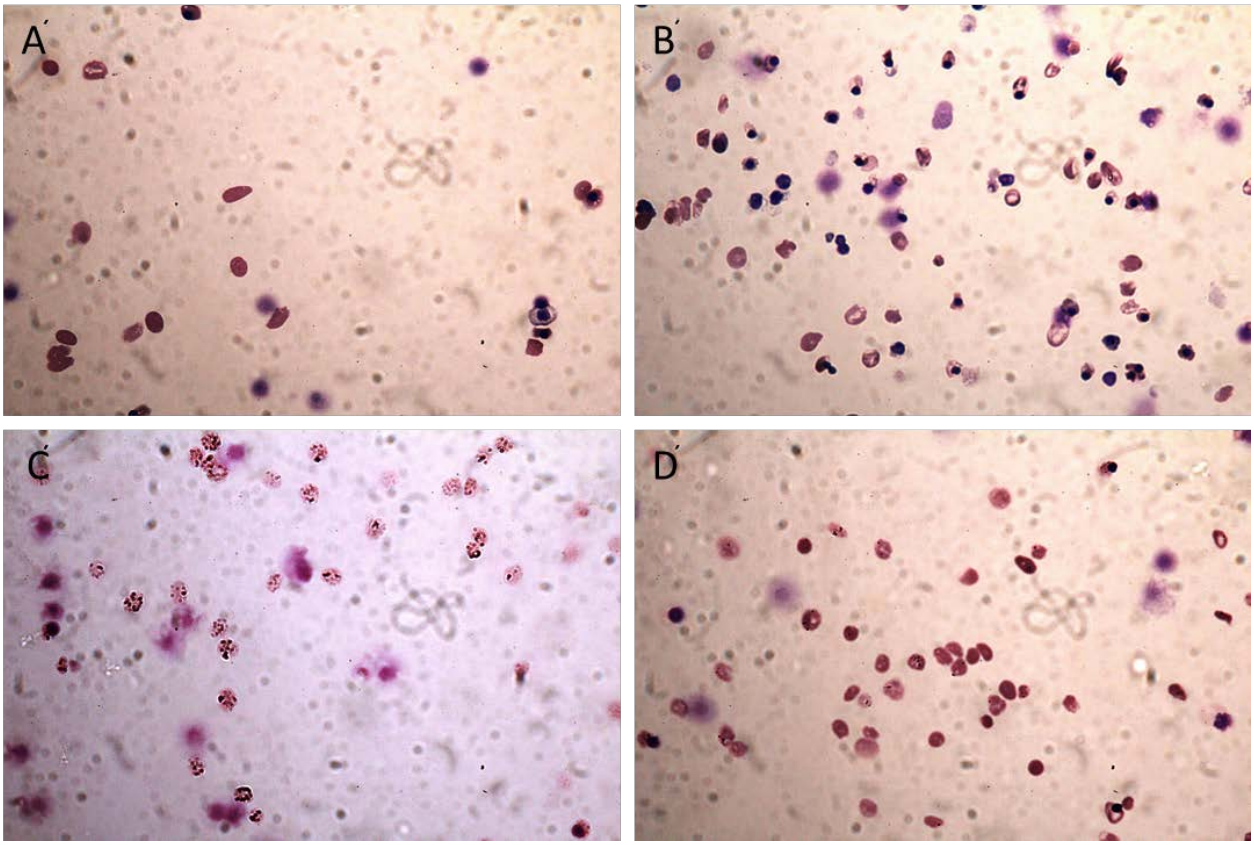

Figure 6.14; (A) In many cases cells are elongated due to parabolic flow profile inside capillary tubing. (B) Cells appear 'patchy' although this could be an effect of cytospin which can distort cells. (C&D) Cells exhibit patches of purple which could be clusters of platelets. NB. Scale bars are not included for these images since the cytospin procedure stretches and distorts cells (x40 magnification).

Figure 6.14B shows ‘patchy’ cells which could indicate development of vacuoles, a hallmark of cellular stress. Pictures C and D show unusual patches of purple on the cells which had not been seen prior to shear stress experiments. It is assumed that these patches are in fact the platelets which were recorded during flow cytometric analysis. Hence it is proposed that megakaryocytes mature by day 15 of the protocol and produce platelets in response to shear stress and/or stress signals released by damaged erythroid precursors. The platelets then attach to damaged areas of the cells. Although to our knowledge this mechanism has not been found previously in CBS erythroid precursors the adhesive properties of platelets and their abilities to repair cell damage are well documented.

6.12 Summary

The use of CFD to estimate shear stress and other unknown physical parameters is becoming widely useful in scale-up studies. However one drawback to this method is that the only way to be certain of its accuracy is to back it up with experimental proof which seems counterintuitive. The estimates obtained for the Celligen BLU bioreactor and Integra Cellspin were realistic in terms of more traditional methods of calculation and were therefore considered experimentally sound. Laminar flow profiles inside capillaries are simple and were considered accurate. As was shown in figure 6.13 once flow is fully developed cells should travel in the centre of the tubing but this is not true for the entry region.

It was expected that entry effects may contribute to some cellular damage, however it was unexpected that it would be so detrimental for 0-500s conditions in the 250µm tubing. These effects were no so pronounced in similar studies, although the flow rates were higher, which was the rationale for adding the second 500µm tubing size. It is extremely important to know the effects of shear stress on differentiating cells, since it has been found to alter cell type and could alter end product in a scale-up process. However this experiment would be better suited to a microdevice in which the shear stress profile is more defined/known and the entry region is better designed.

Regardless the experiment was successful since it obtained its objectives. The high cell counts and low apoptosis rate at 140s makes a strong case for an optimum shear of 0.11 N m^{-2}. This is much lower than other cell types which generally lie in the range of 0.2-3 N m^{-2} but perhaps this is due to the *en vivo* environment of CBS cells where they are unlikely subjected to high shears.

Although it was encouraging to find a candidate condition for optimum shear, conversely the synthesis of platelets under mild shear stresses was ominous in terms of scale-up. Augmented platelet production could contaminate the end product which may then require a further purification step. They may also deplete the media of nutrients necessary for erythrocyte growth.

Chapter 7 – Discussion and Conclusion

7.1 Discussion

RC9b and SFC i55 cell lines were successfully differentiated and expanded at Mountford Laboratories but unexpectedly the process could not be repeated at Heriot Watt University or indeed any other University in the consortium. This conundrum remains unexplained however there are several factors which may have contributed. Firstly, maintaining pluripotency. Although clinical grade pluripotent stem cells were supplied by Roslin in the first instance, new banks were created at University of Glasgow and subsequently transferred to Heriot Watt University. Each passage induces a small amount of spontaneous differentiation which reduces pluripotency. This can build up over the consecutive passages necessary for cell banking/thawing and can easily become augmented since cell culture health is assessed primarily by morphology (a subjective, unstandardized measure) and is easily overlooked. Spontaneous differentiation can also occur if the cells are not thawed quickly and may be vulnerable when in transit on dry ice.

Maintaining pluripotency of stem cells is a well-known challenge in regenerative medicine. Traditionally pluripotent stem cells were grown on MEF feeder cells which continuously secrete growth factors over the lifetime of the culture in response to paracrine signals. Feeder cells however are not amenable to GMP-compliant scale-up culture since they are animal derived, posing the potential transmission of animal pathogens. Although human equivalents have been trialled they do not maintain pluripotency as well as MEFs and require supplementary growth factors.

Regardless of origin feeder cells grow in monolayers with stem cells as a co-culture which would pose an additional challenge in cell separation prior to initiation of the differentiation culture. The secretome composition of the feeder cells is also unknown (this is also true of serum) and in order to reduce variation in end product these components must be removed. It is for these reasons that feeder-free serum-free culture systems for pluripotent stem cells are being developed throughout the field however this has inflicted a new set of challenges. Since feeder cell excretions are living, dynamic responses to paracrine signals emitted by pluripotent stem cells, they are impossible to truly replace through the use of artificially added growth-factors. Additionally many growth factors are cytokines which generally have short half-lives and are readily

degraded when exposed to adverse environmental conditions. Even slight variations in temperature and light can render them inefficient which could have a detrimental effect on the pluripotency of the culture.

As was shown in Chapter 3 the pluripotency of the RC9b and SFC i55 cells was inconsistent in comparison to the Mountford Laboratory cells and may have impacted on later stages of the protocol. Cells which have lost their pluripotency have essentially undergone germline specification into any of three germ layers (mesoderm, endoderm or ectoderm) and since this transition is unidirectional, any which have specified to an erroneous lineage are not available for haematopoietic differentiation, decreasing product yield from the onset.

Conversely many of the differentiations attempted at Heriot Watt University were performed using stem cells which *were* sufficiently pluripotent (as determined by Mountford Laboratories) yet the same overall fold-expansions were never achieved. Day 0-3 embryoid bodies were successfully formed and obligatory expansion attained but for the for the period day 3-10 only an average 8-fold expansion was achieved in comparison to 20-50-fold at University of Glasgow. The marker profile (CD71/CD235a/CD43/CD31) specified presence of haemangioblasts and early erythroid progenitors in accordance with Mountford Laboratory data. However CD34 (haematopoietic stem cell) and CD45 (common leukocyte antigen) were uncharacteristically high. Since CD45 appears on almost all haematopoietic cells except erythrocytes and CD34 is a haematopoietic stem cell marker it could be that the cells were in a state of arrested development and did not suitably progress from germline specification to lineage commitment. Several novel molecules are introduced at day 2/3 of the protocol (FGF-α, SCF, IGF2, TPO and IBMX) one/some of which could be responsible for this developmental failure. Perhaps the most likely candidate would be stem cell factor (SCF) which is first added day two of the protocol and is responsible for haematopoietic commitment and proliferation. Should this cytokine become inoperative it would result in suspension in the haemangioblastic state and lack of proliferation as is was evident in the data. However 3-Isobutyl-1-methylxanthine (IBMX) added on day 3 of the protocol elevates cAMP levels to activate protein kinase A (PKA) which increases differentiation. Since IBMX and consequently PKA modulate timing of differentiation, if IBMX is defective then this could also result in suspension in the haemangioblastic state. Morphologically the cells looked to be progressing through

differentiation in the required way and CD71 (transferrin marker involved in haemoglobin import exclusively found on erythroid lineage cells) was normally >90% so it could be that it was a timing issue which effected proliferation and otherwise they would develop normally only at a slower rate. It is puzzling that morphologically cells differentiated at Heriot Watt University are identical to the Mountford Lab cells aside from proliferation. Perhaps the cells were not in arrested development at all and were only deficient in proliferation alone due to inactive insulin-like growth factor (IGF) which is not involved in haematopoiesis per-se but is a mitogenic hormone which ordinarily stimulates proliferation and cell survival.

In reality the absence of fold-expansion could be attributed to any of the 18 growth factors used during the protocol, especially due to the instability of cytokines in culture. Although every effort was taken to standardize the growth factors (and indeed all aspects of the differentiation culture) inconsistencies in supplier lots, preparation, storage and handling may have affected the potency of these molecules and may have impacted on the outcome of the differentiation culture. Further to this, differences in local physical environment imposed by experimental equipment and operator handling may have also impacted on the process. As was shown in Chapter 3 even the mild shears experienced by external laboratory equipment can induce unwarranted responses in differentiation culture (platelets). It could be (and often is) an oversight in the physical environment of the cell culture and/or their reagents which are the culprits of variation.

The ground covered with pluripotent stem cells in the initial stages of this research could easily be disregarded but the results are significant and scientifically relevant to this study. They highlight universal, reoccurring issues in the manufacture of clinically useful pluripotent-derived cells; that stem cells are often unpredictable and the resultant variabilities are extremely difficult to eradicate. Results regarding these issues are seldom published and in order to transform benchtop stem cell cultures into clinically and commercially viable products all-round improvements in communication, cross-training and method standardization between laboratories are necessary.

Fortunately CD34+ cord blood cells presented an ideal solution to the problems with pluripotent stem cells. Since they are already lineage committed pluripotency issues were eradicated and their differentiation required less growth factors; predominantly hormones which are generally more stable in culture. From commencement of work with CBS cells expansion and differentiation were routinely achieved in-line with Mountford Laboratory data. Although the experiments in this research were designed for use with pluripotent stem cells they were successfully adapted for use with CBS cells.

Two devices were designed for use on this project, initially a microfluidic device. The ultra-scale down approach was successful in reducing reagent costs and was easily integrated into a microscopy platform for in-situ imaging.
However the microfluidic device was difficult to develop. Initially a lot of time should be spent in the design stage, assessing requirements for cell growth, analysis method and anticipating potential problems. Two of the major difficulties experienced during the scope of this research were contamination and leakage as is common with cell culture microdevices. Many of these problems could have been prevented if more time had been spent in the design stage but this was owing to inexperience. Although three forms of sterilization were used during the scope of this research (ethanol, UV and autoclave) only autoclaving resulted in a 100% success rate and hence thermostable materials should be prioritized when selecting materials for microfluidic devices. Leaking is always a reoccurring issue in microfluidics, however carefully considering available bonding methods and standardizing connections with commercially available microfluidic fittings are preventative measures.
The analysis method should also be carefully considered during the designing stage. Microfluidic devices are not ideal for use with flow cytometry analysis (and indeed many other laboratory analysis methods), particularly due to the unexpected lack-lustre fold-expansion, but also because the cells must be removed from the device prior to testing. Therefore a second ‘mesofluidic’ device was implemented which addressed both of these issues.

This device was intended for in-situ analysis of adherent pluripotent cells however this was not amenable to CBS suspension cells due to the flow and vibration of external equipment which made them difficult to visualise. The device did however facilitate the

use of biosensors which was one of the main aims of the project. Retrospectively biosensors are difficult/time-consuming to develop and are not always amenable to sterilisation methods necessary for cell culture. The ruthenium oxygen sensor was the only biosensor which could be sterilized (by ethanol) and remain active. The glucose sensor facilitated a thin film of poly-allyl-amine hydrochloride (PAH) and poly-sodium 4-styrenesulfonate (PSS) which was stripped by ethanol. The HPTS sensor was never successfully fabricated due to the unsuitability of the PDMS polymer.
None of the biosensors trailed could be sterilized by autoclave which should have been considered in the design stage of the project. Regardless the mesofluidic device and oxygen (ruthenium) biosensor were used successfully to analyse the effects of oxygen concentration on differentiating stem cells as was intended.

As shown in Chapter 1 Wagner et al reported that different cell types utilize oxygen at different rates. J774 cells were reported as 31 amol $cell^{-1}$ sec^{-1}, followed by HL60 cells 11.5 amol $cell^{-1}$ sec^{-1} and red blood cells 4 $x10^{-5}$ amol $cell^{-1}$ sec^{-1}. It was unclear where stem cells would lie on this scale although profiling of mitochondria (Chapter 3) found day 8 CBS cells and RC9b cells to be 6 and 3 times fewer than J774 and HL60 cells respectively.
Experimentally the oxygen consumption rate for J774 cells was found to be between 13 and 92 amol $cell^{-1}$ sec^{-1} (dependent on lag/log phase), 2.4 amol $cell^{-1}$ sec^{-1} for RC9b cells a maximum of 3.5 amol $cell^{-1}$ sec^{-1} for CBS cells which equates to 3-5 times less oxygen. Hence although mitochondria presence can be used to ascertain ranking of oxygen utilisation in different cell types it is not accurate in predicting the consumption rate. The method used for detecting mitochondria relates to accumulation of the fluorescent probe due to the ion potential maintained by the proton gradient. Hence the fluorescence intensity could be affected not only by number of mitochondria but upregulated action. As was shown in Chapter 4 oxygen utilization is downregulated in hypoxic conditions indicating a metabolic switch to glycolysis, so mitochondrial action is dynamic and dependent on its physical (and probably biological) environment.
It was found that oxygen consumption rate dropped further to 2 amol $cell^{-1}$ sec^{-1} at day 15-18 following the expulsion of mitochondria. However this is far off (50000 times) the 4 $x10^{-5}$ amol $cell^{-1}$ sec^{-1} predicted for red blood cells which indicates considerable metabolic differences in CBS derived erythroid precursors.

Once the differentiating CBS derived erythroid precursors have expelled their nuclei they are considered reticulocytes, the final cellular stage before erythroid maturation. It is difficult to tell them apart in cytospin pictures but CD71 is a marker for reticulocytes. Even at day 18 CD71 is >90% which indicated that the cells are not maturing into erythrocytes. Reticulocytes retain some mitochondria which may explain the difference in oxygen utilization found during this research. This is problematic on two counts; firstly if the reticulocytes are not maturing into erythrocytes then they will not behave in the same way as adult red blood cells and therefore may not be suitable candidates for blood transfusion. Secondly, since reticulocytes contain mitochondria (which contain DNA) even if these cells were found to be clinically useful, once irradiated (which is the proposed sterilisation method for the project) they may lose their functionality since the roles of mitochondria in erythroid precursors are not entirely understood.
Alternately since cord blood derived stem cells are slightly morphologically, phenotypically and physiologically dissimilar from adult bone marrow derived stem cells, it could be that the erythroid cells they generate will also be different. Assumptions are often made in stem cell therapy research that cells generated will be clinically safe and useful, however there are clues in this research (and others) that this may not be the case. As was shown in Chapter 3 SFC i55 cells have 2-3 times more mitochondria than RC9b cells and it has been found in other studies that they become mutated during reprogramming. Red blood cells generated in this study do not seem to develop or behave in the same way as red blood cells generated from adult haematopoietic stem cells. Hence more research should be performed to ensure the safety and compliance of opposing stem cell types prior to initiation of differentiation studies.

The expansion profiles of cells cultured at 5 and 10% oxygen in the static cultures were only marginally affected in comparison to the control cultures. There were no differences in expansion following day 15 in the differentiation process for cells cultured at 10% oxygen which specifies an advantage in terms of scale-up; the traditional bioreactor sparge rate (40%) could be reduced by half preventing bubble damage. It is surprising that the expansion level diminished under hypoxic conditions prior to day 15 since CBS cells have a low oxygen consumption rate and erythropoiesis is known to be upregulated under hypoxic conditions. It is likely that erythropoietin which is already added to the media accounts for this action already or as earlier

mentioned, it could be that there are broader differences in CBS and AS cells than initially thought. Since these stem cells reside in different niches they may respond to divergent physiological cues.

For example, it was unexpected that higher levels of Hif-1-α were not recorded during the hypoxia experiments. Initially it was expected that the analysis method for Hif-1-α was not sufficient and that Western Blot should be used. Although this is a possibility, flow cytometry is a valid form of analysis for Hif-1. It was also considered that the oxygen levels used in the experiments were not low enough to warrant a response. However it was shown during the course of this research that oxygen utilization was downregulated under hypoxic conditions, which is indicative of a hypoxic response. A third explanation is that in contrast to other stem cell types, CBS cells do not upregulate Hif-1 in response to hypoxia and they have another mechanism for hypoxic response. This is unlikely since Hif-1 is highly conserved and is the master regulator of hypoxia in all known human cell types. This warrants further investigation, since such fundamental differences in stress responses could be detrimental to the development of stem cell-derived red blood cells.

Furthermore AS-derived red blood cells are aged by accumulative ROS which is one of the mechanisms by which they are then marked for apoptosis after 120 days in circulation. For cells produced during this project the survival rate was poor post day 18 (0.6-0.9%) and most cells were marked for apoptosis by day 21 when cultures were ceased. Since there is an increase in ROS at day 21 in comparison to day 18 it is possible that this accumulation contributes to premature cell death. ROS were recorded as high for day 11-14 but were diminished post day 15 indicating that ROS species are produced as a by-product of mitochondrial metabolism. Since the cells are stalled in reticulocyte form (which maintain some mitochondria) there may be an abnormal accumulation of ROS which is detrimental to the cells. AS-derived red blood cells neutralise ROS via cytosolic and membrane bound catalase, glutathione peroxidase and peroxiredoxin-2 so it would be interesting to see if reticulocytes retain these enzymes. The life-span of CBS-derived red blood cells must be improved significantly before they can be considered ideal candidates for cellular therapy.

The shear stress experiments were conducted in capillary tubes of which the shear profile was estimated using CFD. Although it was hoped this would provide an accurate profile of the cells' shear stress environment the results indicate otherwise. The expansion results for 60s were extremely low for both tubing types. Although it is possible that very low shears are highly detrimental to cells it is more likely that these results were caused by entry effects as described in chapter 6. The low flow rate at 60s (10-77 µL/min) coupled with the small entry region may have caused the cells to lyse upon contact with the no-slip layer. Furthermore the expansion profiles of the day 11-14 cells (in particular) and day 15-18 cells are highly erratic, although this could be accounted for by the cells' capacity to proliferate (prior to enucleation) which varies naturally from culture to culture. In order to make the experiment more robust a shear capillary microfluidic device would be better suited in which the shear stress environment could be accurately estimated. Cells should also be counted and analysed for apoptosis/necrosis immediately following the experiment and again every 24 hours post-experiment ascertain the true extent of damage and recovery. Samples of cells analysed by flow cytometry 24 hours after exposure to shear stress showed a high level of platelet markers which diminished over time (not shown) and so it is suspected that in most cases cells are able to recover. The experiment could be improved by completing flow cytometric analysis every 24 hours to track resilience.

This research has presented the presence of platelet markers for mild long-term shear stresses as imposed by the intermittent vibration of the mesofluidic device (-80°C freezer) and short-term shear stresses in capillary tubes. Since platelets were not identified on the cytospin images it is suspected that the platelets attach to damaged areas of the haematopoietic cells as is the case with *en vivo* blood vessels and other types of cells. As shown in the cytospin images, some cells exhibit vacuoles, a hall-mark of cellular stress and others exhibit areas of purple which could be aggregates of platelets. This is backed-up by the flow cytometry data which signifies that between shears of 140 and 1000s (0.1 and 0.8 N m^{-2}) platelets (or their markers) are highly upregulated. These results are somewhat puzzling since for most cell types this is the optimum shear range. Additionally cytospin images revealed that 48 hours post experiment the CBS derived red blood cells had not regained their round/discoid morphology. AS cell-derived red blood cells are known to be highly elastic, able to squeeze through blood capillaries 5-10µm and withstand shears of up to 4 N m^{-2}. Since

CBS-derived red blood cells lack deformability, it can't be said that they are physiologically unalike adult red blood cells. Again this could be due to the fact that they are stalled in reticulocyte form or it could be that the red blood cells produced by CBS cells are more dissimilar to those produced by AS cells than was originally thought.

7.2 Conclusion

The microfluidic approach used for the purposes of this research was successful in reducing experimental costs and providing a continuous means of online monitoring of oxygen consumption with cell growth for the duration of the differentiation culture. Although it was hoped this set-up would implement other types of biosensors it was found that those selected were difficult to develop and/or were not complaint to continuous cell culture and sterilisation techniques. Further work is needed in this area to produce viable options for biosensors for use with cell culture.

It was hoped that this research would produce optimum parameters for stirred tank bioreactor differentiation of red blood cells from human pluripotent stem cells. This was not possible due to the non-transferrable process of haematopoietic differentiation of RC9b and SFC i55 cells. This work along with others has identified the huge challenge in transferring said processes between laboratories and standardizing procedures prior to industrialization. Particularly in the case of stem cells which have proven so unpredictable and unreliable though-out the field. It is believed that these obstacles can be overcome with more in-depth analyses of different types of stem cells prior to initiation of differentiation studies.

The pluripotent stem cell lines were replaced with CD34+ cord blood stem cells which were much easier to culture and the data was reproducible throughout the consortium. It was possible to estimate the optimum oxygenation (40% day 11-14 and 20% post day 15) and agitation rate (37.5rpm based on expansion) for the haematopoietic differentiation of CBS cells in the 5L Celligen BLU bioreactor, as was one of the main aims of the project, however this research has found that this process is not yet ready for scale-up and more time must be spent in the development stage.

Firstly it is projected that the low shears imposed by bioreactor culture may induce synthesis of platelets which could be detrimental to the culture in terms of nutrient depletion and impact on purity of end product. This would require an additional processing step which can be costly and time-consuming to develop.

More importantly this research has highlighted that there are broader differences than initially thought between different types of stem cells and their products. This study has shown the CBS-derived red blood cells generated may not be clinically safe or useful due to their many metamorphoses from adult haematopoietic stem cell derived red blood cells. In order to make this a GMP-compatible scalable process more work must

be done to develop the protocol to ensure the end product is clinically viable red blood cells. An in-depth analysis of stem-cell derived red blood cells must be undertaken which elucidates and diminishes their physiological and metabolic differences.

References

1. Liumbruno, G., Bennardello, F., Lattanzio, A., Piccoli, P. and Rossetti, G. (2009) 'Recommendations for the transfusion of red blood cells', *Blood Transfus,* 7(1), 49-64.

2. Mountford, J. C. and Turner, M. (2011) 'In vitro production of red blood cells', *Transfus Apher Sci,* 45(1), 85-9.

3. Seifried, E. and Roth, W. K. (2000) 'Optimal blood donation screening annotation', *Br J Haematol,* 109(4), 694-8.

4. Stramer, S. L. (2014) 'Current perspectives in transfusion-transmitted infectious diseases: emerging and re-emerging infections', *ISBT Sci Ser,* 9(1), 30-36.

5. Choate, J. and Snyder, E. L. (2011) 'The rise of cellular therapy', *Transfusion and Apheresis Science,* 45(1), 91-97.

6. Kaplan, R. S. and Mikes, A. (2012) 'MANAGING RISKS: A NEW FRAMEWORK', *Harvard Business Review,* 90(6), 48-60.

7. Lee, M. O., Moon, S. H., Jeong, H. C., Yi, J. Y., Lee, T. H., Shim, S. H., Rhee, Y. H., Lee, S. H., Oh, S. J., Lee, M. Y., Han, M. J., Cho, Y. S., Chung, H. M., Kim, K. S. and Cha, H. J. (2013) 'Inhibition of pluripotent stem cell-derived teratoma formation by small molecules', *Proc Natl Acad Sci U S A,* 110(35), E3281-90.

8. Haynes, S. E., Saini, S. and Schowengerdt, K. O. (2015) 'Post-transplant lymphoproliferative disease and other malignancies after pediatric cardiac transplantation: an evolving landscape', *Curr Opin Organ Transplant,* 20(5), 562-9.

9. Vemuri, M. C., Schimmel, T., Colls, P., Munne, S. and Cohen, J. (2007) 'Derivation of human embryonic stem cells in xeno-free conditions', *Methods Mol Biol,* 407, 1-10.

10. Galli, M. C. e. and Serabian, M. e. *Regulatory aspects of gene therapy and cell therapy products : a global perspective*.

11. Pasini, E. M., Kirkegaard, M., Mortensen, P., Lutz, H. U., Thomas, A. W. and Mann, M. (2006) 'In-depth analysis of the membrane and cytosolic proteome of red blood cells', *Blood,* 108(3), 791-801.

12. Bessos, H., Fraser, R. and Seghatchian, J. (2011) 'Scotblood 2010: key presentations of the past, present, and future of transfusion medicine to mark Scottish national blood transfusion service (SNBTS) anniversaries', *Transfus Apher Sci,* 45(2), 213-21.

13. http://www.nhs.uk/conditions/Blood-donation/Pages/Introduction.aspx, 01/06/16

14. Yabut, O. and Bernstein, H. S. (2011) 'The promise of human embryonic stem cells in aging-associated diseases', *Aging (Albany NY)*, 3(5), 494-508.

15. Thomson, M., Liu, S. J., Zou, L. N., Smith, Z., Meissner, A. and Ramanathan, S. (2011) 'Pluripotency factors in embryonic stem cells regulate differentiation into germ layers', *Cell*, 145(6), 875-89.

16. Mölne, J., Björquist, P., Andersson, K., Diswall, M., Jeppsson, A., Strokan, V., Rydberg, L. and Breimer, M. E. (2008) 'Blood group ABO antigen expression in human embryonic stem cells and in differentiated hepatocyte- and cardiomyocyte-like cells', *Transplantation*, 86(10), 1407-13.

17. Okita, K., Ichisaka, T. and Yamanaka, S. (2007) 'Generation of germline-competent induced pluripotent stem cells', *Nature*, 448(7151), 313-7.

18. Gad, S. C. (2007) *Handbook of pharmaceutical biotechnology*, Hoboken, N.J.: Wiley-Interscience ; Chichester : John Wiley [distributor].

19. Hordyjewska, A., Popiołek, Ł. and Horecka, A. (2015) 'Characteristics of hematopoietic stem cells of umbilical cord blood', *Cytotechnology*, 67(3), 387-96.

20. Fisher, J. P. e. o. c., Mikos, A. G. e. o. c., Bronzino, J. D. e. o. c. and Peterson, D. R. e. o. c. *Tissue engineering : principles and practices*.

21. Olivier, E. N., Marenah, L., McCahill, A., Condie, A., Cowan, S. and Mountford, J. C. (2016) 'High-Efficiency Serum-Free Feeder-Free Erythroid Differentiation of Human Pluripotent Stem Cells Using Small Molecules', *Stem Cells Transl Med*.

22. Goldman, D. C., Bailey, A. S., Pfaffle, D. L., Al Masri, A., Christian, J. L. and Fleming, W. H. (2009) 'BMP4 regulates the hematopoietic stem cell niche', *Blood*, 114(20), 4393-401.

23. Gerber, H. P., Malik, A. K., Solar, G. P., Sherman, D., Liang, X. H., Meng, G., Hong, K., Marsters, J. C. and Ferrara, N. (2002) 'VEGF regulates haematopoietic stem cell survival by an internal autocrine loop mechanism', *Nature*, 417(6892), 954-8.

24. Nostro, M. C., Cheng, X., Keller, G. M. and Gadue, P. (2008) 'Wnt, activin, and BMP signaling regulate distinct stages in the developmental pathway from embryonic stem cells to blood', *Cell Stem Cell*, 2(1), 60-71.

25. Pearson, S., Sroczynska, P., Lacaud, G. and Kouskoff, V. (2008) 'The stepwise specification of embryonic stem cells to hematopoietic fate is driven by sequential exposure to Bmp4, activin A, bFGF and VEGF', *Development*, 135(8), 1525-35.

26. Cerdan, C., McIntyre, B. A., Mechael, R., Levadoux-Martin, M., Yang, J., Lee, J. B. and Bhatia, M. (2012) 'Activin A promotes hematopoietic fated mesoderm development through upregulation of brachyury in human embryonic stem cells', *Stem Cells Dev*, 21(15), 2866-77.

27. Pick, M., Azzola, L., Mossman, A., Stanley, E. G. and Elefanty, A. G. (2007) 'Differentiation of human embryonic stem cells in serum-free medium reveals distinct roles for bone morphogenetic protein 4, vascular endothelial growth factor, stem cell factor, and fibroblast growth factor 2 in hematopoiesis', *Stem Cells,* 25(9), 2206-14.

28. Illing, A., Liu, P., Ostermay, S., Schilling, A., de Haan, G., Krust, A., Amling, M., Chambon, P., Schinke, T. and Tuckermann, J. P. (2012) 'Estradiol increases hematopoietic stem and progenitor cells independent of its actions on bone', *Haematologica,* 97(8), 1131-5.

29. Tavakkol, A., Elder, J. T., Griffiths, C. E., Cooper, K. D., Talwar, H., Fisher, G. J., Keane, K. M., Foltin, S. K. and Voorhees, J. J. (1992) 'Expression of growth hormone receptor, insulin-like growth factor 1 (IGF-1) and IGF-1 receptor mRNA and proteins in human skin', *J Invest Dermatol,* 99(3), 343-9.

30. Kaushansky, K., Lok, S., Holly, R. D., Broudy, V. C., Lin, N., Bailey, M. C., Forstrom, J. W., Buddle, M. M., Oort, P. J. and Hagen, F. S. (1994) 'Promotion of megakaryocyte progenitor expansion and differentiation by the c-Mpl ligand thrombopoietin', *Nature,* 369(6481), 568-71.

31. Andersson, L. O., Barrowcliffe, T. W., Holmer, E., Johnson, E. A. and Sims, G. E. (1976) 'Anticoagulant properties of heparin fractionated by affinity chromatography on matrix-bound antithrombin iii and by gel filtration', *Thromb Res,* 9(6), 575-83.

32. Collins, D. M., Murdoch, H., Dunlop, A. J., Charych, E., Baillie, G. S., Wang, Q., Herberg, F. W., Brandon, N., Prinz, A. and Houslay, M. D. (2008) 'Ndel1 alters its conformation by sequestering cAMP-specific phosphodiesterase-4D3 (PDE4D3) in a manner that is dynamically regulated through Protein Kinase A (PKA)', *Cell Signal,* 20(12), 2356-69.

33. Lyman, S. D. and Jacobsen, S. E. (1998) 'c-kit ligand and Flt3 ligand: stem/progenitor cell factors with overlapping yet distinct activities', *Blood,* 91(4), 1101-34.

34. Nitsche, A., Junghahn, I., Thulke, S., Aumann, J., Radonić, A., Fichtner, I. and Siegert, W. (2003) 'Interleukin-3 promotes proliferation and differentiation of human hematopoietic stem cells but reduces their repopulation potential in NOD/SCID mice', *Stem Cells,* 21(2), 236-44.

35. Paul, S. R., Bennett, F., Calvetti, J. A., Kelleher, K., Wood, C. R., O'Hara, R. M., Leary, A. C., Sibley, B., Clark, S. C. and Williams, D. A. (1990) 'Molecular cloning of a cDNA encoding interleukin 11, a stromal cell-derived lymphopoietic and hematopoietic cytokine', *Proc Natl Acad Sci U S A,* 87(19), 7512-6.

36. Goldman, S. J. (1995) 'Preclinical biology of interleukin 11: a multifunctional hematopoietic cytokine with potent thrombopoietic activity', *Stem Cells,* 13(5), 462-71.

37. Sasaki, A., Yasukawa, H., Shouda, T., Kitamura, T., Dikic, I. and Yoshimura, A. (2000) 'CIS3/SOCS-3 suppresses erythropoietin (EPO) signaling by binding the EPO receptor and JAK2', *J Biol Chem*, 275(38), 29338-47.

38. Glader, B. E., Rambach, W. A. and Alt, H. L. (1968) 'Observations on the effect of testosterone and hydrocortisone on erythropoiesis', *Ann N Y Acad Sci*, 149(1), 383-8.

39. Cross, D. A., Alessi, D. R., Cohen, P., Andjelkovich, M. and Hemmings, B. A. (1995) 'Inhibition of glycogen synthase kinase-3 by insulin mediated by protein kinase B', *Nature*, 378(6559), 785-9.

40. Doran, P. M. (2012) *Bioprocess engineering principles*, Second edition. ed., Oxford: Academic.

41. Kim, K. Y., Hysolli, E. and Park, I. H. (2012) 'Reprogramming human somatic cells into induced pluripotent stem cells (iPSCs) using retroviral vector with GFP', *J Vis Exp*, (62).

42. Han, Z. B., Ren, H., Zhao, H., Chi, Y., Chen, K., Zhou, B., Liu, Y. J., Zhang, L., Xu, B., Liu, B., Yang, R. and Han, Z. C. (2008) 'Hypoxia-inducible factor (HIF)-1 alpha directly enhances the transcriptional activity of stem cell factor (SCF) in response to hypoxia and epidermal growth factor (EGF)', *Carcinogenesis*, 29(10), 1853-61.

43. Kim, J. W., Tchernyshyov, I., Semenza, G. L. and Dang, C. V. (2006) 'HIF-1-mediated expression of pyruvate dehydrogenase kinase: a metabolic switch required for cellular adaptation to hypoxia', *Cell Metab*, 3(3), 177-85.

44. Santilli, G., Lamorte, G., Carlessi, L., Ferrari, D., Rota Nodari, L., Binda, E., Delia, D., Vescovi, A. L. and De Filippis, L. (2010) 'Mild hypoxia enhances proliferation and multipotency of human neural stem cells', *PLoS One*, 5(1), e8575.

45. Sisakhtnezhad, S., Alimoradi, E. and Akrami, H. (2016) 'External factors influencing mesenchymal stem cell fate in vitro', *Eur J Cell Biol*.

46. Chen, J., Kang, J. G., Keyvanfar, K., Young, N. S. and Hwang, P. M. (2016) 'Long-term adaptation to hypoxia preserves hematopoietic stem cell function', *Exp Hematol*, 44(9), 866-873.e4.

47. Morikawa, T. and Takubo, K. (2015) 'Hypoxia regulates the hematopoietic stem cell niche', *Pflugers Arch*.

48. Wagner, B. A., Venkataraman, S. and Buettner, G. R. (2011) 'The rate of oxygen utilization by cells', *Free Radic Biol Med*, 51(3), 700-12.

49. Berg, J. M., Tymoczko, J. L., Gatto, G. J., Jr. and Stryer, L. *Biochemistry*, Eighth edition. ed.

50. Yachie-Kinoshita, A., Nishino, T., Shimo, H., Suematsu, M. and Tomita, M. (2010) 'A metabolic model of human erythrocytes: practical application of the E-Cell Simulation Environment', *J Biomed Biotechnol*, 2010, 642420.

51. Wanet, A., Arnould, T., Najimi, M. and Renard, P. (2015) 'Connecting Mitochondria, Metabolism, and Stem Cell Fate', *Stem Cells Dev,* 24(17), 1957-71.

52. Chisti, Y. (2000) 'Animal-cell damage in sparged bioreactors', *Trends Biotechnol,* 18(10), 420-32.

53. Placzek, M. R., Chung, I. M., Macedo, H. M., Ismail, S., Mortera Blanco, T., Lim, M., Cha, J. M., Fauzi, I., Kang, Y., Yeo, D. C., Ma, C. Y., Polak, J. M., Panoskaltsis, N. and Mantalaris, A. (2009) 'Stem cell bioprocessing: fundamentals and principles', *J R Soc Interface,* 6(32), 209-32.

54. Yourek, G., McCormick, S. M., Mao, J. J. and Reilly, G. C. (2010) 'Shear stress induces osteogenic differentiation of human mesenchymal stem cells', *Regen Med,* 5(5), 713-24.

55. Wragg, J. W., Durant, S., McGettrick, H. M., Sample, K. M., Egginton, S. and Bicknell, R. (2014) 'Shear stress regulated gene expression and angiogenesis in vascular endothelium', *Microcirculation,* 21(4), 290-300.

56. Teo A, Mantalaris A, Lim M (2014) ‘Influence of Culture pH on proliferation and cardiac differentiation of murine embryonic stem cells’ Biochem Eng (90) 8-15

57. Chaudhry MA, Bowen B, Piret JM (2009) ‘Culture pH and osmolality influence proliferation and embryoid body yeilds of murine embryonic stem cells’ Biochem Eng Jnl (45) 126-135)

58. Endo, T., Ishibashi, Y., Okana, H. and Fukumaki, Y. (1994) 'Significance of pH on differentiation of human erythroid cell lines', *Leuk Res,* 18(1), 49-54.

59. Sangkuhl, K., Shuldiner, A. R., Klein, T. E. and Altman, R. B. (2011) 'Platelet aggregation pathway', *Pharmacogenet Genomics,* 21(8), 516-21.

60. Alkhamis, T. M., Beissinger, R. L. and Chediak, J. R. (1988) 'Red blood cell effect on platelet adhesion and aggregation in low-stress shear flow. Myth or fact?', *ASAIO Trans,* 34(3), 868-73.

61. Walker, G. M., Zeringue, H. C. and Beebe, D. J. (2004) 'Microenvironment design considerations for cellular scale studies', *Lab Chip,* 4(2), 91-7.

62. Velve-Casquillas, G., Le Berre, M., Piel, M. and Tran, P. T. (2010) 'Microfluidic tools for cell biological research', *Nano Today,* 5(1), 28-47.

63. http://www.tapbiosystems.com/tap/cell_culture/ambr.htm, 26/11/16

64. Shin, Y., Han, S., Jeon, J. S., Yamamoto, K., Zervantonakis, I. K., Sudo, R., Kamm, R. D. and Chung, S. (2012) 'Microfluidic assay for simultaneous culture of multiple cell types on surfaces or within hydrogels', *Nat. Protocols,* 7(7), 1247-1259.

65. Grist, S. M., Chrostowski, L. and Cheung, K. C. (2010) 'Optical oxygen sensors for applications in microfluidic cell culture', *Sensors (Basel),* 10(10), 9286-316.

66. Rohde, C., Gilleland, C., Samara, C., Zeng, F. and Yanik, M. F. (2008) 'High-throughput in vivo genetic and drug screening using femtosecond laser nano-surgery, and microfluidics', *Conf Proc IEEE Eng Med Biol Soc,* 2008, 2642.

67. https://www.dowcorning.com/content/publishedlit/Chapter17.pdf 66

68. van Midwoud, P. M., Janse, A., Merema, M. T., Groothuis, G. M. and Verpoorte, E. (2012) 'Comparison of biocompatibility and adsorption properties of different plastics for advanced microfluidic cell and tissue culture models', *Anal Chem,* 84(9), 3938-44.

69. Becker H, (2002) 'Polymer Microfluidic Devices' Talanta (56) 267-87

70. Lin, Z., Cherng-Wen, T., Roy, P. and Trau, D. (2009) 'In-situ measurement of cellular microenvironments in a microfluidic device', *Lab Chip,* 9(2), 257-62.

71. Chao, H., Mei, W. J., Huang, Q. W. and Ji, L. N. (2002) 'DNA binding studies of ruthenium(II) complexes containing asymmetric tridentate ligands', *J Inorg Biochem,* 92(3-4), 165-70.

72. http://www.abcam.com/protocols/introduction-to-flow-cytometry

73. Schlegel, R. A. and Williamson, P. (2001) 'Phosphatidylserine, a death knell', *Cell Death Differ,* 8(6), 551-63.

74. Medzhitov, R. (2008) 'Origin and physiological roles of inflammation', *Nature,* 454(7203), 428-35.

75. http://www.nature.com/scitable/topicpage/mitochondria-14053590 01/05/16

76. Kim, J. W., Tchernyshyov, I., Semenza, G. L. and Dang, C. V. (2006) 'HIF-1-mediated expression of pyruvate dehydrogenase kinase: a metabolic switch required for cellular adaptation to hypoxia', *Cell Metab,* 3(3), 177-85.

77. Ryu, J. M., Lee, H. J., Jung, Y. H., Lee, K. H., Kim, D. I., Kim, J. Y., Ko, S. H., Choi, G. E., Chai, I. I., Song, E. J., Oh, J. Y., Lee, S. J. and Han, H. J. (2015) 'Regulation of Stem Cell Fate by ROS-mediated Alteration of Metabolism', *Int J Stem Cells,* 8(1), 24-35.

78. Wang, C., Lu, H. and Schwartz, M. A. (2012) 'A novel in vitro flow system for changing flow direction on endothelial cells', *J Biomech,* 45(7), 1212-8.

79. Collins, D. M., Murdoch, H., Dunlop, A. J., Charych, E., Baillie, G. S., Wang, Q., Herberg, F. W., Brandon, N., Prinz, A. and Houslay, M. D. (2008) 'Ndel1 alters its conformation by sequestering cAMP-specific phosphodiesterase-4D3 (PDE4D3) in a manner that is dynamically regulated through Protein Kinase A (PKA)', *Cell Signal,* 20(12), 2356-69.

80. Beebe, D. J., Mensing, G. A. and Walker, G. M. (2002) 'Physics and applications of microfluidics in biology', *Annu Rev Biomed Eng,* 4, 261-86.

81. Acosta-Martinez JP, Papantoniou I, Lawrence K, Ward S, Hoare M (2010) 'Ultra-scale down stress analysis of the bioprocessing of whole human cells as a basis for cancer vaccines' Biotechnol Bioeng 107(6) 953-63